Response to comments

Synergistic radar and radiometer retrievals of ice hydrometeors

This document contains the responses to the comments of each reviewer followed by the marked-up differences of the manuscript and the revised version. For each comment the author's response and, if applicable, the corresponding changes in the manuscript are listed. Line numbers of changes are given with respect to the revised manuscript.
In response to the combined comments of the referees, all computations have been repeated and most of the manuscript has been rewritten. The following general changes have been implemented:

- We have switched to an airborne measurement set-up and the manuscript has been modified accordingly.
- The text in the result section has been shortened.
- Redundant results for scene 2 have been placed in an appendix.
- The selection of tested retrieval habits has been revised and changed.

1 Comments from referee 1

1.1 General comments

Reviewer comment 1

As noted in Section 4.2.4, the a priori assumptions do not describe reality very well. In particular, I suspect that the information content of Dm and N0* is highly dependent on the a priori assumptions of these two variables in the retrieval framework. Especially with a radar measurement, since Z is sensitive to both parameters over a wide range of the parameter space, the relative sensitivity and therefore information content will almost entirely depend on the relative constraints on these parameters imposed by Xa and Sa. As such it is imperative to accurately characterize these. I understand the choice to use the DARDAR constraints, but its clear from the cross-section plots that the model ice particle concentrations vary over a much wider range than the roughly 2 orders of magnitude that Eq. 4 provides over a 220-272 K temperature range. So, when the retrieval results are compared to model reality, it seems that a lot of N0* variability is folded into Dm and this is especially evident in Figures 13 and 14. My overall concern is that it is difficult to interpret some of the results when the model fields and the a priori assumptions differ so strongly.

Author response

To avoid potential misunderstanding we would like to point out that the variation of the a priori mean with temperature, which is given by Eq. 4, does not limit the retrieved values of N_0^* to this range. How much N_0^* is allowed to vary around the a priori mean is determined by the covariance matrix. Since the standard deviation for $\log_{10}(N_0^*)$ at each grid point was set to 2 (c.f. Tab. 3), N_0^* is free to vary over several orders of magnitude in addition to the variation of the a priori profile.
Furthermore, the sentence in Section 4.2.4 was badly formulated and did not really express what we wanted to say there. The a priori assumptions are not generally bad for the model (after all the averaged results for the first scene are good). Rather, they are insufficient to accurately describe the (co-)variability of D_m and N_0^*.
Nonetheless, the point raised by the reviewer certainly remains valid: In absolute terms, the interpretation of the retrieval results is dependent on the a priori assumptions. We argue here, however, that by applying equivalent a priori assumptions in all retrievals, we can still derive conclusions on the benefits of the combined retrieval approach based on a relative interpretation of the retrieval results. Our results indicate that the combined retrieval has to rely less on a priori assumptions than the radar-only retrieval. This is an

important advantage of the combined retrieval since if D_m and N_0^* could be constrained reliably a priori we would not have the uncertainties in the observational record of ice hydrometeors that we see today.

Changes in manuscript

- The discussion of the role of the a priori and its impact on results has been extended by adding the following paragraph to the manuscript:

> **Changes starting in line 481:**
>
> The a priori assumptions used in this study were chosen similar to those of the DARDAR-CLOUD product since they represent well established and validated assumptions for ice cloud retrievals. The role of the a priori is to complement the observations with additional information required to make the retrieval problem tractable. For the hydrometeor retrieval this means that the a priori determines how information from the observations, which alone is insufficient to determine both degrees of freedom of the PSD, is distributed between its D_m and N_0^* parameters. For the radar-only retrieval, this works well for cloud systems containing both ice and snow but leads to biased retrievals of both IWC and IWP when this is not the case (Fig. 9~~. In general, the passive-only and the combined retrievals display~~). The DARDAR product uses co-located lidar observations to resolve the ambiguity where observations from both sensors are available. As our results show, this can be achieved also by combining a radar with passive microwave radiometers. However, while the overlap between lidar and radar is restricted to relatively thin clouds, microwave radiometers can provide sensitivity even inside thick clouds.

- The following paragraph has been added to the discussion of the limitations of the study which clearly states that the retrieval results should not be interpreted in absolute terms:

> **Changes starting in line 529:**
>
> An important limitation of this study is its scope: The aim here was not to develop a production-ready combined retrieval product but rather a proof-of-concept to explore this observational approach. The retrieval results presented here should therefore not be interpreted in absolute terms. The primary results are based on the relative performances of the three retrieval methods: Given equivalent a priori assumptions~~do not describe reality very well. In addition to that, the current implementation of the retrieval is computationally very expensive. For further development of the combined retrieval concept it may therefore be advisable to revisit the applied retrieval method in search for a potentially more suitable alternative~~, the combined retrieval demonstrates higher sensitivity to the microphysical properties than the radar-only retrieval

> and lower errors in terms of IWC than the passive-only retrieval.

- The paragraph starting on line 524 on the limitations of the OEM as retrieval method has been removed since its interpretation caused confusion and it was deemed to be of minor importance for the overall results of the study.

Reviewer comment 2

Forward model error is introduced when the different species present in the model microphysics are combined into one species and when different scattering models are used to represent the ice particles. That this is not represented in Se could lead to over-fitting and poor convergence (I suspect this is part of the reason why the normalized cost is much higher for the radiometer-including retrievals). It should be relatively easy to quantify this error by re-running the simulations with the retrieval assumptions(combining ice species, different scattering models), and I suspect that this error term would dominate the instrument noise term for many channels.

Author response

It is certainly true that the simplified forward model used in the retrieval introduces a forward modeling error and that it will likely dominate the sensor noise. However, we do not agree with the reviewer that this error is easy to quantify. First of all, the error will not be Gaussian and will depend on the cloud composition and the assumed particle shape, so that a more sophisticated error model would be required to describe the error accurately. Fitting such a model to the test scenes would likely yield overly optimistic results as this would mean making use of information which would not be available for a real retrieval scenario.
Because of these difficulties, we decided to not pursue this approach in the study. However, since this is an important point to mention, we will add a paragraph on this issue in the discussion.

Changes in manuscript

> **Changes starting in line 513:**
>
> It should be noted, that none of the presented retrievals accounts for the error caused by the simplified forward model and the choice of the particle model. ~~Unfortunately, no evidence of a relation between the χ^2_y value and the retrieval performance was observed. It thus remains an open question whether and how information on the ice particle shape can be extracted from microwave observations of ice particles~~This has not been pursued here because of the difficulty of fitting a suitable error model to these errors, which are likely non-Gaussian and scene-dependent. However, it is likely that accounting for them can improve retrieval performance and weaken the impact of the particle choice on the retrieval results.

1.2 Specific comments

Reviewer comment 1

Lines 85-88: I recommend the use of geographical spatial references (i.e.,north/south rather than left/right)

Author response

The proposed change has been adopted in the revised version of the manuscript.

Changes in manuscript

> **Changes starting in line 95:**
>
> The first test scene, shown in panel (a), is located in the tropical Pacific and contains a ~~convective storm~~ mesoscale convective system in the ~~right~~ northern half of the scene and its anvil which extends into the ~~left halfof the scene~~southern half. The second scene, shown in panel (b), is located in the North Atlantic and contains an ice cloud in the ~~first quarter~~ southern part and a low-level, mixed-phase cloud in the ~~remainder of the scene~~northern part.

Reviewer comment 2

Line 98 (also 176,252,449): Instead of vertical/horizontal (which are dependent on the convention used for plotting), I recommend the use of concentration/size tocharacterize the dimensions of the particle size distribution.

Author response

The proposed change has been adopted in the revised version of the manuscript.

Changes in manuscript

> **Changes starting in line 105:**
>
> The ~~four panels display the prognosed particle size distributions for the four frozen hydrometeor types together with renderings of the particle shapes used in the forward simulations. As these plots show, the~~ assumed particle size distributions across different ice species vary mostly in their ~~horizontal and vertical scaling~~ scaling with respect to size and concentration, whereas the ~~function~~ normalized shape shows less variability.

> **Changes starting in line 177:**
>
> The PSDs of frozen hydrometeors and rain are represented using the normalized

particle size distribution formalism proposed by Delanoë et al. (2005). The PSD of a hydrometeor species at a given ~~height level is represented by a vertical and a horizontal scaling parameter, the~~ altitude is modeled using a generalized gamma distribution function with four parameters. The mass-weighted mean diameter D_m, which scales the PSD along the size dimension, and the normalized number density N_0^*~~. Alternative parametrizations using mass density and D_m or the mass density and N_0^* have been tested but no considerable effect on retrieval performance has been observed.~~

~~The retrieval computes vertical profiles of the two scaling parameters D_m and N_0^* for each of the two hydrometeor species. The remaining shape of each PSD is described by the shape parameters α and β, not to be confused with the parameters of the mass-size relationship shown in Tab. 1. The shape parameters are set to fixed, species-specific values. This principle is illustrated in Fig. 3. The plot displays the a-priori-assumed shapes of the particle size distribution of frozen and liquid hydrometeors. The retrieved horizontal and vertical scaling parameters~~ , ~~D_m and N_0^*, are used as units for the axes of the plot so that~~ which scales the particle concentration, are the two retrieved degrees of freedom of the PSD.

Changes starting in line 274:

~~In the figure, the cloud signal is displayed in D_m-mass density space and thus shows how the measured passive cloud signal varies with the horizontal and vertical scaling parameters of the PSD. Overlaid onto~~ The cloud signal in the radiometer observations is the difference between the cloudy- and clear-sky brightness temperatures (ΔT_B). The signal in the active observations is here defined as the maximum of the measured profile of radar reflectivity $\mathrm{dBZ_{max}}$. Figure 9 displays the contours of ~~the passive cloudsignal are the isolines of the maximum radar reflectivity returned from the cloud ...~~

Changes starting in line 429:

The results ~~show~~ indicate that the combined observations can ~~simultaneously constrain the horizontal and vertical scaling of~~ constrain the ~~particle size distribution~~size and concentration of particles in the cloud.

Reviewer comment 3

Line 100: A few more details on the Milbrant and Yau microphysics sheme that are relevant to this study would be helpful here. For example: What is the assumed shape(functional form) of the particle size distribution, and what are the prognostic variables(e.g., number concentration, mixing ratio)?

Author response

We followed the reviewers comment and added the requested information to the manuscript.

Changes in manuscript

> **Changes starting in line 99:**
>
> The GEM model uses a two-moment scheme with six types of hydrometeors to represent clouds and precipitation (Milbrandt and Yau, 2005): Two classes of liquid hydrometeors (rain and liquid cloud) and four of frozen hydrometeors (cloud ice, snow, hail and graupel). The particle size distribution (PSD) of each hydrometeor ~~type is parametrized by its particle number concentration and mass density. The full particle size distribution can be prognosed from the two moments using a species-dependent parametrization and mass-size relationship. The~~ class is described by a three-parameter gamma distribution. The prognostic parameters of the model are the slope and intercept parameters of the ~~mass-size relationship are given in Tab. 1. As shown in the table,~~ PSD, which are derived from the predicted mixing ratios and number concentrations. The third parameter, which defines the shape of the ~~masses of all ice particles in the model are assumed to scale with a power of three, which leads to high densities for large particles.~~ PSD, is set to a fixed, species-specific value. For each hydrometeor species a specific mass-size relationship is assumed.

Reviewer comment 4

Line 135: Does the ARTS radar solver also provide analytic Jacobians?

Author response

Yes, it does. A sentence will be added to the description of the forward model to clarify this.

Changes in manuscript

> **Changes starting in line 146:**
>
> Radar reflectivities are computed using ARTS' built-in single-scattering radar solver, which provides analytic Jacobians.

Reviewer comment 5

Line 187: particles should be particle

Author response

The sentence has been removed in the revised version of the manuscript since the information it conveyed was deemed irrelevant.

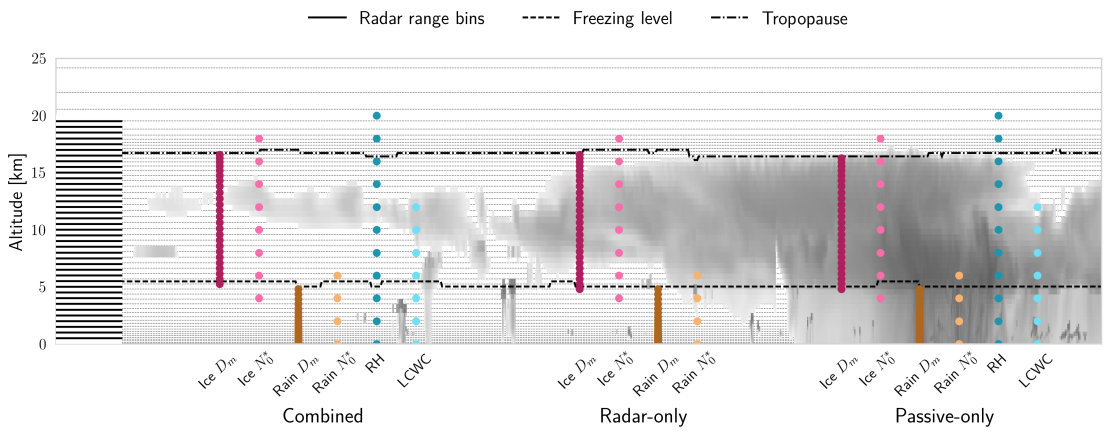

Figure 1.1: Illustration of retrieval quantities and their respective retrieval grids. Grey, dashed lines in the background display the vertical grid of the GEM model. Black, solid lines on the left side display the range bins of the radar observations. Filled markers represent the retrieval grids of each retrieval quantity for the combined, radar-only and passive-only configurations of the retrieval algorithm.

Reviewer comment 6

Line 198: Is Dm also only retrieved at these 10 points, or just N0* (and Dm retrieved in each radar range gate as in Grecu et al. 2016)?

Author response

D_m is actually retrieved at the resolution of the GEM model scenes. Since questions about the retrieval grids were raised also by the other reviewers, we will add an illustration of the grids applied in the different retrieval configurations to the manuscript.

Changes in manuscript

The figure shown in Fig. 1.1 has been added to the manuscript to clarify which variables are retrieved at which resolutions.

Reviewer comment 7

7. Line 256: Actually, this is only one example of how the radar and radiometer measurements can be complementary. Even if the lines were parallel (and thus no information distinguishing size from concentration could be obtained), the radar still locates the cloud and describes its vertical structure. One can imagine a cloud of the same ice water path and particle size at two different heights having different brightness temperatures

due to changes in the water vapor absorption above the cloud having the radar information would provide increased information content about the ice water path in this case than the radiometer measurement alone.

Author response

It is certainly correct that, when a radar sensor is added to a passive observation system, one of the advantages will be the increased resolution. However, what we are interested in are the advantages that neither of the two instruments can provide on its own. If it was only about vertical resolution, then the radar alone would be the ideal observation system. In this sense, we do not consider the vertical resolution a synergy of the two sensors.
To make this clear, we will add an explanation of our definition of synergies between the active and passive observations to the section which discusses the complementary information content.

Changes in manuscript

> **Changes starting in line 262:**
>
> A fundamental question regarding the benefit of combining two remote sensing observations in a retrieval is to what extent the observations contain non-redundant information. The degree of non-redundancy in the combined observations is what we refer to here as complementary information content. We are thus interested in the information that cannot be provided by either of the instruments alone. The higher resolution achieved by adding radar observations to passive ones is therefore not considered as complementary information since the radar alone can provide the increased resolution.

Reviewer comment 8

Table 4: Why are the values for GemSnow and GemGraupel different than in Table 1?

Author response

This was by mistake and has been corrected in the revised version of the manuscript.

Changes in manuscript

Tables 1 and 4 have been corrected and extended in the revised version of the manuscript.

Reviewer comment 9

Figures 7 and 8: Im not sure why these are separate figures it seems like all panels could fit on one page.

Author response

Figures 7 and 8 have been combined into a single figure in the revised manuscript.

Changes in manuscript

Figures 7 and 8 have been combined into a single figure and now look as shown in Fig. 1.2.

Reviewer comment 10

Figure 10 is missing from the manuscript.

Author response

Figure 10 has been included in an Appendix to the revised manuscript with the rest of the analysis of the results from the second test scene.

Changes in manuscript

The figure shown in Fig.1.3 has been added in the appendix of the manuscript.

Reviewer comment 11

Line 374: recommend using represent instead of predict

Author response

The proposed change has been adopted in the revised version of the manuscript.

Changes in manuscript

> **Changes starting in line 365:**
>
> Since snow will have ~~the~~ a stronger impact on the observations, the retrieval in these regions ~~tends to predict~~ will likely tend to represent snow rather than ice, which leads to the low retrieved number ~~densities~~concentrations.

Reviewer comment 12

Line 382: should be reference instead of references

Author response

This has been corrected in the updated version of the manuscript.

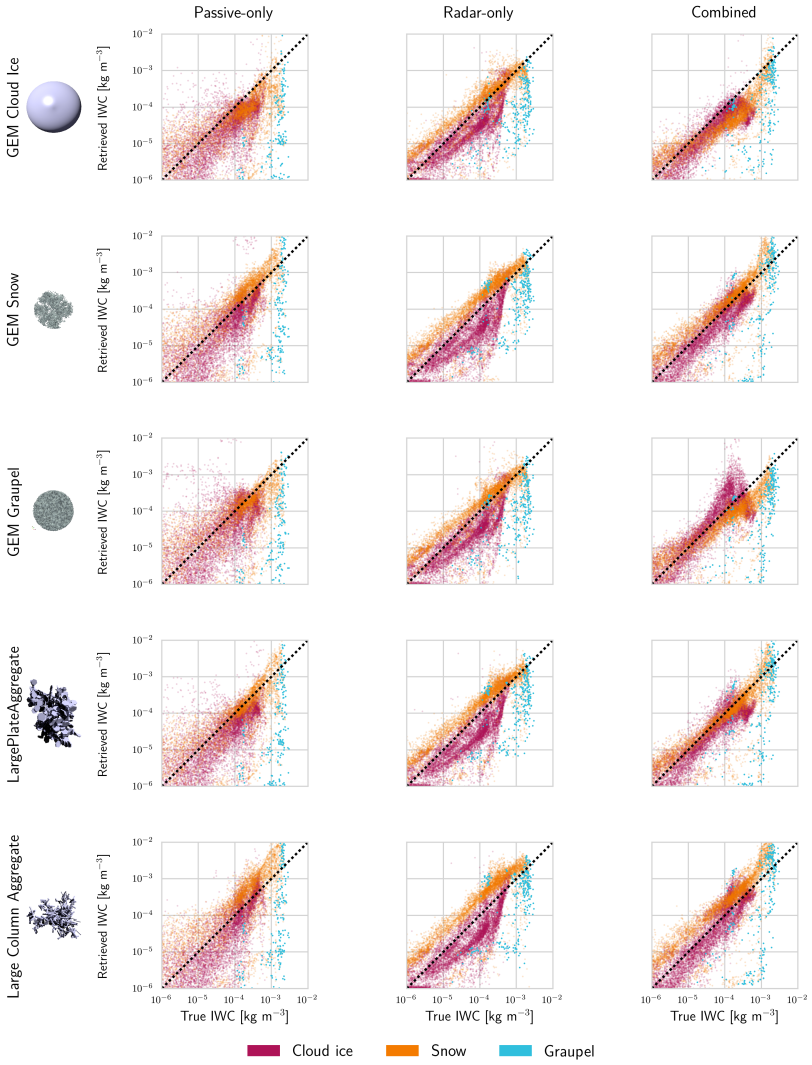

Figure 1.2: Retrieved IWC plotted against reference IWC for the tested retrieval configurations. Each row shows the retrieval results for the particle shape shown in the first panel. The following panels show the retrieval results for the passive-only (first column), the radar-only (second column) and the combined retrieval (third column). Markers are colored according to the prevailing hydrometeor type at the corresponding grid point in the test scene. Due to their sparsity, markers corresponding to graupel are drawn at twice the size of the other markers.

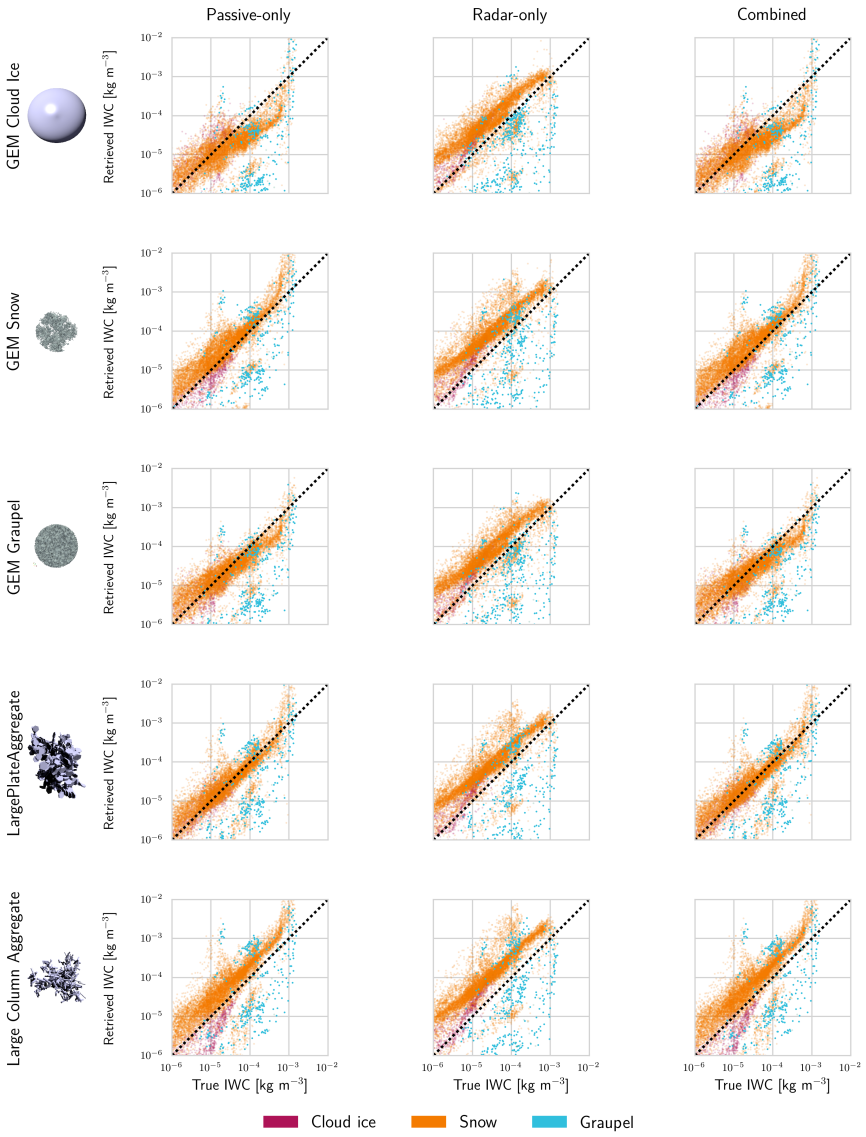

Figure 1.3: Scatter plots of the reference and retrieved IWC for the second test scene. The rows show the retrieval results for a given assumed ice particle model. The first column of each row displays a rendering of the particle model. The following rows display the results for the passive-only, the radar-only and the combined retrieval.

Changes in manuscript

> **Changes starting in line 373:**
>
> The radar-only retrieval does not exhibit any retrieval skill, hardly reproducing any

of the variation of the ~~references~~ reference values.

Reviewer comment 13

Line 414: How are the truncated PSDs (using GemSnow) represented in the forward simulations? Is total ice water content conserved? If so, how is it spread amongthe valid particle sizes equally, or is the truncated mass allocated to the smallest size bin?

Author response

Total IWC is not conserved in the handling of PSDs. The point raised by the reviewer has been investigated by assessing the effect of the truncation on the water content of snow in the forward simulations. The results of the analysis are given in the figure below. As these results show, the effects of the truncation in the forward simulations are negligible.
However, when the GemSnow particle model is used in the retrieval it can introduce significant errors. For this reason as well as another reviewers' comment regarding the choice of tested particles, the selection of particles to be used in the retrieval will be changed for the revised manuscript and the GemSnow particle will be replaced by a habit mix which uses the GemSnow particle for large diameters.

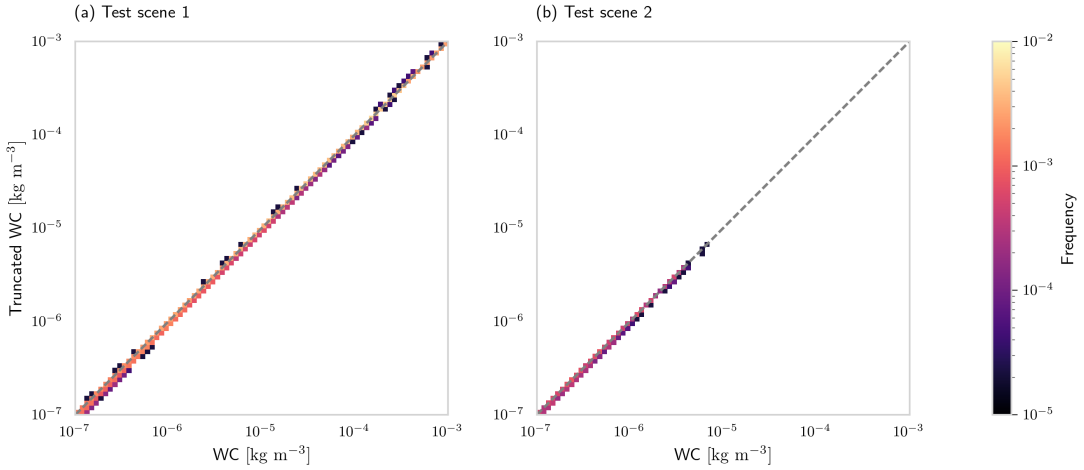

Figure 1.4: Joint distribution of truncated and full snow water content (SWC) for the two test scenes.

Reviewer comment 14

Figure 16: The figure labels/captions aren't clear if they refer to total liquid water content/path or just the cloud liquid water/path.

Author response

We will clarify that the contours refer to liquid cloud water content in the revised version of the manuscript.

Changes in manuscript

To make clear what the labels refer to, they have been changed to liquid cloud water content (LCWC) in the figure. The new figure is shown in Fig. 1.5.

Reviewer comment 15

Line 518: Its interesting that the Plate Aggregate provides the most accurate re-trieval results, even though it isnt similar to the models used in the synthetic measurement simulations. Does the decreasing density with size better replicate the combina-tion of high-density GemCloudIce (which tends to be present in high concentrations atsmall sizes) and lower-density GemSnow (which tends to be dominant at larger sizes)?

Author response

Unfortunately, we cannot give a definitive answer to this question. As panel (a) in Fig. 15 shows, the density of the LargePlateAggregate habit is actually lower than that of snow for large particle sizes. Moreover, the scattering properties certainly also play a role here. From these results alone, we are therefore not able to postulate any direct causality between the particle density and the performance in the retrieval.

Changes in manuscript

To provide more definitive recommendations regarding the choice of the particle model, we have reconsidered the selection of models to test and added the figure shown in Fig. 1.6 to the manuscript. These results indicate that a potential explanation of the good performance of the Large Plate Aggregate is that its scattering properties are intermediate to those of GEM cloud ice and GEM snow.

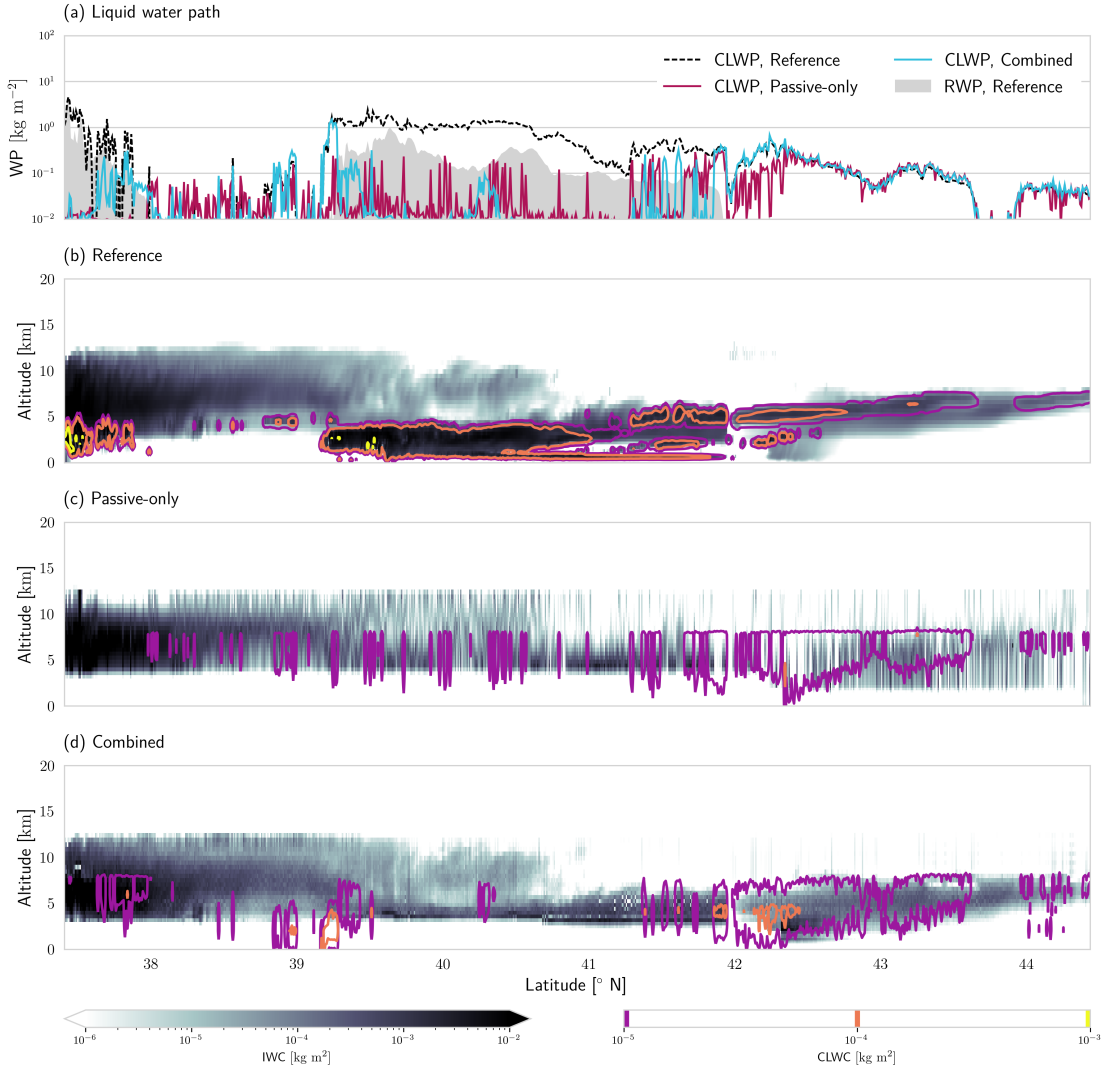

Figure 1.5: Reference and retrieved CLWC and IWC. Panel (a) shows the reference and retrieved LWP for each profile. Panel (b) displays reference LWC contours drawn on top of the total hydrometeor content. Retrieval results for passive-only and combined retrieval are given in Panel (c) and (d).

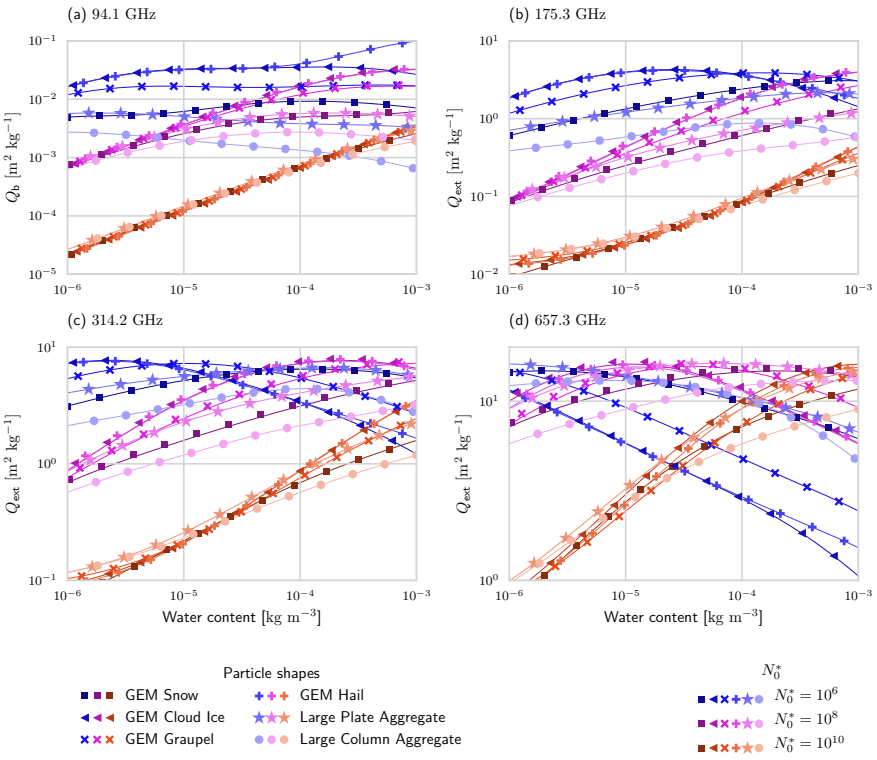

Figure 1.6: Bulk mass backscattering efficiency Q_b at 94.1 GHz (a) and mass attenuation coefficients Q_e at frequencies 175.3 GHz (b), 314.2 GHz (c) and 657.3 GHz (d) for the particle models used in the simulated observations and the retrieval. Different colors show the bulk properties for different values of the N_0^* parameter of the PSD.

2 Comments from referee 2

2.1 Major points

Reviewer comment 1

A major aspect of the study concerns the representation of the particle size distribution which is retrieved by two free parameters (different from the 2 moments of the atmospheric model GEM used to provide the test scenes) and the assumptions of the particle type. The difficulty of connecting atmospheric model output to single scattering properties (which is one of the fundamental assumptions) could be better explained. The motivation why the authors choose their approach and why they test certain settings need to be discussed in the beginning. Couldnt Tab. 1 and 4 be combined and better explained which is used for which purpose? Why is cloud ice the same and GEMsnow and GEMGraupel different in both?

Author response

We agree with the comment that the rather arbitrary choice of tested particles was a weak spot of the study. To improve this, the experiments have been repeated with a more principled selection of particles. The new selection is based on the particle properties described in Ekelund et al. (2020) and covers a broader range of mass-size relationships and scattering parameters. In particular, the GemSnow model has been removed from the selection of test particles because it does not cover small ice particle sizes.

Changes in manuscript

- A paragraph has been added to the description of the GEM test scenes which explains the particle models that have been developed to match the assumptions of the GEM microphysics scheme and that are used to simulate observations.

> **Changes starting in line 110:**
>
> In order to simulate observations from the GEM model scenes, the hydrometeor classes of the GEM microphysics scheme must be associated with particle shapes to define their radiometric properties. The ARTS single-scattering database, described in more detail below, contains particle models which were designed to be consistent with the mass-size relationships assumed in the GEM model. The particle shapes used to represent the GEM model's different hydrometeor types are listed together with their properties in Tab. 1.

- The following text has been added to the description of the retrieval implementation which discusses the difficulty of representing the complex mixture of different particles in the GEM model scenes with a single particle model as well as the new selection of particle models and habit mixes.

  Changes starting in line 228:

  A major difficulty for cloud retrievals is that the observations may not provide sufficient information to distinguish different hydrometeor species. Due to this ambiguity, frozen hydrometeors in the proposed retrieval algorithm are represented using only a single hydrometeor species. It is therefore necessary to find a suitable representation for frozen hydrometeors, which can capture the variability of the four frozen hydrometeor species in the GEM model and ideally also that of real ice hydrometeors.

  The differences between hydrometeor species in the test scenes are due to their different concentrations, sizes and shapes (c.f. Fig. 2). Since two parameters of the PSD of frozen hydrometeor species are retrieved, the retrieval is able to represent the characteristic number concentrations and particle sizes of different hydrometeor species. Variations in particle shape which correlate with particle size can be represented using a habit mix combining crystal shapes at small sizes with aggregates or rimed particles at larger sizes. This provides the retrieval with some flexibility to represent the different shapes present in the test scenes.

  Even with this configuration the simplified retrieval forward model ~~.~~

  ~~The setup and retrieval quantities of the passive-only retrieval are similar to the combined retrieval, with the only difference being that frozen and liquid hydrometeors are retrieved at reduced resolution.For ice,~~ will not be able to represent every possible configuration of mixes of the four ice hydrometeor species in the GEM model. It thus remains unclear which particle shape should be used to best represent this mixture. We therefore choose a set consisting of multiple particle shapes and habit mixes for which we investigate the impact of the particle choice on the retrieval results. The selected particles are listed in Tab. 4. Three of them, GEM Cloud Ice, GEM Snow, and GEM Graupel, correspond to the shapes present in the GEM model scenes. The GEM Snow and Graupel habits were mixed with crystal shapes to ensure that they cover sizes down to around 10 μm. In addition to this, two of the habit mixes distributed with the ARTS SSDB, the Large Plate Aggregate and Large Column Aggregate standard habits, are included in the selection to increase the range of scattering properties it covers.

- The errors in the reported parameters of the mass-size relationship for the GEM Snow and GEM graupel particles have been corrected.

It was, however, not possible to combined Tab. 1 and Tab. 4 because they now convey

slightly different information.

Reviewer comment 2

Although different parameterizations of the hydrometeor types are used to study their effects, vertical changes (development of sedimenting particles) are not considered. Similar polarization effects are not mentioned in the discussion on particle shape. Otherwise the paper nicely discusses the different aspects but in the end I ammissing a clear message on the outcome of the test (choice of particle types). What is recommended for the future?

Author response

The first statement made by the reviewer is not fully correct. Since the retrieval can reduce the concentration of particles and increase their size it can modify the ratio of small and large particles and thus represent the effects of sedimentation on the PSD.
Vertical changes in particle shape, i.e. transition from single crystals to aggregates, are represented indirectly through the particle size. The particle models used here are taken from the standard habits of the ARTS SSDB described in Eriksson et al. (2018). Some of them combine pristine crystals at small particle sizes with aggregate shapes at larger sizes.
Polarization effects in the simulations were ignored for the simple reasons that the model scenes do not provide information on particle orientation or aspect ratios and that suitable scattering data for oriented particles has only recently been released (Brath et al., 2019). For the revised version the sensors are assumed to point at nadir, which justifies neglecting polarization effects. Nonetheless, particle orientation can still have an effect on the observations. We will state clearly in the revised manuscript that polarization effects will have non-negligible impact on the observations of the MWI and ICI sensors. We agree that the choice of the particle models was described and motivated poorly in the manuscript. To address this, we will extend the description of the chosen particle models and try to provide clearer conclusions regarding the outcome of our experiments.

Changes in manuscript

- The following paragraph has been added to Sect. 2.2 stating that for MWI and ICI polarization effects can not be neglected.

> **Changes starting in line 119:**
>
> Moreover, the incidence angles of the beams of ICI and MWI will be around 53° at the Earth's surface. This further complicates the radiative transfer modeling since it requires treating a more complex co-location geometry of the nadir-pointing radar and the passive instruments. At off-nadir viewing angles, polarization also needs to be taken into account, the effects of which can be several Kelvin at the typical viewing angles of microwave imagers

(Xie et al., 2015).

- The discussion of the tested particle shapes has been extended to derive clearer recommendations for the future.

  Changes starting in line 492:

  ~~Given the increased sensitivity of the passive-only and combined retrieval to~~ Only the combined retrieval was able to yield accurate IWC retrievals for both test scenes for suitable choices of the particle model. However, if an unsuitable particle shape is chosen, the ~~assumed particle shape , it would be desirable to know which of the properties of a particle model are most critical for its representativeness. Five different particle models were tested here: The two most dominant from the GEM model and three additional models taken from the ARTS SSDB. The two GEM particles both showed the worst retrieval performance.For the GemCloudIce model~~induced errors may actually outweigh the benefits of the combined retrieval as is the case for the Large Column Aggregate and the GEM Cloud Ice shapes (Fig. 9). Judging from the particle properties displayed in Fig. 4, a likely explanation for ~~its bad performance is its very high density. The GemSnow model has similar density as the 8-ColumnAggregate, but does not reach down to small particle sizes, possibly explaining why it is unsuitable for the retrieval~~ the good performance of the Large Plate Aggregate and the GEM Graupel particle is that their properties are intermediate to those of GEM Cloud Ice and GEM Snow, which are the dominating shapes in the test scenes. For the test scenes considered here, this means that accurate IWC retrievals can be achieved using only a single hydrometeor species with suitable scattering properties which are intermediate to snowflakes and heavily rimed particles. This is in agreement with Ekelund et al. (2020) who found the Large Plate Aggregate to yield good agreement with observations from the GPM Microwave Imager at 183.31 ± 7 GHz. ~~Nonetheless, small performance differences are observed also for the other three models~~

- The following paragraph has been added to the conclusions:

  Changes starting in line 555:

  Regarding the representation of hydrometeors in the retrieval, our results indicate that complex mixes of hydrometeors can be accurately represented using a single, suitable habit mix. In particular, our results indicate that a suitable habit should have scattering properties that are intermediate between strongly rimed and more snow-flake like particles (Fig. 4, 9).

Reviewer comment 3

Not only the two moments of the ice PSD but further variables are retrieved and their information content is nicely shown in Fig. 14. I am surprised that the information on moisture is so low although information along three water vapor lines is provided? This should at least in the upper atmosphere provide information? Is it due to the choice of relative humidity which mainly depends on temperature? I am also skeptical about the results of Fig. 16. Basically, there should be no liquid for temperatures colder than 40 deg C (freezing) but it even reference LWC goes up to 13 km? I would not support the statement on L568 where is the evidence? Similar L527 Liquid water estimation within mixed phase clouds is extremely difficult and if ICI and radar could really do that together this would be worth a separate paper. To better understand the information content, I suggest to plot the profiles of cumulative degrees of freedom for the different retrievals as this could help interprete where and how the synergy works.

Author response

As can be seen in Fig. 8 from Eriksson et al. (2019), the information content on water vapor from ICI alone are at most 4 degrees of freedom for clear-sky scenarios. Since in the retrieval also channels from MWI are included, the expected information content on water vapor should be somewhat higher. However, this is for clear-sky scenarios. In the presence of clouds, the information content will be significantly reduced.
Regarding the results of the retrieved cloud liquid water content (CLWC), Fig. 16 shows quite clearly an improvement, both in terms of CLWC and cloud liquid water path (CLWP), in the results of the combined retrieval compared to the passive-only retrieval. Yes, liquid clouds droplets are present at high altitudes in the first model scene but only below the 230 K isotherm. However, since this is the case only for the first scene, it does not seem relevant for the interpretation of Fig. 16.

Changes in manuscript

To provide a more detailed analysis of the information content regarding humidity and CLWC we followed the referee's suggestion and replaced the bar diagrams in the manuscript with a figure (Fig. 2.1 shown below) displaying the cumulative DFS for all profiles in the test scenes.

Reviewer comment 4

The manuscript is rather lengthy making it difficult for the reader to extract the majorpoints. I strongly suggest a) to move part of the analysis into an appendix (, b) remove double statement (see minor comments, also the LWC plot) and c) to remove figure caption like information (for example L92 or filled contours) from the text. The text must make sense without looking at the figure. Figure only support the statements made in the text. Lengthy descriptions such as "The plot shows.." need to be avoided.

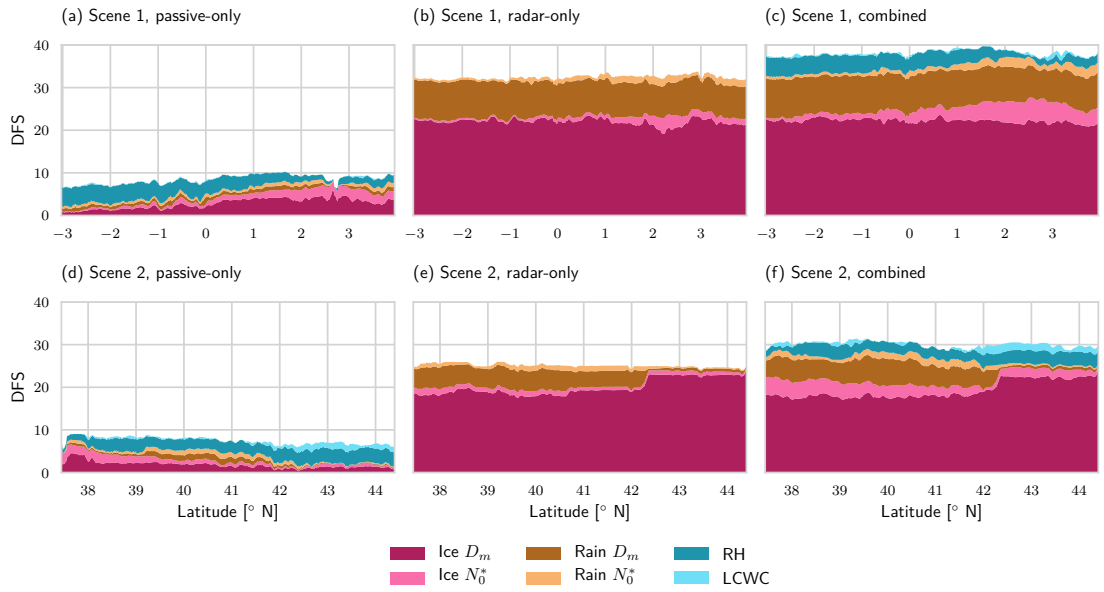

Figure 2.1: Degrees of freedom for signal for all retrieval configurations and both test scenes obtained with the Large Plate Aggregate model. The colored areas in each plot represent the contribution to the cumulative degrees of freedom from each retrieval quantity. Results for the first and second test scene are displayed in the first and second row, respectively. The first, second and third panel in each row show the results for the passive-only, radar-only and the combined retrieval.

Author response

We have followed the referee's recommendations to make the manuscript more concise.

Changes in manuscript

- Descriptions of the figures which display the results in Sect. 3 have been removed.
- The analysis of the results from the second test scene have been moved to an appendix.

2.2 Minor comments

Reviewer comment 1

L39: Is sensitivity really the right word? Range resolution is the main advantage signal-to noise range depends on distance and hydrometeor distribution,

Author response

Following the reviewer's suggestion the sentence has been rewritten.

Changes in manuscript

Most of the introduction has been rewritten and the corresponding expression has been removed.

Reviewer comment 2

L48: MWI will also cover new spectral channels, e.g. 118 GHz

Author response

The 118 GHz spectral band is employed already today by the FY-3 satellites. Nevertheless, we mention the band now also in the introduction.

Changes in manuscript

> **Changes starting in line 63:**
>
> MWI will complement ICI's observations with measurements at traditional millimeter wavelengths as well as a spectral band around the 118 GHz oxygen line. The observations of MWI, which cover the frequency range from 19 GHz up to 183 GHz, will provide additional sensitivity to liquid and frozen precipitation as well as water vapor.

Reviewer comment 3

L62: high-resolution is always relative for a model. I would recommend avoiding this term and use Cloud resolving Model (CRM).

Author response

The proposed improvement has been adopted in the revised version of the manuscript.

Changes in manuscript

> **Changes starting in line 74:**
>
> For this, a combined, variational retrieval is developed and applied to simulated observations of scenes from a ~~high-resolution atmospheric model and used to further explore the synergies between the active and passive observations.~~ cloud-resolving model (CRM).

Reviewer comment 4

L68: After you mention GPM (with scanning radar) it might be good to say that you are only looking at a nadir pointing radar (curtain). The swath center came bit as a surprise.

Author response

The radar type is now stated more explicitly in the introduction.

Changes in manuscript

> **Changes starting in line 75:**
>
> An airborne viewing geometry is assumed for the simulations with all sensors pointing at nadir and close-to overlapping antenna beams.

Reviewer comment 5

L70: There has been quite some literature about combining active and passive MW using a Bayesian framework which should be acknowledged, e.g. Grecu, M., & Olson,W. S. (2006), Johnson et al. (2012) , Munchak, S. J., & Kummerow

Author response

A paragraph listing previous work on synergistic retrievals using radar and passive radiometers at lower microwave frequencies has been added to the introduction.

Changes in manuscript

> **Changes starting in line 51:**
>
> Prominent examples of satellite missions that exploit both of these synergies are the the Tropical Rainfall Measuring Mission (TRMM, Kummerow et al. (1998); Grecu et al. (2004); Muncha) and the Global Precipitation Measurement (GPM, Hou et al. (2014); Grecu et al. (2016); Kummerow e) mission. Since the principal target of these missions are retrievals of liquid hydrometeors, they make use of sensors at comparably low microwave frequencies and hence provide only limited sensitivity to frozen hydrometeors.

Reviewer comment 6

L84: Test scenes have a grid resolution of 1 km horizontally. As this is not the true model resolution I would have recommended to coarse sample the model data (maybe every 5th data point) and include more diverse profiles instead. This might be especially interesting for the scatter plots.

Author response

The point raised by the reviewer here is certainly correct. However, the decision to restrict simulations to two test scenes was motivated primarily by the computational costs of performing the retrievals. The scatter plot in Fig. 10 (shown in Fig. 1.3 in this document), which was unfortunately missing from the manuscript , shows that the emergent structures are consistent for both test scenes. This indicates that the scenes cover sufficient profile variability to be statistically representative.

Reviewer comment 7

Motivation lacking: To perform RT simulations for each GEM profile the PSD needs to be diagnosed from the prognostic GEM variables, i.e. N and m..

Author response

The corresponding paragraph has been rewritten and the sentence removed.

Reviewer comment 8

L92:prognoses means forward in time - you mean diagnosed, calculated, determined.

Author response

The corresponding paragraph has been rewritten and the sentence removed.

Reviewer comment 9

L98: I find the term horizontal and vertical scaling strange why not saying PSD shape is similar but scaling in respect to diameter and number density. At least definethe term clearly the first time that you use it or define a short for it.

Author response

C.f. Comments from Referee 1 - General comment 2.

Reviewer comment 10

L103: model test be careful also at other instances that model can mean too manythings. Here I would say GEM test scenes.

Author response

Since much of the manuscript has been rewritten, this exact sentence is not present anymore. However, attention has been paid to the use of the word model and to ensure that its interpretation is unambiguous.

Reviewer comment 11

L119: Need to clearly say that polarization effects are neglected though these can beseveral Kelvin, e.g. Xie et al., 2015. You ignore this effect but even consider noise reduction.

Author response

C.f. Comments from Referee 2 - General comment 2.

Reviewer comment 12

L157-159: needs to be better motived, references?

Author response

To provide better motivation for the use of the χ^2 statistic the text given below been added to the manuscript.

Changes in manuscript

> **Changes starting in line 159:**

~~To assess the~~ The quality of a retrieved state $\hat{\mathbf{x}}$ and corresponding simulated ~~observation~~ observations $\hat{\mathbf{y}} = \mathbf{F}(\hat{\mathbf{x}})$ ~~, we define~~ is assessed using the following diagnostic quantity:

$$\chi^2_y = \delta\Delta\mathbf{y}^T\mathbf{S}_e^{-1}\delta\Delta\mathbf{y}, \tag{2.1}$$

~~where $\delta\mathbf{y} = \mathbf{y} - \hat{\mathbf{y}}$~~Here, $\Delta\mathbf{y} = \mathbf{y} - \hat{\mathbf{y}}$ is the difference between the fitted and true observations and $\mathbf{S}_e$ is the covariance matrix describing the measurement errors. The quantity χ^2_y ~~is here used to approximate a χ^2-test for the misfit between the observations $\mathbf{y}$ and the retrieval fit $\hat{\mathbf{y}}$. Although a formally correct~~ corresponds to the sum of squared errors in the fitted observations weighted by the uncertainties in each channel or range bin. It should be noted that the quantity has no meaningful interpretation in terms of χ^2 ~~-test for $\delta\mathbf{y}$ should apply a different covariance matrix~~ -statistic for the errors in the fitted observations since they will neither be independent (c.f. Chapter 12 in Rodgers (2000)) ~~, such tests were found to yield very high values that deviate strongly from the expected chi-square distribution. The χ^2_y value used here provides a less strict test in the sense that it will generally be smaller than if the formally correct covariance matrix was used.~~

~~The amount of information contained in a retrieval can be quantified by computing the degrees of freedom for signal (DFS). Let $\mathbf{K} \subset \mathbb{R}^{m\times n}$ be the Jacobian of the forward model $\mathbf{F}$. Then the DFS of the observations can be computed as the trace of the averaging kernel matrix~~

$$\mathbf{A} = (\mathbf{K}^T\mathbf{S}_e^{-1}\mathbf{K} + \mathbf{S}_a^{-1})^{-1}\mathbf{K}^T\mathbf{S}_e^{-1}\mathbf{K}.$$

nor Gaussian due to the presence of forward model error. The value is therefore used here solely as a heuristic to quantify the goodness of the fit to the true observations.

Reviewer comment 13

L172: I doubt that the model has constant vertical resolution. It will be better close to the surface and worse aloft. This should be mentioned than GEM is introduced.

Author response

As suggested by the reviewer, this is mentioned in the revised manuscript when the GEM test scenes are introduced. Moreover, a sketch will be added to the manuscript which displays the GEM model grid and the grids of all retrieval quantities for the retrievals.

Changes in manuscript

The following text has been added to the description of the model scenes.

Changes starting in line 92:

> The vertical resolution of the model scenes varies between 250 and 500 m below an altitude of 18 km and decreases steadily above that.

In addition to this, the figure shown in Fig. 1.1 has been added in Sect. 2.3.2 of the revised manuscript.

Reviewer comment 14

L 174: for all hydrometeor species of the model? It would be helpful to first introduce all retrieval quantities I was missing a motivation for the paragraph around L195. How do you define the freezing level (and later the troposphere)? How do they vary in both test scenes? The model also likely has supercooled liquid water above the freezing layer how is this treated?

Author response

For the simulated observations, supercooled liquid is treated in just the same way as liquid water below the freezing level. As described in the paragraph around L. 211 (old manuscript version), cloud liquid water in the retrieval is treated as purely absorbing and simulated using a parametrized absorption model. Moreover, it is restricted to temperatures of 230 K and up.

Changes in manuscript

Fig. 1.1 has been added to the manuscript, which displays all retrieval variables as well as the freezing level and the tropopause. Moreover, the following text explaining the definitions of freezing level and tropopause has been added to the manuscript:

> **Changes starting in line 193:**
>
> As additional constraints, the retrieval of frozen hydrometeors is restricted to the region between the freezing ~~layer and the tropopause, whereas the retrieval of liquid~~ level, here defined simply as the 273.15 K-isotherm, and the approximate altitude of the tropopause. The altitude of the tropopause is approximated as the first grid point at which the lapse rate is negative and temperature below 220 K. The retrieval of rain hydrometeors is restricted to below the freezing ~~layer.~~
> ~~To further regularize the retrieval , N_0^* for ice is retrieved at only 10 equally-spaced grid points between freezing layer and the tropopause. Similarly, D_m and~~ level.

Reviewer comment 15

L 198: Vertical resolution of retrieval grid: Why 4 points? The freezing layer must be very different for both cased. Maybe a sketch would be helpful as later on lines 230 the different vertical resolutions for other variables is discussed?

Author response

We have revised the retrieval implementation and now use fixed retrieval grids with a resolution of 2 km for the N_0^* parameters. Reducing the resolution of the retrieval grids for the N_0^* parameters was found to aid the convergence of the retrieval.

Changes in manuscript

The sketch requested by the reviewer has been added to the manuscript (c.f. comment above).

2.2.1 Reviewer comment 16

L281: How do I know that Large Plate is the best performing model? Which parameter,plot, table does show that?

Author response

This sentence has been removed from the revised version of the manuscript.

Reviewer comment 17

L283-L307: Can be shortened significantly

Author response

The proposed change has been adopted in the revised version of the manuscript.

Changes in manuscript

Changes starting in line 304:

The χ^2_y values of the three retrieval configurations, displayed in Panel (a)~~of the figure displays the χ^2_y value (normalized by the dimension of the measurement space) for each profile in the scene. A high value of χ^2_y indicates that the retrieved state is not consistent with the input observations. The χ^2_y value for~~ , give an indication of how well the retrievals are able to fit the observations. For the radar-only retrieval~~is remarkably low throughout most~~ , the values are much smaller than 1 for most parts of the scene~~. This may indicate that the retrieval is insufficiently regularized, allowing it to fit the noise in the observations. The~~ , while for the passive-only and combined retrieval ~~, on the contrary, have a normalized χ^2_y value around 1 over most of the scene. Since the presented values are normalized, the value 1 corresponds to~~ they are around the expected value of ~~the approximated chi-square distribution of χ^2_y. All three retrievals exhibit a region of elevated χ^2_y values near the core of the convective system. In particular the high values of~~ 1. This indicates that the radar-only retrieval overfits the observations, while the passive-only and combined

retrievals ~~indicate that the retrieval was not able to find a good fitto the observations here.~~

~~Panel (b) displays the retrieved column-integrated IWC, the ice water path (IWP). The IWP is given in dB relative to the reference IWP since, owing to the high dynamic range of the reference values,~~ achieve the expected fit. The exception is the ~~curves could otherwise not be distinguished. Although all methods reproduce the reference IWP fairly well, the combined retrieval yields the best overall agreement with~~ region around 3° N, where the cloud is particularly thick and consists of a mix of different hydrometeor types. Here, especially the passive-only retrieval has problems fitting the observations.

In terms of IWP, all methods provide fairly good estimates of the reference values ~~. Exceptions are the regions of high χ^2_y values where the~~ with the combined retrieval consistently yielding the smallest deviations. Larger differences between the methods are observed when comparing the retrieval ~~failed to find a good fit to the observations.~~

~~Panel (c) shows the IWC field retrieved using the passive-only retrieval . Despite a certain resemblance in the overall structure between the retrieved and reference IWCfield, the results do not reproduce~~ results in terms of IWC. While the vertical structure of the cloud ~~very well. It should be noted, however, that the displayed mass-density range extends below the sensitivity limit of the passive-only observations around 10^{-5} kg m^{-3} (c.f. Fig. 4), which explains the smeared-out appearance of the results to some extent.~~

~~The~~ is captured only very roughly by the passive retrieval, it is better resolved by the radar-only ~~results, shown in panel (d), reproduce the vertical structure of the cloud well. Nonetheless, when compared to the reference IWC field, certain discrepancies are visible: The~~ and the combined retrieval. On closer inspection, however, it becomes evident that the radar-only retrieval ~~tends to overestimate the mass density at the bottom~~ deviates systematically from the reference IWC in specific regions of the cloud~~and underestimate the mass concentrations at the top~~ , such as for example the upper part of the cloud ~~.~~

~~The results of the combined retrieval are displayed in panel (e). Although some artifacts are clearly visible in the retrieved IWC field, the retrieval reproduces the vertical structure well. In particular,~~ between 0°N and 2°N. These deviations are corrected in the results from the combined retrieval~~succeeds to correct some of the systematic deviations of the radar-only retrieval : The mass density at cloud base is reduced and increased at cloud top~~, although certain retrieval artifacts are visible.

Reviewer comment 18

L332: There can I see that? Give figure?

Author response

The sentence has been removed from the revised version of the manuscript.

Reviewer comment 19

L325: The two paragraph here give similar information -> streamline

Author response

The proposed change have be adopted in the revised version of the manuscript.

Changes in manuscript

Changes starting in line 320:

~~Similar to the radar-only retrieval, the results of the combined retrieval are located close to the diagonal. But the clusters observed in the radar-only results are to large extent merged in the combined results. Moreover, except for the results obtained with the GemCloudIce particle shape, the two clusters move in closer towards the diagonal. The combined retrieval thus improves the IWC retrieval for the specific hydrometeor species in the scene.~~ is biased for specific hydrometeor classes. In the combined and even the passive-only results, this effect is weaker and the clusters are generally moved towards the diagonal. For graupel, all retrievals perform badly but this is likely due to it being present only in the core of the convective system where the signals from all sensors can be expected to be saturated.
~~Nonetheless, the results for the GemCloudIce particle stand out in the~~ Comparing the results ~~. Even though the systematic deviations observed in~~ for different particle models, a clear dependency is evident in the passive-only and the combined results while the radar-only retrieval ~~are reduced for most particle shapes, for this specific shape they are instead increased. The retrieval error is particularly large for snow, which is strongly underestimated for reference mass concentrations around 10^{-4} kg m^{-3}.~~

Reviewer comment 20

L333-344: I would put this to the appendix

Author response

Following the reviewer's advice, the analysis of the second test scene has been moved to the appendix.

Reviewer comment 21

L444: Here it needs to be made clearer how this goes beyond what GPM is doing.

Author response

To clarify how our work goes beyond what GPM does, a paragraph detailing this has been added to the discussion.

Changes in manuscript

> **Changes starting in line 421:**
>
> The novelty of this work for lies, in part, in the application of ICI's sub-millimeter channels, which sets it apart from the combined retrievals developed for the TRMM and GPM missions. Moreover, the development of a fully consistent variational retrieval in which all retrieval quantities are retrieved simultaneously using the observations from all sensors is also novel. This allows comparison of the combined retrieval to equivalent radar-only and passive-only configurations and therefore a direct analysis of the synergies between the active and passive observations.

Reviewer comment 22

L495: does not say much about the general validity of the assumption. Here you should dig in a bit more. What is the role of a priori and covariances?

Author response

Following the suggestion of the reviewer we will the discussion of the a priori assumptions has been extended.

Changes in manuscript

C.f. the first change listed for Comments from Referee 1 - General comment 1.

Reviewer comment 23

L560: Rethink the bullet structure. 2. Is not an independent result. For each result refer to the part of the manuscript where you can clearly see that. Especially result 3 should be detailed how do ICI channel advance the currently available data?

Author response

The bullet points have been removed in the revised manuscript and replaced by a text which presents the conclusion in a logically coherent way.

Changes in manuscript

> **Changes starting in line 540:**

The main ~~conclusions from the results presented above are: The complementary information in active and passive microwave observations canconstrain two degrees of freedom of the PSD~~ conclusion from this work is that the combination of radar and sub-millimeter radiometer observations can, to some extent, constrain both the size and number concentration of frozen hydrometeors ~~. This reduces systematic retrieval errors for specific hydrometeor species whose properties are not well described by the a priori assumptions. Especially the sub-millimeter channels of the ICI radiometer contribute to the synergistic information content for ice particles.~~

~~In addition to this~~(Fig. 5). The increased sensitivity of the combined retrieval to the microphysical properties of hydrometeors helps to improve the accuracy of IWC retrievals and avoid systematic errors observed in an equivalent radar-only retrieval (Fig. 8, 9). Moreover, the combined retrieval ~~also shows improved profiling capabilities for warm and supercooled liquid clouds~~showed clear sensitivity to particle number concentrations and was able reproduce their vertical structure in regions where the cloud composition is homogeneous (Fig. 10, 11).

The results ~~presented in this study~~ particularly highlight the ~~complementarity of the active and passive observations : Although the radar provides observations at high vertical resolution, they contain insufficient information on the microphysical properties of hydrometeors . The passive-only observations, on the contrary, have low vertical resolution, but are more sensitive to cloud microphysics allowing a potentially more accurate IWP retrieval than what can be obtained from the radar alone. A synergistic retrieval using both types of observations allows combining the high vertical resolution of the radar with the sensitivity to cloud microphysics~~ importance of sub-millimeter observations for combined retrievals of frozen hydrometeors. While observations at currently available microwave frequencies provide information complementary to that from a radar-only for thick clouds with very large particles ($D_m > 800$ μm, IWC $> 10^{-4}$ kg m^{-3}), frequencies above 200 GHz provide additional information on cloud microphysics (Fig. 5) at smaller particles sizes and water content ($D_m > 200$ μm, IWC $> 10^{-5}$ kg m^{-3}).

Reviewer comment 24

Fig. 3: Is it really worth having the slightly different size distribution shapes for frozen and liquid? Isnt there a stronger difference between different frozen hydrometeors

Author response

This is certainly true but in most clouds ice and rain can be distinguished fairly well a priori, which simplifies treating them as different species using different PSD shapes. Distinguishing between different frozen hydrometeors is difficult to do a priori and using multiple species of hydrometeors in the retrieval was found to cause ambiguities which the retrieval is not able to resolve.

Reviewer comment 25

Figures 7 and 8: Im not sure why these are separate figures it seems like allpanels could fit on one page.

Author response

Figures 7 and 8 will be combined into a single figure in the revised manuscript.

Changes in manuscript

C.f. Comments from Referee 1 - Specific comment 9.

Reviewer comment 26

Fig. 4 and also in text: cloud signal say that this is dTB.

Author response

Following the reviewers recommendation, the passive cloud signal will be referred to in the text as ΔT_B and the radar signal as $\mathrm{dBZ}_{\max}$.

Changes in manuscript

Fig. 5 and its caption have been changed as shown in Fig. 2.2. In addition to this, the paragraph describing the results has been changed as follows.

Changes starting in line 272:

~~Figure 4 displays the simulated passive cloud signal , i.e. the brightness temperature difference between clear sky and cloudy sky simulation, as filled contours for a selection of channels of the MWI and ICI sensors. For given values of N_0^* and D_m, the corresponding ice mass density is given by the relation~~

$$m = \frac{\pi\rho}{4^4} N_0^* D_m^4.$$

~~In the figure, the cloud signal is displayed in D_m-mass density space and thus shows how the measured passive cloud signal varies with the horizontal and vertical scaling parameters of the PSD. Overlaid onto~~ The cloud signal in the radiometer observations is the difference between the cloudy- and clear-sky brightness temperatures (ΔT_B). The signal in the active observations is here defined as the maximum of the measured profile of radar reflectivity $\mathrm{dBZ}_{\max}$. Figure 4 displays the contours of ~~the passive cloudsignal are the isolines of the maximum radar reflectivity returned from the cloud~~ΔT_B and $\mathrm{dBZ}_{\max}$ with respect to D_m and the cloud's water content, which

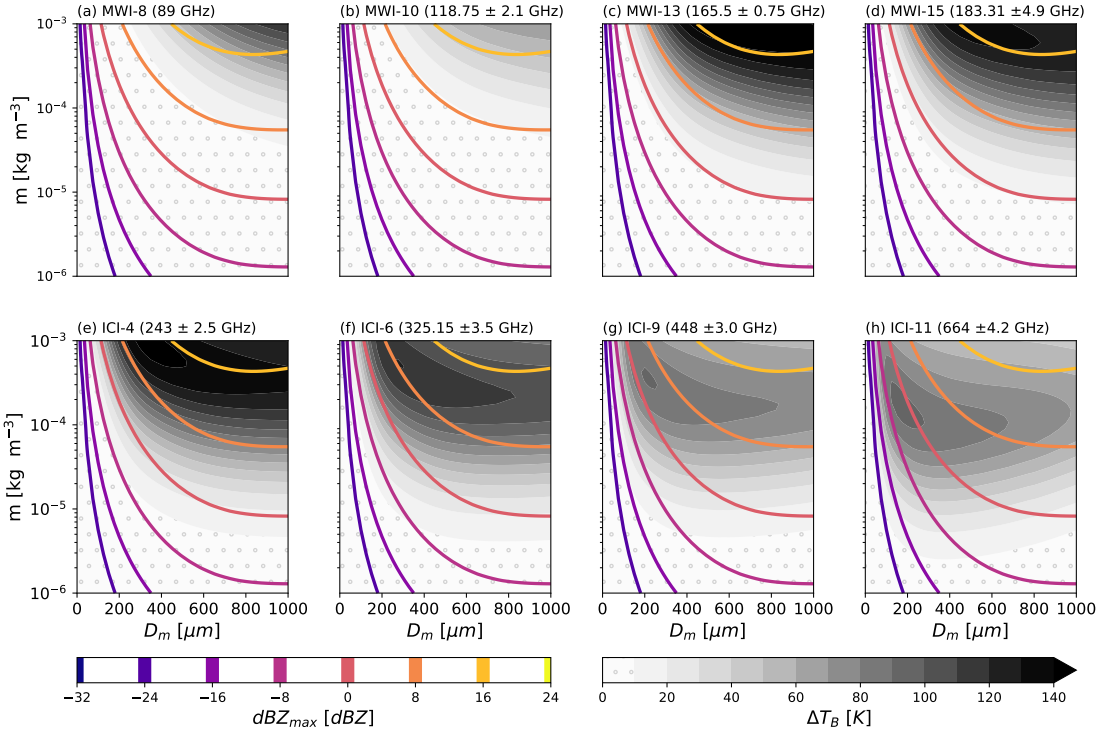

Figure 2.2: Simulated observations of a homogeneous, 5 km thick cloud layer with varying water content m and mass-weighted mean diameter D_m. The panels display the maximum radar reflectivity in dBZ ($\mathrm{dBZ}_{\mathrm{max}}$) overlaid onto the cloud signal (ΔT_B) measured by selected radiometer channels of the MWI (first row) and ICI radiometers (second row).

is proportional to N_0^*:

$$\mathrm{WC} = \frac{\pi \rho}{4^4} N_0^* D_m^4, \tag{2.2}$$

with ρ the density of ice.

Reviewer comment 27

Fig. 5: Can you add freezing layer height?

Author response

Freezing level height has been added to Fig. 5.

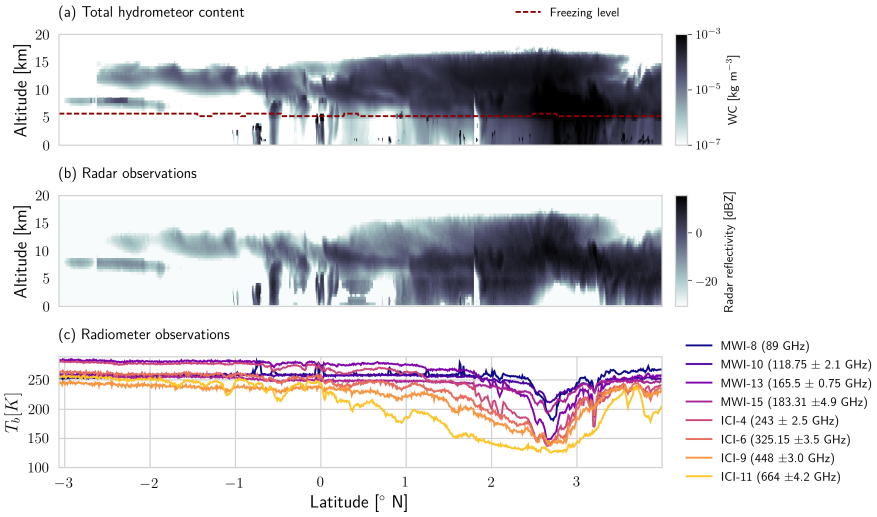

Figure 2.3: Total water content (WC) and simulated observations for the first test scene. Panel (a) displays the total water content in the scene, i.e. the sum of the water content of all hydrometeor species of the GEM model. Panel (b) shows the simulated radar reflectivities. Panel (c) displays the simulated brightness temperatures for a selection of channels of the MWI and ICI radiometers.

Changes in manuscript

The freezing level has been added to Fig. 5, which now looks as shown in Fig. 2.3.

Reviewer comment 28

Fig. 6: It would be nice to see the absolute values of IWP somewhere. Maybe you could add another time series with IWP as the sum of the different components such that the reader can see where the different categories (cloud, graupel, snow and hail) contribute most?

Author response

We will add absolute IWP and its decomposition into different hydrometeor classes to Fig. 6.

Changes in manuscript

Total IWP and its decomposition into contributions from different hydrometeor classes have been added to panel (b) of Fig. 6, which now looks as shown in Fig. 2.4.

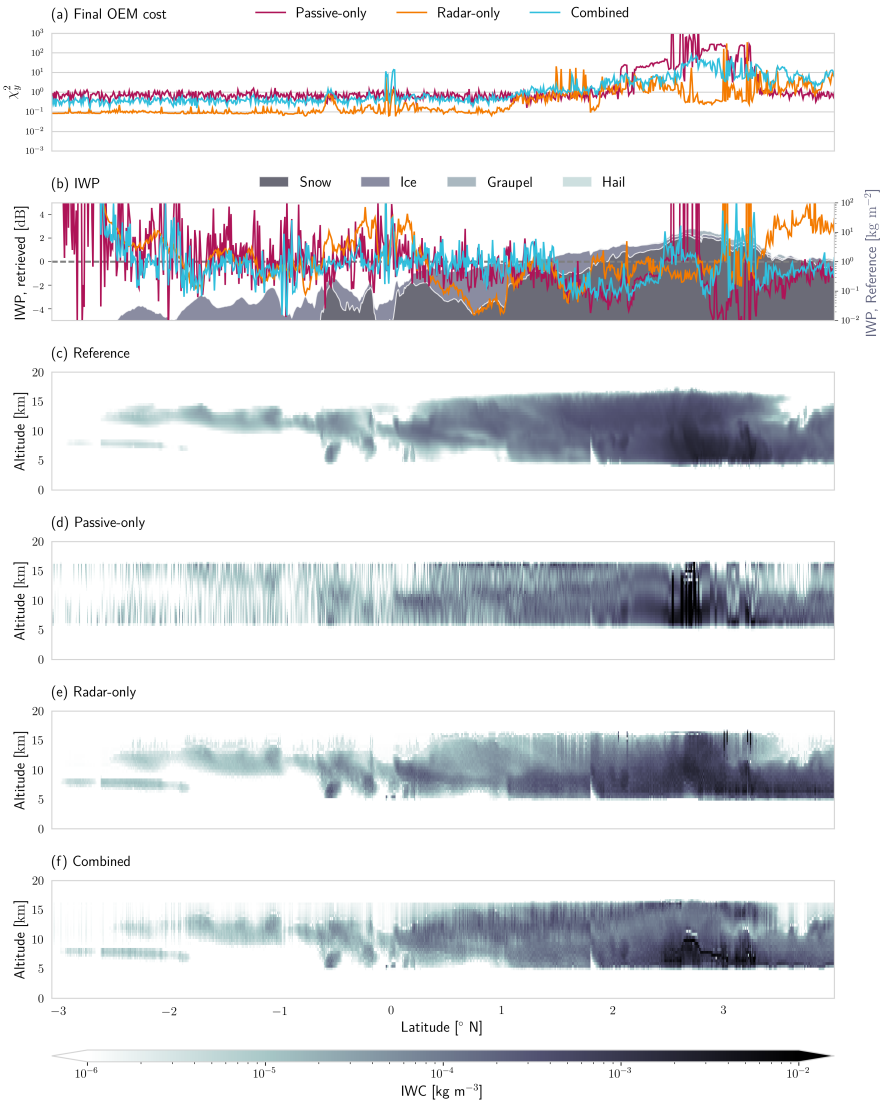

Figure 2.4: Results of the ice hydrometeor retrieval for the first test scene using the Large Plage Aggregate particle shape. Panel (a) displays the value of the χ^2_y diagnostic normalized by the dimension of the measurement space of the corresponding retrieval. Panel (b) displays retrieved IWP in dB relative to the reference IWP. Reference IWP and the contributions from different hydrometeor classes are displayed by the filled areas in the background. Panel (c) shows the reference IWC from the model scene. Panel (d), (e) and (f) display the retrieval results for the passive-only, radar-only and combined retrieval, respectively.

Reviewer comment 29

Fig. 7: I think it is retrieved vs. truth. The word following is not really exact. Why not put 7 and 8 together?

Author response

Fig. 7 and 8 have been merged and the caption has been corrected.

Changes in manuscript

C.f. Comments from Referee 1 - Reviewer comment 9.

Reviewer comment 30

Fig. 9: Could go to the appendix

Author response

Fig. 9 has been moved to the appendix.

Reviewer comment 31

Fig. 10 I only see the caption???

Author response

C.f. Comments from Referee 1 - Reviewer comment 10.

Reviewer comment 32

Tab. 1. Assumed particle model information for each hydrometeor class given by GEM-model. In fact it could be good to combine it

Author response

In order to give a better overview of the particle models that are used in the retrieval Tab. 4 will be extended in the revised version of the manuscript. This, however, would make merging Tab. 1 and 4 slightly confusing so we decided against the reviewers recommendation.

Reviewer comment 33

Tab.3 : I would recommend to add a first column with a spelled out name

Author response

We have added the column to the revised version of the manuscript.

Changes in manuscript

The proposed column has been added to the table which now looks as is shown in Tab. 2.1.

Table 2.1: A priori uncertainties and correlation lengths used in the retrieval.

Retrieval target		Combined / Radar-only		Passive-only	
Name	Retrieved quantity	σ_q	l_q [km]	σ_q	l_q [km]
Ice, N_0^*	$\log_{10}(N_{0,\mathrm{Ice}}^*)$	2	2	2	5
Ice, D_m	Ice $D_{m,\mathrm{Ice}}$	300 μm	2	300 μm	5
Rain, N_0^*	$\log_{10}(\mathrm{Rain}\ N_0^*)$	2	2	2	5
Rain, D_m	$D_{m,\mathrm{Rain}}$	300 μm	2	300 μm	5
Relative humidity (RH)	$\mathrm{arctanh}(\frac{2\cdot\mathrm{RH}}{1.2} - 1.0)$	0.5^*	2^*	0.5	2
Cloud liquid water content (CLWC)	$\log_{10}(\mathrm{CLWC})$	1^*	2^*	1	2

*: Not retrieved in radar-only retrieval

2.3 Grammar, typos and reformulations

The authors would like to thank the reviewer for the additional comments, all of which will be incorporated into the revised manuscript.

3 Comments from referee 3

3.1 Major comments

Reviewer comment 1

The paper is presented as an application for ICI in combination with a Cloudsat like configuration but it is not clear to me what geometry of observations the authors are thinking about. They state "As mentioned above, the same incidence angle as for the passive radiometers is assumed also for the radar. In practice, this could be achieved by remapping the radar observations to the lines of sights of the passive beam". Are they thinking about a scanning W-band radar? or at a off-nadir pointing radar? If the former is true then they should discuss what is a realistic technological solution (and what are the consequences in terms of sensitivity) and the authors should refer to state of the art scanning W-band radar concepts (there is none at the moment!); if the latter is true they should discuss what are the consequences of such a selection (e.g. forground clutter) and they need to convince me that what we could gain from such a configuration compensate from the loss of information introduced by pointing in such a slanted direction. There should be a certain degree of realism in what we are trying to simulate, especially if this was part of an ESA study.

Author response:

The reviewer raises a very relevant point with his comment. To address this, we have changed our simulation setup to simulate perfectly co-located observations at nadir. Realistic modeling of a space-borne viewing geometry (at least in a variational retrieval) is currently not feasible due to the computational complexity. We still deem this sufficient for the scope of the study, i.e. studying the fundamental synergies between active and passive observations. In addition to this, we follow the recommendation made in the second comment and will pitch the application more towards air borne observations.

Changes in manuscript

All calculations have been repeated for the assumed airborne viewing geometry and the manuscript has been adapted accordingly.

Reviewer comment 2

"The beams of all three sensors are modeled as perfectly coincident pencil beams". Again this is quite an assumption. Non uniform beam filling will play a key factor. This is one

of the many simplifications (no polarization, no multiple scattering,1D, ...) that needs to be clearly listed at the beginning of Sect.2.2.1 (some appear only at page 27). For this reason I would actually pitch more towards an airborne configuration where these simplification indeed can be realistically assumed or of a radar with a radiometric mode (where you can actually match footprints). Otherwise the (not massive) gain of having a radar-radiometer combination that you show later on can be completely washed out by the errors introduced to these assumptions. I imagine that you may also have airborne data where to test how realistic your forward model is.

Author response

As mentioned above, we will follow the reviewer's suggestion to pitch the application of the combined retrievals more towards combined retrievals. We also state these limitations more clear in Sect. 2.2.1 and discuss their implications more thoroughly.

Changes in manuscript

> **Changes starting in line 116:**
>
> ~~A number of simplifications are applied for the generation of the synthetic cloud observations: Firstly, the~~ An airborne sensor configuration is simulated to test the retrieval. The beams of all three sensors are ~~modeled as~~ assumed to point at nadir and to be perfectly coincident pencil beams. ~~Secondly, a synthetic observation is generated for each vertical profile from the model scenes by simulating a one-dimensional, plane-parallel atmosphere, the properties of which are taken from the corresponding model profile. It follows from these modeling decisions that the atmosphere is assumed to be homogeneous across the beams of the active and passive sensors and that they all sense the same atmospheric volume. This is certainly not~~ Multiple scattering effects in the radar observations as well as the effects of particle orientation are neglected. Although these assumptions may be justified for an airborne configuration, this will not be the case for space-borne observations ~~and will incur a forward modeling error that is not accounted for in this study. Since the focus of this study are the fundamental synergies between the active and passive observations, quantifying the impact of beam width and inhomogeneity is left for future investigation~~from ICI and MWI. Moreover, the incidence angles of the beams of ICI and MWI will be around 53° at the Earth's surface. This further complicates the radiative transfer modeling since it requires treating a more complex co-location geometry of the nadir-pointing radar and the passive instruments. At off-nadir viewing angles, polarization also needs to be taken into account, the effects of which can be several Kelvin at the typical viewing angles of microwave imagers (Xie et al., 2015).

Reviewer comment 3

Fig 2: these PSDs look very weird to me. Why do they have the plateau at small sizes? y-axis units are obviously wrong unless you are renormalizing by some mass (but it is

not explained).

Author response

The reviewer is of course right, the units on the axis of the plots were indeed wrong and will be corrected in the revised manuscript. Otherwise, the PSDs correspond to the modified-gamma functions that are assumed in the Milbrandt and Yau (2005) microphysics scheme.

Changes in manuscript

The y-units of the figure have been corrected which now looks as shown in Fig. 3.1.

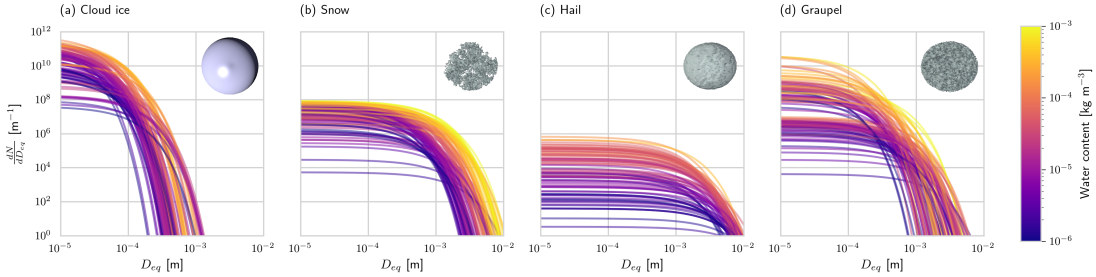

Figure 3.1: Realizations of particle size distributions from the test scenes used in this study. The particle number concentration is plotted with respect to the volume-equivalent diameter D_{eq}. Shown are the PSDs corresponding to 100 randomly chosen grid points with a water content higher than 10^{-6} kg m^{-3}. Line color encodes the corresponding water content. Inlets display visualizations of the particle shape assumed for each hydrometeor species.

Reviewer comment 4

Fig 3: sorry I do not follow what is this (what is the y-axis?), and why this plot is meaningful.

Author response

We have removed this plot from the revised version of the manuscript.

Reviewer comment 5

Eq.6: Clearly with values lower than 230 K it does not make any sense (negative RH, or large than1.1???)

Author response

We would like to thank the author to point out this inconsistency, as there are indeed two mistakes in Eq. 6. The right equation should be

$$\phi(t) = \begin{cases} 0.7, & 270\ \mathrm{K} < t \\ 0.7 + 0.01 \cdot (t - 270), & 220 < t \leq 270\ \mathrm{K}\ . \\ 0.2, & t < 220 \end{cases} \tag{3.1}$$

This will of course be corrected in the updated version of the manuscript.

Changes in manuscript

> **Changes starting in line 202:**
>
> $$\underline{\phi}\underline{\mathrm{RH}}(t) = \begin{cases} 0.7 & ,270\ \mathrm{K} < t \\ 0.7 - 0.01 \cdot (270 - t) & ,220 < t \leq 270\ \mathrm{K}\ . \\ 0.2 & ,t < 220\mathrm{K} \end{cases} \tag{3.2}$$

Reviewer comment 6

Line 210; this means that the vertical resolution changes with the surface temperature, really weird choice.

Author response

We agree with the reviewer that the chosen retrieval grids may not have been optimal. We will change them to fixed-resolution grids for the revised manuscript.

Changes in manuscript

Computations have been repeated with fix-resolution grids and the manuscript has been rewritten accordingly.

Reviewer comment 7

fIG4 : not clear to me why the scattering depression is not increasing at higher frequencies. I would expect that the optical thickness would drastically increase increasing frequency. Is this due to very large asymmetry parameters then? But this is not what I do see in Fig.5 (though Fig4 is of course a very idealized case) If this is the case then results will be very dependent on particle habits (which may introduce additional uncertainties in the retrieval)

Author response

It is correct that extinction increases rapidly with frequency, but the final scattering depression depends also on other factors. One consideration is the background absorption due to gases. A higher gas absorption decreases the effect of scattering, and this effect generally increases with frequency. It is correct that also the asymmetry parameter needs to be considered, which increases with frequency. A higher asymmetry parameter gives a lower depression for a given cloud optical depth, see Fig. 5 of Eriksson et al. (2015).
It can be hard to judge the scattering depression in a figure like Fig. 5, as the clear-sky values differ between the channels. In the version found below, extracted scattering depressions are shown in the second panel. For high-clouds with moderate cloud optical depth, the scattering depression increases monotonously with frequency, while in the most dense cloud region (around lat 2.7) this is not the case for the reasons discussed above.

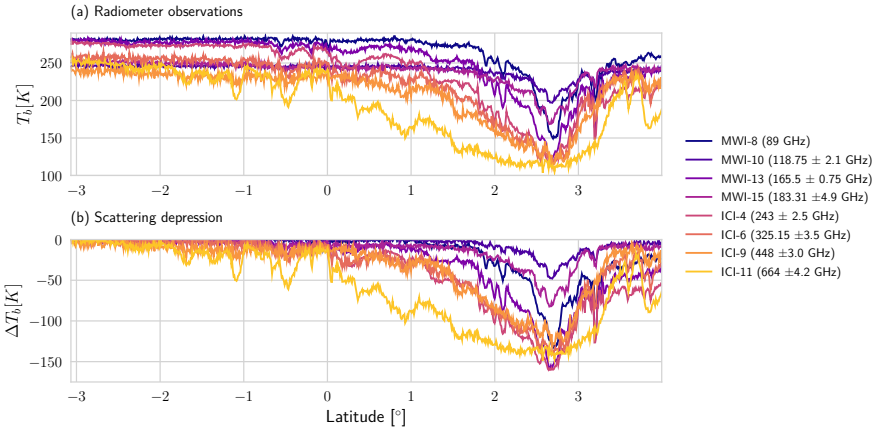

Figure 3.2: Simulated brightness temperatures (Panel (a)) and cloud signal depressions computed for selected channels of the MWI and ICI radiometers for the first test scene.

Reviewer comment 8

8) Line 275: not clear what you mean, in Tab.4 there are 6.

Author response

What was meant here is that different ice shapes are tested for the single frozen hydrometeor species which is used in the retrieval. Tab. 4 lists the different shape models that were investigated.
Since the section describing the selection of particle models will be rewritten, this sentence will be reformulated to make it clearer.

Changes in manuscript

C.f. Comments from Referee 2 - General comment 1

Reviewer comment 9

9) extends below the sensitivity limit of the passive-only observations around 10-5 kg m-3 : very sloppy sentence. Passive microwave radiometer are sensitive to integrated contents!

Author response

As response to a comment from another reviewer the corresponding paragraph will be rewritten and this sentence will be removed.

Changes in manuscript

> **Changes starting in line 310:**
>
> ~~It should be noted, however, that the displayed mass-density range extends below the sensitivity limit of the passive-only observations around 10^{-5} kg m^{-3} (c.f. Fig. 4), which explains the smeared-out appearance of the results to some extent.~~

Reviewer comment 10

Fig 6d: this retrieval looks really weird. Where are all the stripes coming from? Certainly this does not look like acloud, or? What kind of constraint have you imposed on the cloud top?

Author response

It is true that the passive only retrieval does not perform well in terms of the vertical structure of IWC. The reason for this is that the passive observations alone do not provide much information on the vertical distribution of ice. To correct for this, further regularization would be necessary which is not applied here in order to keep the comparison to the other retrieval methods fair. All of this is discussed in the discussion section of the manuscript.

Reviewer comment 11

"In general, the radar-only results exhibit only very weak dependency on the particle model, making the results for different particle shapes virtually indistinguishable." Again another dangerous sentence. We know (unfortunately) that this is not true (otherwise our ice problems would be sorted). Here my guess is that you have not properly explored the backscattering variability (particularly looking at the different degree of riming). It is notclear to me whether there is enough variability in your ARTS database, I guess

you are more focused at ice particles (including aggregates) but you are not considering really rimed particles. Regions where graupel is present should be avoided from the discussion of the radar-only retrieval for the simple reason that in those regions attenuation correction and multiple scattering effects make the problem very tricky. I guess that the radiometer as well is in serious trouble when entering those areas. Again, I would not start tackling regions the observation system is not tailored for.

Author response

As mentioned above, we will revise the particle habits used in the retrieval, but we expect that particle shape will continue to have a smaller impact on our radar-only retrieval. What the results shown in scatter plot in Fig. 7 and 8 indicate is that the uncertainty which can be attributed to the particle size distribution (PSD) is larger than that introduced by the assumed particle shape. However, it is difficult in general to draw a clear line between particle shape and PSD. This is especially true if particle size is described by Dmax, and the PSD is defined accordingly. In this case, IWC of a given PSD will depend on the particle's effective density, and e.g. degree of riming becomes critical. Accordingly, to what extent retrieval errors are due to shape or PSD, depend partly on definitions.
The ARTS single scattering database does include several types of rimed particles. Two of them are the GEM Graupel and GEM Hail models which are used in the simulation of the synthetic observations. For the retrieval, however, it is true that we did not include rimed particles in the tested particle models but this will be changed for the revised version of the manuscript.
Both the forward simulations and the retrieval handle attenuation consistently. We therefore think it is worth considering even regions where graupel is present as this allows us to assess the uncertainties caused by not having a realistic representation of rimed particles in the retrieval.
It is certainly correct that for space-borne observations multiple scattering needs to be considered and this will add complexity to the retrieval. Here, however, we can avoid this extra complexity as we use simulated observations which do not include multiple scattering.

Reviewer comment 12

Fig.10 is missing!!!

Author response

Fig. 10 was unfortunately missing from the manuscript. The figure will be included in the appendix of the revised version together with the analysis of the second test scene.

Changes in manuscript

C.f. Comments from Referee 1 - Specific comment 10.

Reviewer comment 13

Since the calculation of the AVK involves the forward model Jacobian, this effectmust be related to the non-linearity of the forward model well I would avoid such veryspeculative statements.

Author response

Following the suggestion of the reviewer, the sentence will be removed from the manuscript.

Changes in manuscript

The sentence has been removed from the manuscript.

Reviewer comment 14

You need to be very careful how you present the results in Fig. 14. The conclusions that I can draw is the following: a CloudSat like radar is pro-viding much more information than the ICI+MWI radiometers when characterizing ice particles (really the radiometer is providing some additional water vapour information). As a result we should invest in the former and not the latter. While I may agree with the previous statement and strongly support a CloudSat-like radar on an operational mission my feeling is that you are pitching your radiometer system at the wrong kind of scenes (I already see an improvement going from the first to the second scene). I would have selected completely different scenes (including high latitude clouds with mixed phase). It is to me an overkill to try to retrieve D_M of rain for these scenes from your PMW radiometer suite of sensor. If you have any skill in warm rain you should properly prove it

Author response

Our interest in this study is neither arguing for one nor the other observation system. The question that we want to address is whether combined observations have extra value compared to separate observations. Such combined observations could be achieved by performing joint flights with the aircraft carrying the ISMAR sub-millimeter radiometer and another one carrying a radar, by flying a cloud radar in constellation to Metop-SG, or by adding a sub-millimeter radiometer to the platform carrying some future cloud radar. We consider it out of the scope of this study to judge the cost effectiveness of either of these solutions.
As the referee clearly favours radars, we would like to balance this by mentioning that passive instruments have an additional strength in their much higher areal coverage. The swath of ICI and MWI is about three orders of magnitude broader than that of CloudSat and EarthCARE.
Although a cloud radar certainly provides more information on frozen hydrometeors than ICI, our results clearly show that also radar observations alone are insufficient to accurately determine the microphysical properties of ice hydrometeors (Fig. 4, 7).

The passive adds information on the microphysics of the clouds to the radar (note the significant increase in information content on N_0^* in Fig. 14) which helps to reduce retrieval uncertainties (Fig. 11). Although it is not clear whether these improvements carry over to space-borne observations, our results clearly show this as a synergy between the passive and active observations (esp. Fig. 4, 11, 14).
The cloud scenes used in the manuscript were selected with the aim of providing a representative sampling of the type of clouds present in the two model scenes that were available for the study. We did not want to cherry pick scenes were the retrieval works well to provide a more realistic assessment of the retrieval.
Rain must be handled in the retrieval due to its effect on the passive radiances. However, we never claim that we have any skill in retrieving warm rain and so we do not agree that we are required to prove to have it.

Reviewer comment 15

LWP and Fig.16. I have a serious problem here. The cloud I see on the right is a liquid cloud. So how it is possible that your radiometer is doing sobadly in the LWP retrieval and why the combined is so much better? I guess this must go back to understanding surface emissivity and integrated water vapour (maybe somecomments there should be made to explain what kind of surface/IWP we are dealingwith). You have not included radar path integrated attenuation in your retrieval (like istypically done in radar retrievals) but this could of course help in this case.

Author response

The cloud in the right of the scene is a mixed-phase cloud. There are several explanations for why the retrieval does not work well here: First of all, our observations setup does not make use of the channels around 23 GHz, which are typically used for retrieving LWP. And also here the performance of the passive-only retrieval suffers from the lack of a priori information on the vertical position of the cloud. Since liquid water at higher altitudes has a stronger impact on the observations, the retrieval puts too little cloud water too high in the atmosphere because of its inability to locate it properly. This is discussed in Sect. 4.2.3 of the manuscript.

Reviewer comment 16

I do not think that for OE to work The forward model must be linear as stated at line 544.

Author response

The OEM can of course be applied to non-linear problems but a complication that arises is that it can get stuck in secondary minima. The sentence will be corrected in the revised version of the manuscript.

Changes in manuscript

The section discussing limitations of the OEM has been removed from the manuscript since it was deemed to be of minor importance.

Reviewer comment 17

17)Sect.4 and 5: a lot of waffling here (e.g. the three bullet conclusion, you need to be much more quantitative and linked to what you have proved; the three statements are something I could have formulated on my own without making any simulation). Again the conclusions must be related to the cloud regime you are considering (and cannot be valid for all!)

Author response

One of the main advantages that we see in the combined retrieval is that it actually works for a wide range of different cloud regimes. If the cloud regime was known a priori, good results can probably be achieved using only a radar and suitable a priori assumptions. In general, however, this is not the case, which leads to the uncertainties that we currently have in the observational record for IWP and IWC.
For the revised manuscript, we will rewrite the conclusion and parts of the discussion to make it more concise and the point mentioned above more clear.

Changes in manuscript

C.f. Comments from Referee 2 - Specific comment 23

3.2 Minor comments

Reviewer comment 1

I would avoid the use of ice mass density and use ice water content

Author response

The proposed changes will be adopted in the revised version of the manuscript.

Changes in manuscript

Water content is now used consistently across the manuscript to refer to the mass density of hydrometeors.

Reviewer comment 2

Table 2: it would be good to see footprints as well

Author response

Since in the revised manuscript an airborne viewing geometry will be considered the footprint sizes of MWI and ICI are not relevant anymore.

Reviewer comment 3

Line 130: dBZ are the wrong units for a std of a reflectivity!

Author response

We are unsure what the reviewer is referring to here since quantifying uncertainty in the radar observations in dBZ seems to fairly common. This is for example how it is handled in the DARDAR cloud (Delanoë and Hogan, 2010) product as well as in the study by Jiang et al. (2019).

Reviewer comment 4

Line 180: The remaining shape of each PSD is described by the shape parameters alpha and beta, not to be confused with the parameters of themass-size relationship shown in Tab. 1.; very confusing. Why are you using the same letters????

Author response

We used the same letters to be consistent with the definition and used in Delanoë et al. (2014) and Cazenave et al. (2019). However, since the explicit values of the α and β parameters are probably of little interest for the average reader, we will simply refer to Cazenave et al. (2019) and not name the parameters explicitly.

Changes in manuscript

Changes starting in line 182:

~~The retrieval computes vertical profiles of the two scaling parameters D_m and N_0^* for each of the two hydrometeor species. The remaining shape of each PSD is described by the shape parameters α and β, not to be confused with the parameters of the mass-size relationship shown in Tab. 1. The shape parameters are set to fixed, species-specific values. This principle is illustrated in Fig. **??**. The plot displays the a-priori-assumed shapes of the particle size distribution of frozen and liquid hydrometeors. The retrieved horizontal and vertical scaling parameters , D_m and N_0^*, are used as units for the axes of the plot so that~~ which scales the particle concentration, are the two retrieved degrees of freedom of the PSD. The other two parameters describe the shape of the ~~PSD becomes independent of the retrieved mass density and number concentration. For frozen hydrometeors, the values of the shape parameters α and β are chosen identical to~~ normalized PSD. The same shape

parameters as in version 3 of the DARDAR-CLOUD product ~~(Cazenave et al., 2019) . For liquid hydrometeors, the shape parameters are chosen so that they are equivalent to~~ (Cazenave et al., 2019) are chosen for frozen hydrometeors. For rain, they are chosen to match the shape used ~~by~~ in the GEM model for rain drops. ~~All calculations involving particles size distributions use the volume-equivalent diameter D_{eq} as size variable.~~

Reviewer comment 5

Line 193: wrong units

Author response

This will be corrected in the revised version of the manuscript.

Changes in manuscript

Changes starting in line 188:

For ~~liquid hydrometeors~~rain, a fixed value for N_0^* of ~~10^6 m^4~~ 10^6 m^{-4} is assumed and the a priori profile for D_m is determined similarly as for frozen hydrometeors.

Reviewer comment 6

Line 199: English

Author response

This will be corrected in the revised version of the manuscript.

Changes in manuscript

Changes starting in line 196:

~~To further regularize the retrieval , N_0^* for ice is retrieved at only 10 equally-spaced grid points between freezing layer and the tropopause. Similarly, D_m and~~ level. The retrieval of the N_0^* ~~for rain are retrieved at 10 respectively 4 points between surface and freezing layer~~parameters is further regularized by retrieving them at reduced vertical resolution of 2 km

Author response 7

Line 35 page 2 (not really limited,this is a wide range!!)

Author response

The corresponding sentence will be reformulated in the revised manuscript.

Changes in manuscript

> **Changes starting in line 41:**
>
> ~~The observing frequencies that are currently available for measuring ice from space are limited to the microwave, infrared and optical domain. Infrared and optical sensors provide sensitivity to small ice particles but cannot sense significant parts of the ice mass of thicker clouds due to saturation of~~ The currently most accurate information on the global distribution of ice water content (IWC) is provided by the CloudSat radar. A main strength of these observations is their vertical resolution, in the ~~signal. Microwave observations , in contrast, provide sensitivity throughout the whole atmospheric column but are insensitive to small ice particles. Although radars and lidars generally provide greater sensitivity than their passive counterparts, they are ultimately limited by the same principles~~order of 500 m.

Reviewer comment 8

Line 54 page 2. maybe it is worth mentioning all the heritage coming from radar-radiometer retrievals with W-band (Ka and Ku-band) radars with PMW radiometers.

Author response

Following the suggestion of the reviewer, a paragraph that mentions previous work on synergistic retrievals using radar and passive radiometers at lower microwave frequencies will be added to the introduction.

Changes in manuscript

C.f. Comments from Referee 2 - Minor comment 5

Reviewer comment 9

Line 229: troposphere is too generic

Author response

The use of the word *troposphere* and should have been *tropopause*. This will be corrected in the revised version of the manuscript.

Changes in manuscript

The section has been rewritten

> **Changes starting in line 246:**
>
> Fig. 4 provides an overview of the bulk mass backscattering efficiencies and mass attenuation coefficients of the selected particles computed for three different values of the N_0^* ~~is retrieved at three equally spaced grid points between freezing layer and troposphere, while D_m is retrieved at five. For liquid hydormeteors, the retrieval grids for N_0^* and D_m are reduced to two equally spaced points between surface and freezing layer. Relative humidity is retrieved at a vertical resolution of 2 km~~parameter of the PSD. Mass backscattering efficiency and attenuation coefficient are defined as the ratio of the corresponding cross-section σ and the bulk water content:

Author response 11

250: rho is not defined

Reviewer comment

ρ will be defined in the revised version of the manuscript.

Changes in manuscript

> **Changes starting in line 276:**
>
> Figure 2.2 displays the contours of ~~the passive cloudsignal are the isolines of the maximum radar reflectivity returned from the cloud~~ΔT_B and $\mathrm{dBZ}_{\mathrm{max}}$ with respect to D_m and the cloud's water content, which is proportional to N_0^*:
>
> $$\mathrm{WC} = \frac{\pi\rho}{4^4} N_0^* D_m^4, \tag{3.3}$$
>
> with ρ the density of ice.

Reviewer comment 12

Line 4: 272.5????

Author response

This mistake will be corrected in the revised version of the manuscript.

Changes in manuscript

> **Changes starting in line 186:**
>
> $$N_0^* = \exp\left(-0.076586 \cdot (T - 272.5273.15) + 17.948\right), \tag{3.4}$$

Reviewer comment 10

Fig 4 caption: you need to include how thick is the layer.

Author response

This will be included in the revised version of the manuscript.

Change in manuscript

This has been changed in the revised manuscript and the figure and caption now looks as is shown in Fig. 2.2.

4 Marked-up differences

Synergistic radar and radiometer retrievals of ice hydrometeors

Simon Pfreundschuh[1], Patrick Eriksson[1], Stefan A. Buehler[2], Manfred Brath[2], David Duncan[1,4], Richard Larsson[3], and Robin Ekelund[1]

[1]Department of Space, Earth and Environment, Chalmers University of Technology, 41296 Gothenburg, Sweden
[2]Meteorologisches Institut, Fachbereich Geowissenschaften, Centrum für Erdsystem und Nachhaltigkeitsforschung (CEN), Universität Hamburg, Bundesstraße 55, 20146 Hamburg, Germany
[3]Max Planck Institute for Solar System Research, Justus-von-Liebig-Weg 3, 37077 Göttingen, Germany
[4]Now at European Centre for Medium-Range Weather Forecasts, Shinfield Park, Reading RG2 9AX, United Kingdom

Correspondence: Simon Pfreundschuh (simon.pfreundschuh@chalmers.se)

Abstract. ~~The upcoming~~ Remote sensing observations at sub-millimeter wavelengths provide higher sensitivity to small hydrometeors and low water content than observations at millimeter wavelengths, which are traditionally used to observe clouds and precipitation. Hence they are employed increasingly in field campaigns to study cloud microphysics and will be integrated into the global meteorological observing system to measure the global distribution of ice in the atmosphere. A milestone in this development is the launch of the Ice Cloud Imager (ICI) radiometer ~~, to be launched~~ on board the second generation of European operational meteorological satellites (Metop-SG), ~~will be the first microwave imager to provide~~ which will make sub-millimeter observations of ~~the atmosphere. The Microwave Imager (MWI) radiometer will be flown on the same satellites and complement the ICI sensor with observations at traditional millimeter wavelengths. The addition of these two new passive microwave sensors to the global system of earth observation satellites opens up opportunities for synergistic satellite missions aiming to maximize the scientific return of the Metop-SG program. This study analyzes~~ ice clouds available operationally. Observations at these novel wavelengths provide valuable information not only on their own but also in combination with complementary observations at other wavelengths. This study investigates the potential benefits of combining ~~observations of the MWI and ICI radiometers with a 94-GHz~~ passive sub-millimeter radiometer observations with a hypothetical W-band cloud radar for the retrieval of frozen hydrometeors. ~~Starting from a simplified numerical experiment, it is shown that the complementary information content in the radar and radiometer observations can help to better constrain the particle size distribution of ice particles in the atmosphere. The feasibility of the combined retrieval is demonstrated by applying a one-dimensional, variational cloud-retrieval algorithm~~ Using a simplified cloud-model, the information content of the combined observations is investigated and the capacity of the observations to constrain the microphysical properties of ice hydrometeors is established. A synergistic retrieval algorithm for airborne observations is proposed and applied to simulated observations from a ~~high-resolution atmospheric model. Comparison of the results with passive- and radar-only versions of the retrieval algorithm confirms that synergies between the active and passive observations allow an improved retrieval of microphysical properties of frozen hydrometeors. The effect~~ cloud-resolving model. Results from the synergistic retrieval are compared to equivalent radar- and passive-only implementations in order to assess the benefits of the synergistic sensor configurations. The impact of the assumed ice particle shape on the ~~results is analyzed and found to be critical for obtaining~~

good retrieval performance. In addition to thisretrieval results is assessed for all retrieval implementations. Although they show greater sensitivity to the assumed particle shape, the synergistic retrieval shows observations can better constrain the microphysics of the cloud, which decreases uncertainties in retrieved ice water content and improves the retrieval of particle number concentrations. Our results also indicate improved sensitivity to liquid water in both warm and supercooled cloudscloud water content for the synergistic configuration compared to a passive-only setup. The results of this study clearly demonstrate the potential of the combined observations to constrain the microphysical properties of ice hydrometeors, which can help to reduce errors in retrieved profiles of mass- and number densitiessynergistic sensor configuration to improve retrievals of frozen hydrometeors. The developed synergistic retrieval algorithm can be applied with only minor modifications to suitable airborne observations from sub-millimeter radiometers such as the International Sub-Millimetre Airborne Radiometer.

1 Introduction

Ice clouds hydrometeors play an important role in many weather- and climate-related processes in the atmosphere. They interact with incoming and outgoing radiation and thus for both weather and climate. They influence the Earth's energy budget . Moreover, as through their interaction with incoming and outgoing radiation, constitute a part of the global hydrological cycle and due to their relation are coupled to the dynamics of the atmosphere (Bony et al., 2015)in multiple ways (Bony et al., 2015) . Because of this, observations of ice clouds provide important information to constrain the are required for understanding the role of clouds in a changing climate (Boucher et al., 2013), to provide information on the dynamical state of the atmosphere in numerical weather prediction (NWP) models (Geer et al., 2017) as well as to validate predictions from and to validate climate models (Waliser et al., 2009).

Despite the importanceof observations of ice clouds for climate and weather predictionDespite this importance, today's global observing system cannot provide accurate information on the global distribution of ice in the atmosphere (Eliasson et al., 2011; Duncan and Eriksson, 2018). The main difficulty in sensing atmospheric ice from space is A major difficulty of measuring atmospheric ice using remote sensing lies in the large variability of sizesand concentrations , concentrations and shapes in which ice particles occur in the atmosphere. The wide spectrum of ice crystal sizes, which ranges from micro- to millimeter scales, can only be partially resolved by currently available space-borne sensors.

The sensitivity of a remote sensing system to ice particles of a given size is determined mainly by its observing frequencies. The scattering of radiation by ice particlesis strongest for sizes roughly equal to the wavelength, λ, of the radiation. For particleswith sizes much smaller than λ, the sensitivity decreases rapidly, making them practically invisible to the sensor. Although the strength of the interaction between particles and radiation decreases as the wavelength becomes much larger than the particle size, it remains strong enough for the cloud signal to saturate in the presence of thicker clouds, leading to loss of sensitivity further down the line of sight. Current operational observation systems used to study clouds can be divided into two groups by virtue of their observing frequency and their corresponding capabilities and limitations. Microwave sensors employ wavelengths ranging down to about 1 mm. Compared to the sizes of ice particles, the wavelengths are very long and therefore sensitive only to very large ice particles. At the same time, they provide the advantage of penetrating even thick clouds. Optical

and infrared sensors use radiation with wavelengths from around 15 µm down to several hundred nano meters. Although these relatively short wavelengths make them sensitive to small ice particles, their signal saturates for thick clouds, which makes them insensitive to the ice mass further down the line of sight. Although radars and lidars allow detection of lower ice water contents than their passive counterparts, they are ultimately limited by the same principles.

~~The observing frequencies that are currently available for measuring ice from space are limited to the microwave, infrared and optical domain. Infrared and optical sensors provide sensitivity to small ice particles but cannot sense significant parts of the ice mass of thicker clouds due to saturation of~~ The currently most accurate information on the global distribution of ice water content (IWC) is provided by the CloudSat radar. A main strength of these observations is their vertical resolution, in the ~~signal. Microwave observations , in contrast, provide sensitivity throughout the whole atmospheric column but are insensitive to small ice particles. Although radars and lidars generally provide greater sensitivity than their passive counterparts, they are ultimately limited by the same principles~~order of 500 m. However, the radar lacks scanning capability and the swath width is just 1.5 km wide, to be contrasted with the swath width of passive imagers which is on the order of 1000 km. A potentially less obvious limitation is that CloudSat performs a single-frequency measurement. Since this limits the information per range bin to one degree of freedom, a priori information is required as additional constraint on microphysical properties such as particle size, concentration and shape.

A way to overcome the limitations of single-frequency radars is to combine them with observations from passive sensors, which typically provide measurements at multiple frequencies and a significantly wider swath. Two types of synergies can be distinguished for such an observation scenario: A local synergy, which consists of using the co-located radar and radiometer observations to obtain more accurate hydrometeor retrievals, and the non-local synergy, which uses the vertically resolved radar observations to support passive-only retrievals across the wide swath of the passive sensor. Prominent examples of satellite missions that exploit both of these synergies are the the Tropical Rainfall Measuring Mission (TRMM, Kummerow et al. (1998); Grecu et al) and the Global Precipitation Measurement (GPM, Hou et al. (2014); Grecu et al. (2016); Kummerow et al. (2015)) mission. Since the principal target of these missions are retrievals of liquid hydrometeors, they make use of sensors at comparably low microwave frequencies and hence provide only limited sensitivity to frozen hydrometeors.

~~To narrow the size-sensitivity gap between the infrared and traditional microwave sensors, the upcoming~~ With the upcoming launch of the Ice Cloud Imager (ICI) a new passive microwave sensor will become operational, which is dedicated to observing ice hydrometeors from space. ICI will extend the ~~microwave frequencies available for studying clouds~~ range of currently available microwave frequencies with channels at 243, 325, 448 and 664 GHz ~~(Eriksson et al., 2019). This extension of~~ (Eriksson et al., 2020). This will narrow the size-sensitivity gap between the infrared and traditional microwave sensors by extending the smallest currently available microwave wavelength from 1.6 mm at 183 GHz down to the sub-millimeter domain (0.45 mm at 664 GHz) ~~will~~ and significantly improve the size-sensitivity of space-borne microwave observations of clouds.

Together with ICI, ~~also~~ the newly developed Microwave Imager (MWI) will be flown on the satellites of the Metop-SG program. MWI will complement ICI's observations with measurements at traditional millimeter wavelengths as well as a

spectral band around the 118 GHz oxygen line. The observations of MWI, which cover the frequency range from 19 GHz up to 183 GHz, will provide additional sensitivity to liquid and frozen precipitation as well as water vapor.

The advent of space-borne With ICI sub-millimeter radiometry of clouds brings with it great potential for the study will reach operational status. This has of course sparked interest in its potential for studying ice in the atmosphere. The information content and retrieval performance from of radiometer observations alone has been studied in detail for column-integrated ice mass (Jiménez et al., 2007; Wang et al., 2017; Brath et al., 2018) water content (Jiménez et al., 2007; Wang et al., 2017; Brath et al., 2018; Eriks as well as for the vertical distribution of ice in the atmosphere (Birman et al., 2017; Grützun et al., 2018; Aires et al., 2019). Also the concept of combining Although not directly related to ICI, the combination of millimeter and sub-millimeter radiometer observations with active observations from a cloud radar has been investigated (Evans et al., 2005; Jiang et al., 2019) by Evans et al. (2005) and Jiang et al. (2019).

This work applies the concept of synergistic radar and sub-millimeter radiometer retrievals to the upcoming ICI and MWIsensors by combining them with a conceptual In this study, we are interested in the local synergies of co-located MWI/ICI-type radiometer observations combined with observations from a W-band cloud radar. It extends previous studies on this observational technique by providing an in-depth analysis of the fundamental synergies between the active and passive observations that help to improve the retrieval ice in the atmosphere. radar. In particular, this study investigates to which extent the combined active and passive observations can constrain the microphysics of ice particles in the atmosphere. Starting from a simplified numerical experiment, the complementarity of the information content of the active and passive observations is demonstrated. In addition to this, simulated results from a synergistic, variational cloud-retrieval algorithm are presented. The algorithm is applied to synthetic observations of cloud we aim to answer the question what additional information can be gained from combined observations compared to observations from the radar or MWI and ICI alone. For this, a combined, variational retrieval is developed and applied to simulated observations of scenes from a high-resolution atmospheric model and used to further explore the synergies between the active and passive observations. cloud-resolving model (CRM). An airborne viewing geometry is assumed for the simulations with all sensors pointing at nadir and close-to overlapping antenna beams. Our work extends the previous work by Evans et al. (2005) and Jiang et al. (2019) by comparing the performance of the combined retrieval to that of equivalent radar- and passive-only retrievals, which allows us to quantify the value added by the synergistic observations. In addition to that, the impact of the assumed scattering properties of ice hydrometeors on the retrieval is investigated.

The presented research has been conducted as part of a larger study funded by

This study consists of two principal parts: In the first part, simulated observations from a simplified cloud model are used to perform a preliminary study of the European Space Agency, which evaluated the concept of a future radar mission to fly in constellation with ICI on board the satellites of the Metop-SG program. Inspired by the concept of the Global Precipitation Measurement (GPM, Hou et al. (2014)) mission, the approach of this tentative mission is to perform vertically-resolved, high-accuracy retrievals of hydrometeors from the co-located active and passive observations at the swath center of the passive imager. The results of combined retrieval could then be used to constrain complementary information content of radar and passive radiometer observations. In the second part, the developed synergistic retrieval algorithm is applied to simulated

observations from a CRM to investigate the performance benefits of the combined observations compared to radar- and passive-only ~~profile retrievals with the aim of extending the profiling capabilities of the radar to the wide swath of the passive imager.~~

configurations. Following this introduction, Section 2 introduces the test data, sensor configuration and the developed retrieval algorithm on which the study is based. This is followed by the experimental results on the information content of the combined observations and the ~~retrieval results of the joint retrieval on selected test scenes~~ simulated retrieval results in Section 3. The article closes with a discussion of the results in Section 4 and conclusions in Section 5.

2 Methods and data

~~The synergistic retrieval is tested using simulated observations of cloud scenes from a high-resolution atmospheric circulation model. This section presents the selected reference cloud scenes, sensor configuration and basic modeling assumptions used in the radiative transfer simulations. In addition to this, the theoretical formulation of the combined cloud-retrieval algorithm is introduced.~~

2.1 Reference cloud scenes

The cloud scenes ~~that will be~~ which are used for the testing of the retrieval were produced by Environment and Climate Change Canada using a high-resolution NWP configuration of the Global Environmental Multiscale (GEM) Model (Côté et al. (1998)). ~~For this study, we restrict ourselves to two designated, two-dimensional test scenes, which are displayed in Fig. 1. The test scenes have~~ Two test scenes with a horizontal resolution of 1 km and ~~both extend over~~ an extent of 800 km were selected. The vertical resolution of the model scenes varies between 250 and 500 m below an altitude of 18 km and decreases steadily above that. The scenes, displayed in Fig. 1, were chosen with the aim of covering a large range of cloud structures and compositions so as to ensure a realistic assessment of the retrieval. The first test scene, shown in panel (a), is located in the tropical Pacific and contains a ~~convective storm~~ mesoscale convective system in the ~~right~~ northern half of the scene and its anvil ~~that~~ which extends into the ~~left halfof the scene~~southern half. The second scene, shown in panel (b), is located in the North Atlantic and contains an ice cloud in the ~~first quarter~~ southern part and a low-level, mixed-phase cloud in the ~~remainder of the scene~~northern part.

The GEM model uses a two-moment scheme with six types of hydrometeors to represent clouds and precipitation (Milbrandt and Yau, 2005): Two classes of liquid hydrometeors (rain and liquid cloud) and four of frozen hydrometeors (cloud ice, snow, hail and graupel). The particle size distribution (PSD) of each hydrometeor ~~type is parametrized by its particle number concentration and mass density. The full particle size distribution can be prognosed from the two moments using a species-dependent parametrization and mass-size relationship. The~~ class is described by a three-parameter gamma distribution. The prognostic parameters of the model are the slope and intercept parameters of the ~~mass-size relationship are given in Tab. 4. As shown in the table,~~ PSD, which are derived from the predicted mixing ratios and number concentrations. The third

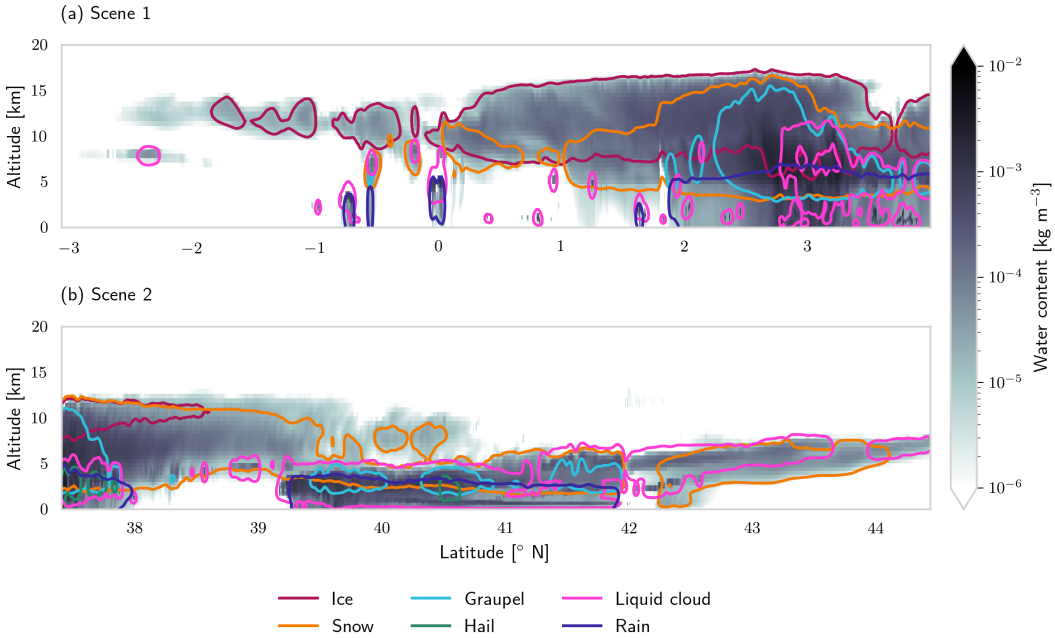

Figure 1. The distribution of total ~~hydrometeor mass~~ water content including all hydrometeor classes in the two cloud scenes used to test the retrieval. Colored lines show the ~~$m = 10^{-5}$ kg m^{-3}~~ 10^{-5} kg m^{-3} contour ~~for different~~ of the water content of each hydrometeor ~~species~~class.

parameter, which defines the shape of the ~~masses of all ice particles in the model are assumed to scale with a power of three, which leads to high densities for large particles.~~

~~Particle model names, IDs and parameters α, β of the mass-size relationships $m = \alpha D_{\text{max}}^{\beta}$, where D_{max} is the maximum diameter of the particle. The ID column contains the particle shape identifier of the particle model in the Eriksson et al. (2018) scattering database. Hydrometeor species Particle shape ID α β Cloud ice GemCloudIce 31 440 3 Snow GemSnow 32 52.4 3 Graupel GemGraupel 33 209.4 3 Hail GemHail 34 471.2 3 Rain LiquidSphere 25 523.6 3 Liquid cloud LiquidSphere 25 523.6 3~~ PSD, is set to a fixed, species-specific value. For each hydrometeor species a specific mass-size relationship is assumed.

Examples of particle size distributions of frozen hydrometeors are displayed in Fig. 2. The ~~four panels display the prognosed particle size distributions for the four frozen hydrometeor types together with renderings of the particle shapes used in the forward simulations. As these plots show, the~~ assumed particle size distributions across different ice species vary mostly in their ~~horizontal and vertical scaling~~ scaling with respect to size and concentration, whereas the ~~function~~ normalized shape shows less variability. ~~Furthermore, an~~ An important characteristic of the model can be identified here, which will help to better understand the retrieval results presented later: Cloud ice in the model is characterized by high particle number ~~densities~~ concentrations and small particle sizes, whereas snow ~~exhibits~~ has lower number concentrations and larger particles.

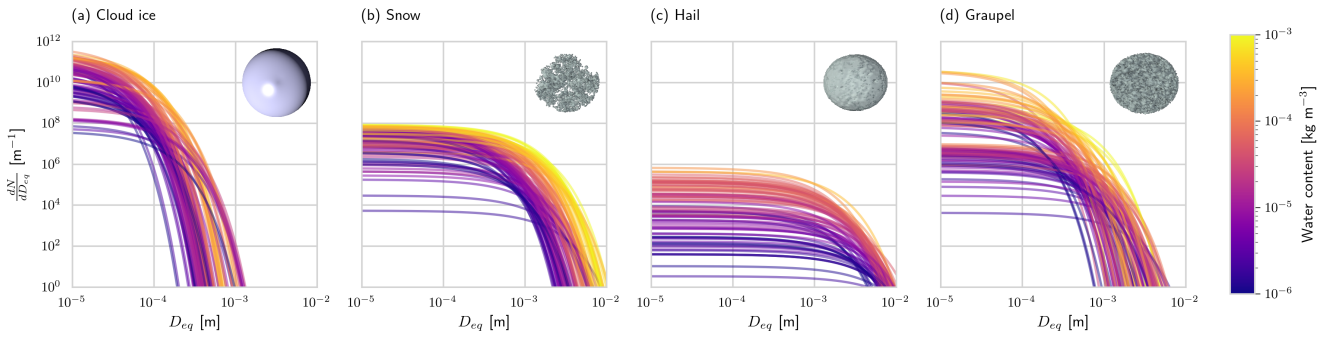

Figure 2. Realizations of particle size distributions from the ~~cloud~~ test scenes used in this study. The ~~number~~ particle ~~density~~ number concentration is plotted with respect to the volume-equivalent diameter D_{eq}. Shown are the PSDs corresponding to 100 randomly chosen grid points with a ~~mass concentration~~ water content higher than 10^{-6} kg m^{-3}. Line color encodes the corresponding ~~mass density~~water content. Inlets display visualizations of the particle shape assumed for each hydrometeor species.

Table 1. Particle shapes used to represent the hydrometeor species of the GEM model scenes. The mass size relationship is given in terms of the parameters of a fitted power law of the form $m = \alpha \cdot D_{\mathrm{max}}^{\beta}$ with D_{max} the maximum diameter and m in kg m^{-3}.

GEM hydrometeor class	Associated particle shape	Size range		Mass size relationship	
	Name (ID)	$D_{\mathrm{eq,\,min}}$ [µm]	$D_{\mathrm{eq,\,max}}$ [µm]	α	β
Liquid cloud	LiquidSphere (25)	1	$5 \cdot 10^4$	480	3
Rain	LiquidSphere (25)	1	$5 \cdot 10^4$	480	3
Ice cloud	GEM Cloud Ice (31)	10	$3 \cdot 10^3$	440	3
Snow	GEM Snow (32)	94	$5 \cdot 10^3$	24	2.86
Graupel	GEM Graupel (33)	94	$5 \cdot 10^3$	170	2.96
Hail	GEM Hail (34)	94	$5 \cdot 10^3$	540	3.02

2.2 ~~Simulated cloud observations~~

~~A simulated observation is generated for each vertical profile in the model test scenes. The simulations apply the same microphysics scheme as the model, which means that they use the same six hydrometeor classes and PSD parametrizations.~~ In order to simulate observations from the GEM model scenes, the hydrometeor classes of the GEM microphysics scheme must be associated with particle shapes to define their radiometric properties. The ARTS single-scattering database, described in more detail below, contains particle models which were designed to be consistent with the mass-size relationships assumed in the GEM model. The particle shapes used to represent the GEM model's different hydrometeor types are listed together with their properties in Tab. 1.

2.1.1 ~~Sensor configuration~~

~~Simulations of observed passive brightness temperatures are performed for the 11 highest-frequency channels of the MWI radiometer and all channels of the ICI radiometer. The passive observations are combined with a W-band cloud radar similar to the CloudSat Cloud Profiling Radar (CPR) (Stephens et al., 2002; Tanelli et al., 2008).~~

2.2 Simulated cloud observations

~~A number of simplifications are applied for the generation of the synthetic cloud observations: Firstly, the~~ An airborne sensor configuration is simulated to test the retrieval. The beams of all three sensors are ~~modeled as~~ assumed to point at nadir and to be perfectly coincident pencil beams. ~~Secondly, a synthetic observation is generated for each vertical profile from the model scenes by simulating a one-dimensional, plane-parallel atmosphere, the properties of which are taken from the corresponding model profile. It follows from these modeling decisions that the atmosphere is assumed to be homogeneous across the beams of the active and passive sensors and that they all sense the same atmospheric volume. This is certainly not~~ Multiple scattering effects in the radar observations as well as the effects of particle orientation are neglected. Although these assumptions may be justified for an airborne configuration, this will not be the case for space-borne observations ~~and will incur a forward modeling error that is not accounted for in this study. Since the focus of this study are the fundamental synergies between the active and passive observations, quantifying the impact of beam width and inhomogeneity is left for future investigation~~from ICI and MWI. Moreover, the incidence angles of the beams of ICI and MWI will be around 53° at the Earth's surface. This further complicates the radiative transfer modeling since it requires treating a more complex co-location geometry of the nadir-pointing radar and the passive instruments. At off-nadir viewing angles, polarization also needs to be taken into account, the effects of which can be several Kelvin at the typical viewing angles of microwave imagers (Xie et al., 2015).

2.2.1 Sensor configuration

The sensor configuration assumed for the simulated observations includes the 11 highest-frequency channels of the MWI radiometer and all ICI channels. For the radar, a nadir-pointing W-band cloud radar with similar characteristics as the CloudSat Cloud Profiling Radar (CPR, Stephens et al. (2002); Tanelli et al. (2008)) is assumed.

Observations from the ICI radiometer are simulated by performing a single, non-polarized radiative transfer simulation located at the centers of the pass bands of each double-sideband channel and averaging the resulting brightness temperatures. For channels with multiple polarizations, only a single simulation is performed. To compensate for this, the noise of the corresponding channel is reduced by a factor of $\sqrt{2}$. The simulated ICI channels and assumed noise levels are presented in Tab. 2. ~~The off-nadir viewing angle of ICI is assumed to be 48° at the sensor.~~

Observations from the MWI radiometer are simulated in a similar manner ~~as those from ICI . However, from~~ to those of ICI except that for MWI only channels with frequencies larger than or equal to 89 GHz are used. The reason for this is that the footprints of the channels with frequencies lower than 89 GHz will have full-width at half maximum of 50 km compared to only 10 km for the MWI's higher-frequency channels ~~. Due~~ and 16 km for ICI's channels. For a spaceborne configuration, these channels were deemed unlikely to be beneficial for a synergistic retrieval due to the very small overlap of the footprints

of these ~~low-frequency~~ channels with that of the radar~~, it is assumed they would not be beneficial for a synergistic retrieval and are therefore disregarded here~~. The included MWI channels are listed in Tab. 2.

Table 2. Channels of the MWI and ICI radiometers used in the retrieval.

MWI			ICI		
Channel	Freq. [GHz]	Noise [K]	Channel	Freq. [GHz]	Noise [K]
MWI-8	89	1.1	ICI-1	183.31 ± 7.0	0.8
MWI-9	118.75 ± 3.2	1.3	ICI-2	± 3.4	0.8
MWI-10	± 2.1	1.3	ICI-3	± 2.0	0.8
MWI-11	± 1.4	1.3	ICI-4	243 ± 2.5	$\frac{1}{\sqrt{2}} \cdot 0.7$
MWI-12	± 1.2	1.3	ICI-5	325.15 ± 9.5	1.2
MWI-13	165.5 ± 0.75	1.3	ICI-6	± 3.5	1.3
MWI-14	183.31 ± 7.0	1.2	ICI-7	± 1.5	1.5
MWI-15	± 6.1	1.2	ICI-8	448 ± 7.2	1.4
MWI-16	± 4.9	1.2	ICI-9	± 3.0	1.6
MWI-17	± 3.4	1.2	ICI-10	± 1.4	2.0
MWI-18	± 2.0	1.3	ICI-11	664 ± 4.2	$\frac{1}{\sqrt{2}} \cdot 1.6$

The frequency of the the cloud radar is chosen to be 94 GHz similar to the CloudSat CPR. The vertical resolution of the nadir-pointing radar observations is assumed to be 500 m ranging from 0.5 to 20 km in altitude. The minimum sensitivity is set to be -30 dBZ and the noise at each range gate is modeled to be independent with standard deviation 0.5 dBZ. ~~As mentioned above, the same incidence angle as for the passive radiometers is assumed also for the radar. In practice, this could be achieved by remapping the radar observations to the lines of sights of the passive beams.~~

2.2.2 Radiative transfer simulations

All simulations presented in this study were performed using Version 2.3~~.1245~~.1279 of the Atmospheric Radiative Transfer Simulator (ARTS, Buehler et al. (2018)). Radar reflectivities are computed using ARTS' built-in single-scattering radar solver, which provides analytic Jacobians. For the simulation of passive radiances, a hybrid solver is used which combines the DISORT (Stamnes et al., 2000) scattering solver with the ARTS standard scheme for pencil beam radiative transfer. The hybrid solver has been added to ARTS specifically for this study and provides approximate, analytical Jacobians, which are required for ~~the~~ variational retrievals of hydrometeors. All simulations are performed assuming an ocean surface with emissivities calculated using the Tool to Estimate Sea-Surface Emissivity from Microwaves to sub-Millimeter waves (TESSEM, Prigent et al. (2017)). Polarization is neglected in all simulations performed in this study. ~~Particle scattering data are taken from the ARTS scattering data base (hereafter ARTS-SSDB, Eriksson et al. (2018)).~~ Gaseous absorption is modeled using the absorption models from Rosenkranz (1993) for N_2, O_2 and from Rosenkranz (1998) for H_2O.

Single scattering data for hydrometeors are taken from ARTS single scattering data base (ARTS SSDB, Eriksson et al. (2018)). The database provides scattering data for a wide range of hydrometeor shapes including particles designed specifically to be consistent with assumptions of the GEM microphysics scheme. It also provides a number of predefined habit mixes, referred to as standard habits, designed to cover the full range of particle sizes relevant for microwave observations of ice hydrometeors.

2.3 Retrieval algorithm

A one-dimensional, variational cloud retrieval algorithm is proposed ~~to retrieve distributions of frozen hydrometeors from the combined active and passive observations. The algorithm~~ which uses the optimal estimation method (OEM~~) developed by Rodgers (2000). The retrieved state $\mathbf{x} \in \mathbb{R}^n$ is determined by fitting a forward model $\mathbf{F} : \mathbb{R}^n \rightarrow \mathbb{R}^m$ to a set of observations $\mathbf{y} \in \mathbb{R}^m$. The best fit is determined by minimizing a cost function of the form~~

$$\mathcal{L}(\mathbf{x},\mathbf{y}) \propto (\mathbf{F}(\mathbf{x}) - \mathbf{y})^T \mathbf{S}_e^{-1} (\mathbf{F}(\mathbf{x}) - \mathbf{y}) + (\mathbf{x} - \mathbf{x}_a)^T \mathbf{S}_a^{-1} (\mathbf{x} - \mathbf{x}_a).$$

~~The cost function $\mathcal{L}(\mathbf{x},\mathbf{y})$ corresponds to the negative log-likelihood of the a posteriori distribution of the state $\mathbf{x}$ under the assumptions of Gaussian a priori distribution with mean $\mathbf{x}_a$ and covariance matrix $\mathbf{S}_a$ as well as zero-mean Gaussian measurement error with covariance matrix $\mathbf{S}_e$~~, Rodgers (2000)) to fit an atmospheric state to given observations.

~~To assess the~~ The quality of a retrieved state $\hat{\mathbf{x}}$ and corresponding simulated ~~observation~~ observations $\hat{\mathbf{y}} = \mathbf{F}(\hat{\mathbf{x}})$ ~~, we define~~ is assessed using the following diagnostic quantity:

$$\chi_y^2 = \delta\Delta\mathbf{y}^T \mathbf{S}_e^{-1} \delta\Delta\mathbf{y}, \tag{1}$$

~~where $\delta\mathbf{y} = \mathbf{y} - \hat{\mathbf{y}}$~~Here, $\Delta\mathbf{y} = \mathbf{y} - \hat{\mathbf{y}}$ is the difference between the fitted and true observations and $\mathbf{S}_e$ is the covariance matrix describing the measurement errors. The quantity χ_y^2 ~~is here used to approximate a χ^2-test for the misfit between the observations $\mathbf{y}$ and the retrieval fit $\hat{\mathbf{y}}$. Although a formally correct~~ corresponds to the sum of squared errors in the fitted observations weighted by the uncertainties in each channel or range bin. It should be noted that the quantity has no meaningful interpretation in terms of χ^2~~-test for $\delta\mathbf{y}$ should apply a different covariance matrix~~ -statistic for the errors in the fitted observations since they will neither be independent (c.f. Chapter 12 in Rodgers (2000)) ~~, such tests were found to yield very high values that deviate strongly from the expected chi-square distribution. The χ_y^2 value used here provides a less strict test in the sense that it will generally be smaller than if the formally correct covariance matrix was used.~~

~~The amount of information contained in a retrieval can be quantified by computing the degrees of freedom for signal (DFS). Let $\mathbf{K} \in \mathbb{R}^{m \times n}$ be the Jacobian of the forward model $\mathbf{F}$. Then the DFS of the observations can be computed as the trace of the averaging kernel matrix~~

$$\mathbf{A} = (\mathbf{K}^T \mathbf{S}_e^{-1} \mathbf{K} + \mathbf{S}_a^{-1})^{-1} \mathbf{K}^T \mathbf{S}_e^{-1} \mathbf{K}.$$

nor Gaussian due to the presence of forward model error. The value is therefore used here solely as a heuristic to quantify the goodness of the fit to the true observations.

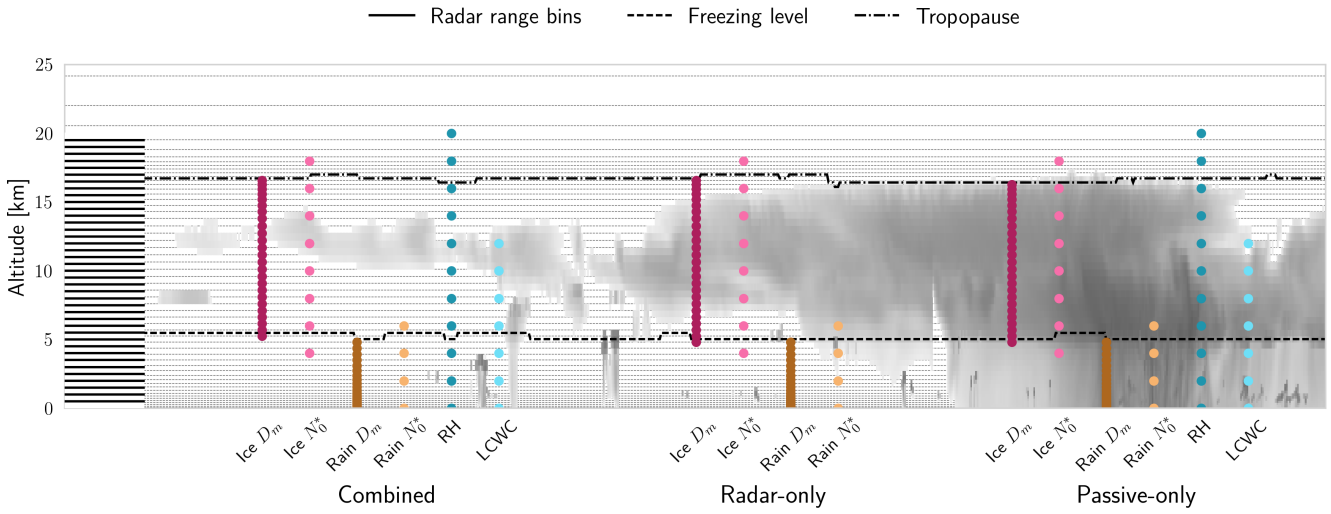

Figure 3. Illustration of retrieval quantities and their respective retrieval grids. Grey, dashed lines in the background display the vertical grid of the GEM model. Black, solid lines on the left side display the range bins of the radar observations. Filled markers represent the retrieval grids of each retrieval quantity for the combined, radar-only and passive-only configurations of the retrieval algorithm.

2.3.1 Measurement space

The input for the ~~retrieval algorithm~~ synergistic retrieval is the combined observation vector $\mathbf{y}$ consisting of the concatenated single-instrument observations from the cloud radar and the two radiometers. Measurement errors are assumed to be independent and Gaussian distributed with standard deviations according to the noise characteristics given in Section 2.2.1. For the single-instrument retrievals the measurement vector consists only of observations from either the radar or the radiometers.

2.3.2 State space

The proposed retrieval solves for ~~distributions of one frozen and one liquid hydrometeor species in the atmospheric column together~~ profiles of two degrees of freedom of the PSDs of frozen hydrometeors and rain along with profiles of ~~atmospheric humidity~~ relative humidity (RH) and liquid-cloud ~~mass density. The retrieval uses the same vertical grid as the model scenes, which have a vertical resolution of about 500 m throughout the troposphere. If not specified otherwise, retrieval quantities are retrieved at this resolution~~water content (LCWC). An illustration of the retrieved quantities and their respective retrieval grids for the combined and single-instrument configurations of the retrieval are given in Fig. 3.

~~Distributions of hydrometeors in the atmospheric column~~

The PSDs of frozen hydrometeors and rain are represented using the normalized particle size distribution formalism proposed by Delanoë et al. (2005). The PSD of a hydrometeor species at a given ~~height level is represented by a vertical and a horizontal scaling parameter, the~~ altitude is modeled using a generalized gamma distribution function with four parameters.

The mass-weighted mean diameter D_m, which scales the PSD along the size dimension, and the normalized number density N_0^*. Alternative parametrizations using mass density and D_m or the mass density and N_0^* have been tested but no considerable effect on retrieval performance has been observed.

The retrieval computes vertical profiles of the two scaling parameters D_m and N_0^* for each of the two hydrometeor species. The remaining shape of each PSD is described by the shape parameters α and β, not to be confused with the parameters of the mass-size relationship shown in Tab. 4. The shape parameters are set to fixed, species-specific values. This principle is illustrated in Fig. 3. The plot displays the a-priori-assumed shapes of the particle size distribution of frozen and liquid hydrometeors. The retrieved horizontal and vertical scaling parameters , D_m and N_0^*, are used as units for the axes of the plot so that which scales the particle concentration, are the two retrieved degrees of freedom of the PSD. The other two parameters describe the shape of the PSD becomes independent of the retrieved mass density and number concentration. For frozen hydrometeors, the values of the shape parameters α and β are chosen identical to normalized PSD. The same shape parameters as in version 3 of the DARDAR-CLOUD product (Cazenave et al., 2018). For liquid hydrometeors, the shape parameters are chosen so that they are equivalent to (Cazenave et al., 2019) are chosen for frozen hydrometeors. For rain, they are chosen to match the shape used by in the GEM model for rain drops. All calculations involving particles size distributions use the volume-equivalent diameter D_{eq} as size variable.

PSD parametrizations for frozen and liquid hydrometeors used in the cloud retrieval.

The temperature-dependent a priori profile for N_0^* of for frozen hydrometeors is determined using the relation from Delanoë et al. (2014)

$$N_0^* = \exp\left(-0.076586 \cdot (T - 272.5273.15) + 17.948\right), \tag{2}$$

where T is in K. The a priori profile for of D_m for frozen hydrometeors is chosen so that the a priori mass density IWC is equal to 10^{-6} kg m^{-3}. For liquid hydrometeorsrain, a fixed value for N_0^* of 10^6 m^4 10^6 m^{-4} is assumed and the a priori profile for D_m is determined similarly as for frozen hydrometeors. Values of the mass-weighted mean diameter D_m for both hydrometeor species

Since the N_0^* parameters vary over several orders of magnitude they are retrieved in $\log_{10}$-space for both frozen hydrometeors and rain. The D_m parameters, in contrast, are retrieved in linear space, whereas the normalized number concentration parameter . Alternative parametrizations using water content and D_m or the water content and N_0^* is retrieved in $\log_{10}$ spacehave been tested but no considerable effect on retrieval performance has been observed. As additional constraints, the retrieval of frozen hydrometeors is restricted to the region between the freezing layer and the tropopause, whereas the retrieval of liquid level, here defined simply as the 273.15 K-isotherm, and the approximate altitude of the tropopause. The altitude of the tropopause is approximated as the first grid point at which the lapse rate is negative and temperature below 220 K. The retrieval of rain hydrometeors is restricted to below the freezing layer.

To further regularize the retrieval , N_0^* for ice is retrieved at only 10 equally-spaced grid points between freezing layer and the tropopause. Similarly, D_m and level. The retrieval of the N_0^* for rain are retrieved at 10 respectively 4 points between surface and freezing layerparameters is further regularized by retrieving them at reduced vertical resolution of 2 km. This was

~~necessary to avoid~~ found necessary to keep the retrieval from getting stuck in spurious local minima. ~~An approach similar to this one is also~~ This resembles the approach taken in the GPM combined precipitation retrievals (Grecu et al., 2016)~~.~~, where the PSD parameter scaling the particle concentration is also retrieved at reduced resolution.

~~Humidity in the atmospheric column is retrieved in units of relative humidity~~ Relative humidity is retrieved at a vertical resolution of ~~1 km~~2 km. However, ~~instead of retrieving relative humidity directly ,~~ the values are not retrieved directly but instead an inverse hyperbolic ~~tangens~~ tangent transformation is applied to the relative humidity profile~~ϕ~~:

$$x = \text{arctanh}\left(\frac{2\phi}{1.1}\frac{2\text{RH}}{1.2} - 1.0\right) \tag{3}$$

The transformation restricts the retrieved relative humidity values to the range ~~of $[0.0, 1.1]$~~between 0 and 120%. The a priori profile for relative humidity is ~~arbitrarily chosen as~~ set to

$$\phi\text{RH}(t) = \begin{cases} 0.7 & ,270\ \text{K} < t \\ 0.7 - 0.01 \cdot (270 - t) & ,220 < t \leq 270\ \text{K} \cdot \\ 0.2 & ,t < 220\text{K} \end{cases} \tag{4}$$

~~The retrieval of liquid cloud mass density, here referred to as liquid water content (LWC), is performed at seven equally spaced altitude levels~~ LCWC is retrieved at a resolution of 2 km but is restricted to the region between the surface and the 230 K isotherm. In contrast to frozen ~~and liquid hydrometeors , cloud water is modeled~~ hydrometeors and rain, the PSD of liquid cloud droplets is not explicitly resolved in the retrieval forward model~~to be purely absorbing using the absorption~~. Instead, liquid cloud droplets are modeled as purely absorbing quantity using the model by Liebe et al. (1993) for suspended liquid cloud droplets. ~~Liquid cloud mass density~~ Note that this is the case only for the retrieval. For the simulated observations, liquid cloud droplets are handled as any other hydrometeor species in the GEM model. LCWC is retrieved in $\log_{10}$-space and the a priori profile is set to a fixed value of 10^{-6} kg m^{-3} in the permitted region of the atmosphere.

The a priori distributions of the 6 retrieval quantities (N_0^* and D_m for frozen and liquid hydrometeors, ~~relative humidity ϕ, cloud water~~RH, CLWC) are assumed to be independent so that the overall a priori covariance matrix $\mathbf{S}_a$ has block-diagonal structure. Within each block, vertical correlations between the values of a given retrieval quantity at different altitudes are assumed to be exponentially decaying. ~~Hence, the correlation~~ The covariance of the values of retrieval quantity q at points i and j of the retrieval grid is computed as

$$(\mathbf{S}_{a,q})_{i,j} = \sigma_{q,i}\sigma_{q,j} \cdot \exp\left(-\frac{d(i,j)}{l_q}\right), \tag{5}$$

where $\sigma_{q,i}$ is the a priori uncertainty assumed for retrieval quantity q at grid point i, $d(i,j)$ the vertical distance between the grid points and l_q the quantity-specific correlation length. The assumed a priori uncertainties and correlation lengths for the retrieval quantities are summarized in Tab. 3.

~~As baselines for the assessment of the combined~~ The radar-only version of the retrieval is similar to the combined version except that RH and LCWC are not retrieved. Instead, perfect knowledge of the true RH profile is assumed while LCWC is

Table 3. A priori uncertainties and correlation lengths used in the retrieval.

Retrieval target	~~Quantity q~~	Combined / Radar-only		Passive-only	
Name	Retrieved quantity	σ_q	l_q [km]	σ_q	l_q [km]
~~$\log_{10}(N^*_{0,\text{frozen}})$~~ Ice, N^*_0	$\log_{10}(N^*_{0,\text{Ice}})$	2	2	2	5
~~$D_{m,\text{ice}}$~~ Ice, D_m	Ice $D_{m,\text{Ice}}$	300 µm	2	300 µm	5
~~$\log_{10}(N^*_{0,\text{liquid}})$~~ Rain, N^*_0	~~2~~ $\log_{10}$(Rain N^*_0)	2 ~~$D_{m,\text{liquid}}$~~	~~500 µm~~ 2	2	5
~~$\text{arctanh}(\frac{2\cdot\phi}{1.1} - 1.0)$~~ Rain, D_m	$D_{m,\text{Rain}}$	300 µm	2	300 µm	5
Relative humidity (RH)	$\text{arctanh}(\frac{2\cdot\text{RH}}{1.2} - 1.0)$	0.5*	2*	0.5	2
~~$\log_{10}(m_{\text{liquid cloud}})$~~ Cloud liquid water content (CLWC)	$\log_{10}$(CLWC)	1*	2*	1	2

*: Not retrieved in radar-only retrieval

neglected. In addition to a two-moment radar-only retrieval, also a ~~radar-only and a passive only-retrieval are performed. The radar-only retrievaluses the same implementation as~~ one-moment version (M1), in which only the D_m parameter is retrieved has been tested. For completeness, retrieval results for IWC will be reported also for the M1 version. However, to allow for better comparison with the combined and passive-only retrieval, for the remaining results only the two-moment version is considered. For the passive-only retrieval, the retrieval quantities and grids are the same as for the combined retrieval~~, but only retrieves frozen and liquid hydrometeors. For the radar-only retrieval, perfect knowledge of the atmospheric humidity profile is assumed but liquid cloud is ignored in the~~ . However, higher correlations lengths are assumed, which are shown in Tab. 3

2.3.3 Representation of ice particle shape

A major difficulty for cloud retrievals is that the observations may not provide sufficient information to distinguish different hydrometeor species. Due to this ambiguity, frozen hydrometeors in the proposed retrieval algorithm are represented using only a single hydrometeor species. It is therefore necessary to find a suitable representation for frozen hydrometeors, which can capture the variability of the four frozen hydrometeor species in the GEM model and ideally also that of real ice hydrometeors.

The differences between hydrometeor species in the test scenes are due to their different concentrations, sizes and shapes (c.f. Fig. 2). Since two parameters of the PSD of frozen hydrometeor species are retrieved, the retrieval is able to represent the characteristic number concentrations and particle sizes of different hydrometeor species. Variations in particle shape which correlate with particle size can be represented using a habit mix combining crystal shapes at small sizes with aggregates or rimed particles at larger sizes. This provides the retrieval with some flexibility to represent the different shapes present in the test scenes.

Even with this configuration the simplified retrieval forward model ~~.~~ ~~The setup and retrieval quantities of the passive-only retrieval are similar to the combined retrieval, with the only difference being that frozen and liquid hydrometeors are retrieved at reduced resolution. For ice,~~ will not be able to represent every possible

configuration of mixes of the four ice hydrometeor species in the GEM model. It thus remains unclear which particle shape should be used to best represent this mixture. We therefore choose a set consisting of multiple particle shapes and habit mixes for which we investigate the impact of the particle choice on the retrieval results. The selected particles are listed in Tab. 1. Three of them, GEM Cloud Ice, GEM Snow, and GEM Graupel, correspond to the shapes present in the GEM model scenes. The GEM Snow and Graupel habits were mixed with crystal shapes to ensure that they cover sizes down to around 10 µm. In addition to this, two of the habit mixes distributed with the ARTS SSDB, the Large Plate Aggregate and Large Column Aggregate standard habits, are included in the selection to increase the range of scattering properties it covers. Fig. 4 provides an overview of the bulk mass backscattering efficiencies and mass attenuation coefficients of the selected particles computed for three different values of the N_0^* ~~is retrieved at three equally spaced grid points between freezing layer and troposphere, while D_m is retrieved at five. For liquid hydormeteors, the retrieval grids for N_0^* and D_m are reduced to two equally spaced points between surface and freezing layer. Relative humidity is retrieved at a vertical resolution of 2 km.~~ parameter of the PSD. Mass backscattering efficiency and attenuation coefficient are defined as the ratio of the corresponding cross-section σ and the bulk water content:

$$Q = \frac{\sigma}{\mathrm{WC}} \tag{6}$$

For high values of N_0^*, which are typical for cloud ice, the radiometric properties of particle shapes differ only for large masses at the two highest frequencies considered. For low N_0^* values, which are more typical for snow, the particles' properties differ considerably at all masses and frequencies. At the two lowest frequencies, the Large Column Aggregate, Large Plate Aggregate and GEM Snow are the least efficient scatterers or absorbers of radiation whereas GEM Graupel, Gem Hail and GEM Cloud Ice are more efficient. This behavior is also observed at the two higher frequencies, except for the lowest N_0^* value for which a reversal of the ordering occurs as the bulk mass increases. The mass backscattering efficiency at 94 GHz shows the greatest relative variability across different bulk water contents and N_0^* values, spanning six orders of magnitudes, while for the mass attenuation coefficients at the other frequencies the variability spans at most three orders of magnitude.

3 Results

The first part of this section presents results from a numerical experiment ~~that~~ which investigates the complementary information content of the active and passive microwave observations. Results of the combined and the ~~baseline~~ single-instrument retrievals applied to the reference cloud scenes are presented in the ~~remaining partof this section~~second part.

3.1 Complementary information content

A fundamental question regarding the benefit of combining two remote sensing observations in a retrieval is to what extent the observations contain non-redundant information. The degree of non-redundancy in the combined observations is what we refer to here as complementary information content. We are thus interested in the information that cannot be provided by either of

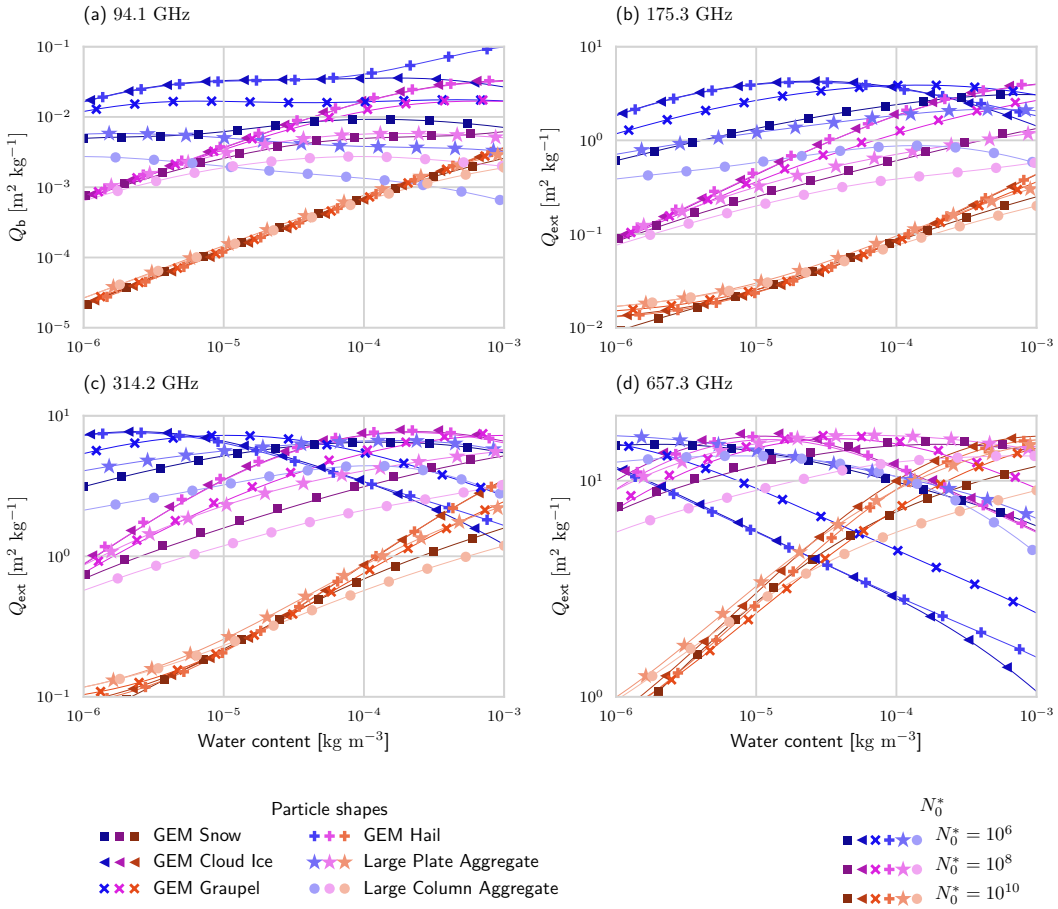

Figure 4. Bulk mass backscattering efficiency Q_b at 94.1 GHz (a) and mass attenuation coefficients Q_e at frequencies 175.3 GHz (b), 314.2 GHz (c) and 657.3 GHz (d) for the particle models used in the simulated observations and the retrieval. Different colors show the bulk properties for different values of the N_0^* parameter of the PSD.

Table 4. Particle models used to represent ice hydrometeors used in the retrieval. The mass size relationship is given in terms of the parameters of a fitted power law of the form $m = \alpha \cdot D_{\text{max}}^{\beta}$ with D_{max} the maximum diameter and m in kg m^{-3}.

Name	Shapes used	Size range		Mass size relationship	
	Name (ID)	$D_{\text{eq, min}}$ [µm]	$D_{\text{eq, max}}$ [µm]	α	β
CloudIce	GEM CloudIce (11)	10	3000	440	3
GEM Snow	8-Column Aggregate (8)	10	127	65	3
	GEM Snow (32)	107	5000	24	2.86
GEM Graupel	8-Column Aggregate (8)	10	179	65	3
	GEM Graupel (33)	107	5000	170	2.96
Large Plate Aggregate	Thick Plate (15)	16	200	110	3
	Large Plate Aggregate (33)	160	3021	0.21	2.26
Large Column Aggregate	Block Column (12)	10	200	110	3
	Large Column Aggregate (22)	160	3021	0.25	2.43

the instruments alone. The higher resolution achieved by adding radar observations to passive ones is therefore not considered as complementary information since the radar alone can provide the increased resolution.

In order to explore ~~this~~ the complementary information content in the radar and radiometer observations, an idealized, homogeneous cloud layer with a thickness of ~~4 km located~~ 5 km centered at an altitude of 10 km in a tropical atmosphere is considered. The cloud is assumed to consist of a single species of frozen hydrometeors represented using the PSD parametrization which is also used in the retrieval and described in Sec. ~~2.3.2~~2.3.2. As particle model, the ~~8-ColumnAggregate~~ 8-Column Aggregate (ID 8) from the ARTS SSDB is used.

The question that is addressed here is whether the combination of active and passive observations is able to constrain both the ~~horizontal and the vertical scaling factors of the PSD~~ size and concentration of the ice particles in the cloud. To investigate this, the N_0^* and D_m parameters of the homogeneous cloud layer are varied and observations of the cloud ~~layer~~ are simulated. ~~Figure 5 displays the simulated passive cloud signal , i.e. the brightness temperature difference between clear sky and cloudy sky simulation, as filled contours for a selection of channels of the MWI and ICI sensors. For given values of N_0^* and D_m, the corresponding ice mass density is given by the relation~~

$$m = \frac{\pi \rho}{4^4} N_0^* D_m^4.$$

~~In the figure, the cloud signal is displayed in D_m-mass density space and thus shows how the measured passive cloud signal varies with the horizontal and vertical scaling parameters of the PSD. Overlaid onto~~ The cloud signal in the radiometer observations is the difference between the cloudy- and clear-sky brightness temperatures (ΔT_B). The signal in the active observations is here defined as the maximum of the measured profile of radar reflectivity dBZ$_{\text{max}}$. Figure 5 displays the contours of ~~the passive cloudsignal are the isolines of the maximum radar reflectivity returned from the cloud~~ΔT_B and dBZ$_{\text{max}}$

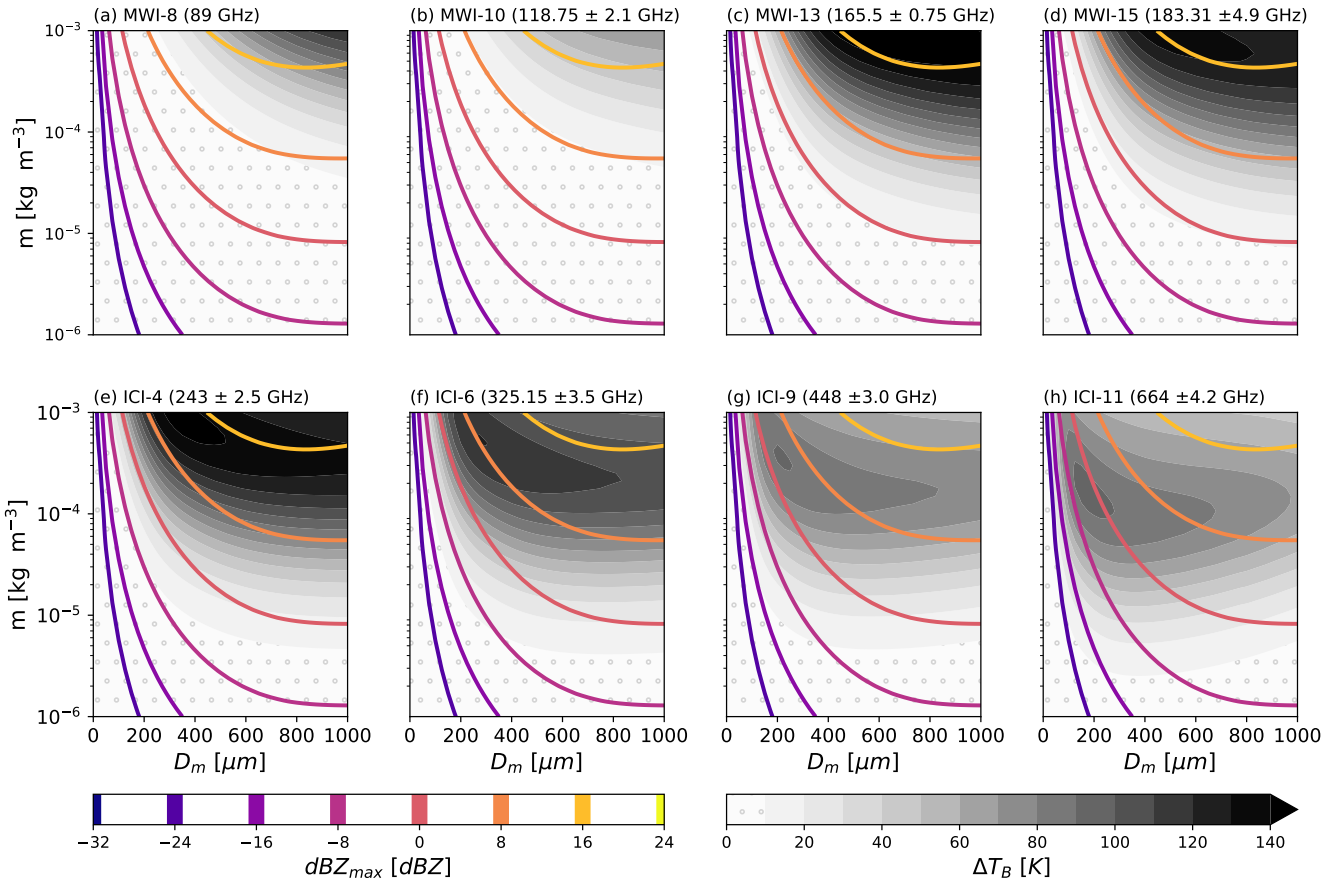

Figure 5. Simulated observations of a homogeneous, 5 km thick cloud layer centered at 10 km with varying water content m and mass-weighted mean diameter D_m. The panels display the maximum radar reflectivity in dBZ (dBZ_{max}) overlaid onto the cloud signal (ΔT_B) measured by selected radiometer channels of the MWI (first row) and ICI radiometers (second row).

with respect to D_m and the cloud's water content, which is proportional to N_0^*:

$$\mathrm{WC} = \frac{\pi\rho}{4^4} N_0^* D_m^4, \tag{7}$$

with ρ the density of ice.

~~The contours of the measured active and passive cloud signals show~~ Along the dBZ_{max}-contours the cloud composition changes but the observed signal stays the same. This shows the ambiguity of the ~~single-instrument measurements~~ radar observations with respect to the ~~parameters of the PSD: Along these contours the signal does not change, while the cloud compositiondoes~~cloud composition. A necessary condition for a ~~combined cloud retrieval~~ passive observation at a given frequency to be able to resolve this ambiguity is that the contours of the active and passive signals cross each other. The panels in Fig. 5 thus provide an indication to what extent the information in the radar measurement and the corresponding passive

radiometer channel provide complementary information on the ~~parameters~~ two degrees of freedom of the PSD. ~~Considering the panels corresponding to the MWI channels, the~~ The results show that the ~~observations contain~~ MWI channels provide complementary information only for very dense clouds consisting of ~~very~~ large particles. In contrast to that, the ICI observations exhibit crossing contours already at lower ~~m~~ water content and D_m values, indicating ~~that the complementary information content in these observations is higher~~ complementary information for less dense clouds ~~consisting of~~ and smaller particles.

3.2 Retrieval results

To assess the performance of the combined cloud retrieval, the developed algorithm has been applied to the two designated cloud scenes. The same retrievals have been performed with a radar-only and a passive-only version of the algorithm to serve as baselines for the evaluation of the combined retrieval. Each retrieval was performed multiple times using the different ice particle models ~~. The tested particle shapes are listed together with the corresponding mass-size relations and ARTS SSDB identifier~~ listed in Tab. ~~4~~1. Since the results for both test scenes are qualitatively similar, ~~not all analyses are shown for both scenes. Instead, these~~ results from the second scene are provided in App. A. Complete results for all retrieval quantities, both scenes and all tested particle shapes are provided as ~~a~~ digital supplement to this article.

~~Particle model name, ARTS scattering database ID and parameters α, β of the mass-size relationships of the particle habits used in the retrieval. Name ID α β GemCloudIce 31 440 3 GemSnow 32 24.0072 2.8571 GemGraupel 33 172.7527 2.9646 8 ColumnAggregate 8 65.4480 3 PlateType1 9 2.4770 0.7570 LargePlateAggregate 20 2.2571 0.2085~~

~~The forward-simulated observations that~~ The simulated observations which were generated to test the retrievals are shown for the first test scene in Fig. 6. Independent Gaussian noise with standard deviations according to sensor specifications has been added to the simulated observations to account for sensor noise. It is important to note ~~,~~ that the simulated observations ~~which are~~ used to test the retrieval assume different microphysics than what is assumed in the retrieval~~:~~. The synthetic observations are computed using the six hydrometeor classes from the GEM model, while the retrieval forward model assumes only two classes of hydrometeors.

3.2.1 ~~Mass concentrations~~Water content

~~To provide an overview over how well the different retrieval methods are able to reproduce the cloud structures in the test scene, the retrieved ice water content (IWC)~~ Retrieved IWC obtained using the Large Plate Aggregate particle model for the first test scene is ~~shown in Figure 7.~~ displayed together with the reference IWC field in Fig. 7. The reference IWC is defined here as the sum of the ~~mass densities of all frozen hydrometeor species. This means that the reference IWC is the sum~~ masses of the four frozen hydrometeor species ~~represented~~ in the GEM model ~~, whereas the retrieved IWC is simply the mass density of the single frozen hydrometeor species assumed in the retrieval. The results shown here were obtained using the LargePlateAggregate as particle model, which was found to be one of the best performing particle models.~~

scenes.

The normalized χ^2_y values of the three retrieval configurations, displayed in Panel (a)~~of the figure displays the χ^2_y value (normalized by the dimension of the measurement space) for each profile in the scene. A high value of χ^2_y indicates that the~~

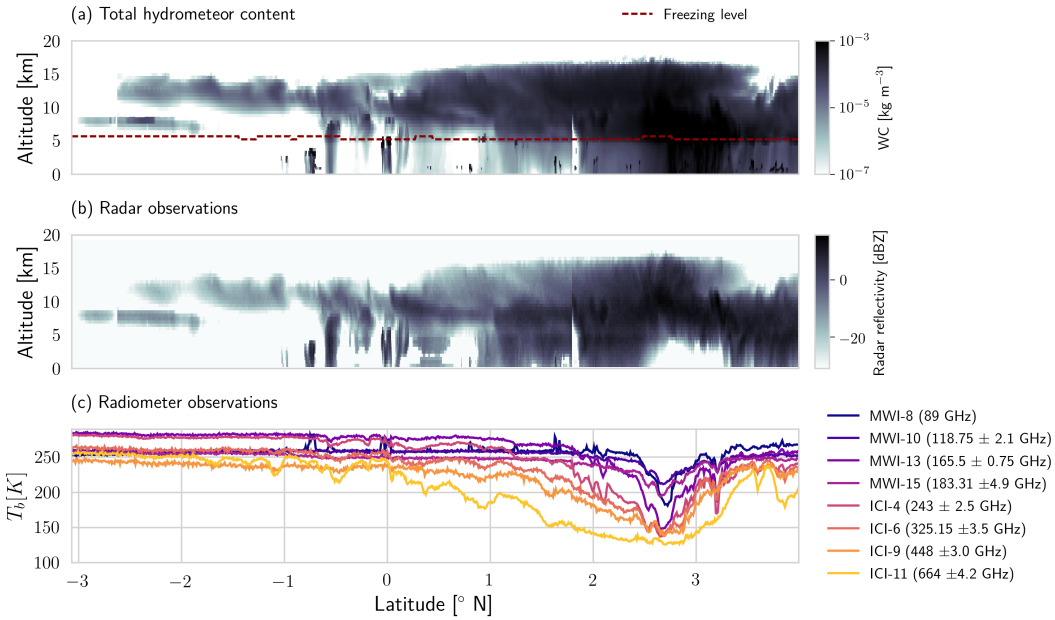

Figure 6. Total ~~hydrometeor~~ water content (~~HMC~~WC) and simulated observations for the first test scene. Panel (a) displays the total ~~hydrometeor~~ water content in the scene, i.e. the sum of the ~~mass densities~~ water content of all hydrometeor species of the GEM model. Panel (b) shows the simulated radar reflectivities. Panel (c) displays the simulated brightness temperatures for a selection of ~~the~~ channels of the MWI and ICI radiometers.

~~retrieved state is not consistent with the input observations. The χ^2_y value for~~ , give an indication of how well the retrievals are able to fit the observations. For the radar-only retrieval~~is remarkably low throughout most~~ , the values are much smaller than 1 for most parts of the scene~~. This may indicate that the retrieval is insufficiently regularized, allowing it to fit the noise in the observations. The~~ , while for the passive-only and combined retrieval ~~, on the contrary, have a normalized χ^2_y value around 1 over most of the scene. Since the presented values are normalized, the value 1 corresponds to~~ they are around the expected value of ~~the approximated chi-square distribution of χ^2_y. All three retrievals exhibit a region of elevated χ^2_y values near the core of the convective system. In particular the high values of~~ 1. This indicates that the radar-only retrieval overfits the observations, while the passive-only and combined retrievals ~~indicate that the retrieval was not able to find a good fitto the observations here.~~

~~Panel (b) displays the retrieved column-integrated IWC, the ice water path (IWP). The IWP is given in dB relative to the reference IWP since, owing to the high dynamic range of the reference values,~~ achieve the expected fit. The exception is the ~~curves could otherwise not be distinguished. Although all methods reproduce the reference IWP fairly well, the combined retrieval yields the best overall agreement with~~ region around 3° N, where the cloud is particularly thick and consists of a mix of different hydrometeor types. Here, especially the passive-only retrieval has problems fitting the observations.

In terms of IWP, all methods provide fairly good estimates of the reference values ~~. Exceptions are the regions of high χ^2_y values where the~~ with the combined retrieval consistently yielding the smallest deviations. Larger differences between the methods are observed when comparing the retrieval ~~failed to find a good fit to the observations.~~

~~Panel (c) shows the IWC field retrieved using the passive-only retrieval . Despite a certain resemblance in the overall structure between the retrieved and reference IWCfield, the results do not reproduce~~ results in terms of IWC. While the vertical structure of the cloud ~~very well. It should be noted, however, that the displayed mass-density range extends below the sensitivity limit of the passive-only observations around 10^{-5} kg m^{-3} (c.f. Fig. 5), which explains the smeared-out appearance of the results to some extent.~~

~~The~~ is captured only very roughly by the passive retrieval, it is better resolved by the radar-only ~~results, shown in panel (d), reproduce the vertical structure of the cloud well. Nonetheless, when compared to the reference IWC field, certain discrepancies are visible: The~~ and the combined retrieval. On closer inspection, however, it becomes evident that the radar-only retrieval ~~tends to overestimate the mass density at the bottom~~ deviates systematically from the reference IWC in specific regions of the cloud~~and underestimate the mass concentrations at the top~~ , such as for example the upper part of the cloud ~~.~~

~~The results of the combined retrieval are displayed in panel (e). Although some artifacts are clearly visible in the retrieved IWC field, the retrieval reproduces the vertical structure well. In particular,~~ between $0°N$ and $2°N$. These deviations are corrected in the results from the combined retrieval~~succeeds to correct some of the systematic deviations of the radar-only retrieval : The mass density at cloud base is reduced and increased at cloud top~~, however certain retrieval artifacts remain visible.

~~To make the~~ For a more quantitative assessment of the retrieval performance~~more quantitative, the reference mass concentrations are~~ , retrieved water content is plotted against the ~~retrieved values~~ reference water content in Fig. ~~7 and 8. The plots show the results for all different retrieval configurations and tested particle models. Markers in the plots are color-coded according to the prevailing hydrometeor type (by mass density) in the reference scene in order to allow assessment of the retrieval performance for the different hydrometeor types of the GEM model.~~

~~Not surprisingly, the results from the~~ 8. In terms of precision, the passive-only retrieval ~~exhibit the strongest deviations from the diagonal. Since the passive channels alone contain only limited~~ performs worst while both the radar-only and combined retrieval yield much smaller spread in the retrieved values. This is not surprising considering that the passive observations do not contain sufficient information on the vertical distribution of ~~ice in the atmosphere, the retrieval cannot be expected~~ IWC to yield accurate results at the resolution ~~considered here. Although rather weak, a certain effect of the ice particle model on the retrieval results can be observed. In particular, the GemCloudIce model leads to a systematic underestimation of ice mass densities, which are less pronounced for the other particle models.~~

~~Reference IWC plotted against retrieved IWC for the tested retrieval configurations. Each row shows the retrieval results for the particle shape shown in the first panel. The following panels show the retrieval results for the passive only (first column), the radar only (second column) and the combined retrieval (third column). Markers are colored according to the prevailing hydrometeor type at the corresponding grid point in the test scene. Due to their sparsity, markers corresponding to graupel are drawn at twice the size of the other markers.~~

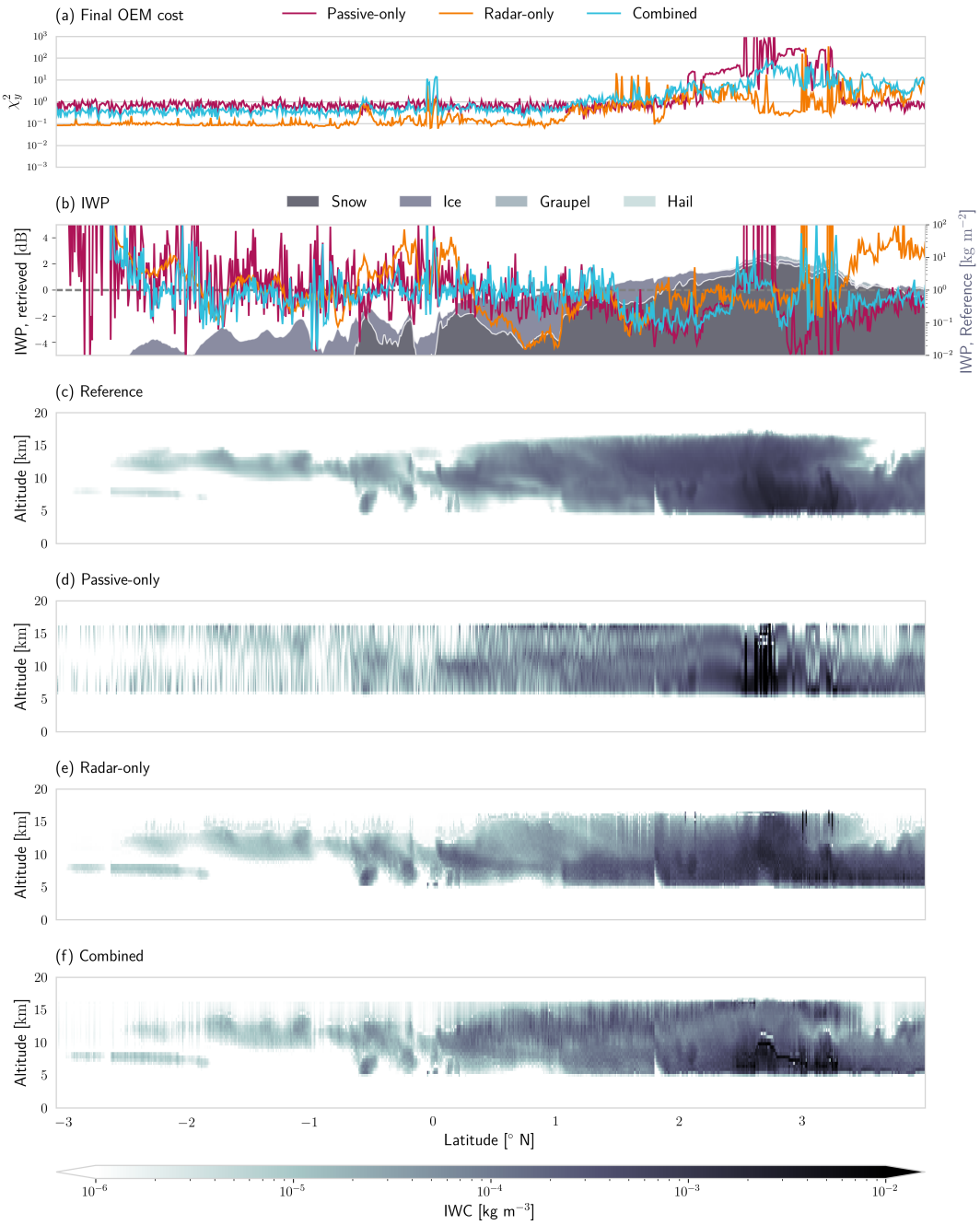

Figure 7. Results of the ice hydrometeor retrieval for the first test scene using the Large Plage Aggregate particle model. Panel (a) displays the value of the χ^2_y diagnostic normalized by the dimension of the measurement space of the corresponding retrieval. Panel (b) displays retrieved IWP in dB relative to the reference IWP. Reference IWP and the contributions from different hydrometeor classes are displayed by the filled areas in the background. Panel (c) shows the reference IWC from the model scene. Panel (d), (e) and (f) display the retrieval results for the passive-only, radar-only and combined retrieval, respectively.

~~The results from the radar-only retrieval are more accurate than the passive-only retrieval, with almost all retrieval results located fairly close to the diagonal. The most distinct feature of the radar-only results, however, is the emergence of two clusters that extend along the diagonal but are displaced above respectively below it. The color coding of the markers reveals that these clusters correspond to grid points dominated by ice for the cluster below the diagonal and snow for the cluster located above the diagonal. This indicates~~ of the model scenes. In terms of overall accuracy, i.e. systematic deviations from the diagonal, no clear differences between the three configurations are visible. However, the color-coding with respect to hydrometeor species reveals that the radar-only retrieval ~~systematically underestimates mass densities for cloud ice but overestimates the mass density of snow. The effect is observed for all tested particle shapes and thus likely independent of it. In general, the radar-only results exhibit only very weak dependency on the particle model, making the results for different particle shapes virtually indistinguishable.~~

~~Another feature that stands out in the radar-only resultsis that the retrieval does not work for graupel. This, however, can be understood by comparing the radar reflectivities shown in Fig. 6 with the cloud structure displayed in Fig. 1. It becomes apparent that graupelin this scene is located where the radar signal is fully attenuated. Since there is no signal to retrieve the mass density from, this explains the bad performance of the radar-only retrieval for these grid points.~~

~~Similar to the radar-only retrieval, the results of the combined retrieval are located close to the diagonal. But the clusters observed in the radar-only results are to large extent merged in the combined results . Moreover, except for the results obtained with the GemCloudIce particle shape, the two clusters move in closer towards the diagonal. The combined retrieval thus improves the IWC retrieval for the specific hydrometeor species in the scene.~~ is biased for specific hydrometeor classes. In the combined and even the passive-only results, this effect is weaker and the clusters are generally moved towards the diagonal. For graupel, all retrievals perform badly but this is likely due to it being present only in the core of the convective system where the signals from all sensors can be expected to be saturated.

~~Nonetheless, the results for the GemCloudIce particle stand out in the~~ Comparing the results ~~. Even though the systematic deviations observed in~~ for different particle models, a clear dependency is evident in the passive-only and the combined results while the radar-only retrieval ~~are reduced for most particle shapes, for this specific shape they are instead increased. The retrieval error is particularly large for snow, which is strongly underestimated for reference mass concentrations around 10^{-4} kg m^{-3}.~~

~~Same as Fig. 7 but for the remaining particle shapes.~~

~~The results for the second test scene obtained using the LargePlateAggregate particle model are shown in Fig. A1. As mentioned above, the results are qualitatively very similar to those of the first scene. Also here, the final OEM cost, shown in Panel (a), displays a region of increased cost for the passive-only and combined retrievals. This is again a region of very dense cloud which consists of graupel and snow. Also similar to the first scene, the passive only retrievaldoes not reproduce the structure of the cloud well. Although the cloud top is placed at the right position, neither the vertical structure of the cloud nor its base are resolved. The radar-only retrieval resolves the vertical structure of the cloud well, but overestimates the ice mass density in the scene. The combined retrieval also resolves the vertical structure of the cloud well and corrects the overestimation observed in the radar-only resultsto some extent~~is affected the least. For the combined and passive-only retrieval, the effect is

consistent across the methods, with the GEM Cloud Ice and Large Column Aggregate yielding the largest deviations and the Large Plate Aggregate yielding the most accurate results.

To summarize retrieval performance for all tested retrieval methods and particle shapes, the distributions of the logarithmic error

$$\mathrm{E}_{\log_{10}} = \log_{10}\left(\frac{x_{\text{retrieved}}}{x_{\text{reference}}}\right) \tag{8}$$

for the retrieved IWC and IWP are displayed in Fig. 9. ~~The logarithmic error in the IWC retrieval~~ In addition to the two-moment version of the radar-only retrieval, this figure also displays results of the single-moment version of the retrieval, which was actually found to yield better IWC retrievals for the second test scene.

The error for IWC has been computed ~~only for~~ considering only grid points where either reference or retrieved IWC is larger than 10^{-6} kg m^{-3}. ~~Considering first the results of the IWC retrieval, shown in Panel (a) and (b), the plots confirm the findings from the analysis above: The combined retrieval generally~~ Similar to the results presented above, the combined retrieval yields the smallest retrieval errors for suitable choices of the particle model. Although the ~~spread of the retrieval errors~~ two-moment radar-only retrieval performs similar to the combined retrieval in terms of precision, it yields significant systematic errors for the second scene. The reason for this can be understood considering the cloud composition displayed in Fig. 1. Since the clouds in the second test scene consist mostly of snow, the bias of the radar-only retrieval ~~is lower in~~ with respect to this specific hydrometeor species (c.f. Fig. 8 and also Fig. A2) leads to the large observed systematic errors for the second scene. The single-moment radar-only retrieval does not produce the same large systematic errors for the second scene, ~~the combined retrieval yields smaller systematic errors~~ but instead produces systematic errors for the first scene. The passive-only retrieval yields the largest errors in terms of retrieved IWC due its low vertical resolution.

~~Compared in~~ In terms of IWP, however, the ~~results are different. Especially~~ errors of the passive-only retrieval ~~yields much lower errors for the retrieved IWP, making the results comparable if not better than those of~~ are decreased making the retrieval comparable to the other methods. For the radar-only and combined retrievals, the precision is generally increased but the systematic deviations observed ~~in the~~ for IWC persist. This leads, particularly for the second test scene, to significant systematic errors in the ~~radar-only-retrieved IWP~~ IWP retrieved by the two-moment radar-only retrieval.

~~In addition to this, the passive-only and the combined retrieval exhibit~~ Also in these results, a strong dependence ~~of the retrieval error~~ on the applied particle model ~~. Especially the GemCloudIce and GemSnow particle models yield large retrieval errors for IWC and IWP. The other three particle models, however, consistently yield smaller retrieval than the GemCloudIce and GemSnow models~~is observed for the passive-only and combined retrievals. The errors are particularly large for the GEM Cloud Ice and the Large Column Aggregate. Although the impact is stronger for the M1 version, the particle shape has less impact on the retrieval performance of the radar-only retrieval and does not affect the large systematic errors observed for the second test scene.

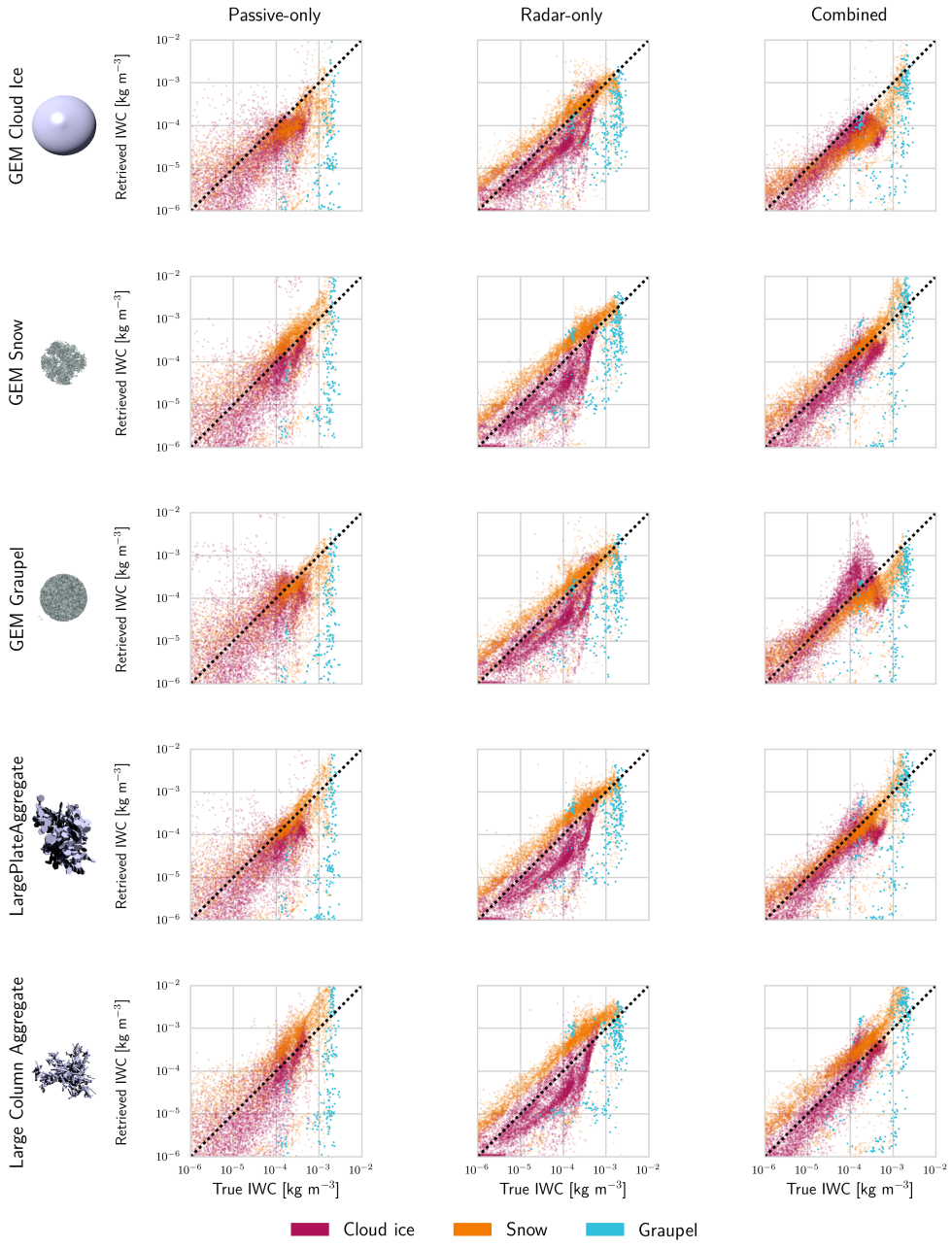

Figure 8. ~~Results of the ice hydrometeor retrieval~~ Retrieved IWC plotted against reference IWC for the ~~second test scene. Panel (a) displays the value of the χ^2_y diagnostic normalized by the dimension of the measurement space of the corresponding~~ tested retrieval configurations. ~~Panel (b)~~ Each row shows ~~retrieved IWP in dB relative to~~ the ~~reference IWP. Panel (c) displays~~ retrieval results for the ~~reference mass concentrations from~~ particle shape shown in the ~~model scene~~first panel. ~~Panel (d), (e) and (f) display~~ The following panels show the retrieval results for the passive-only (first column), the radar-only (second column) and the combined retrieval (third column). Markers are colored according to the prevailing hydrometeor type at the corresponding grid point in the test scene. Due to their sparsity, ~~respectively~~markers corresponding to graupel are drawn at twice the size of the other markers.

~~Scatter plots for the retrieval results from the second scene are shown in Fig. 10. Except for the lack of cloud ice in the scene, the results are similar to what has been observed in the first scene: The radar-only retrieval overestimates the mass density of snow in the scene. This effect is corrected by the combined retrieval for most of the tested particle shapes. The exception is the GemCloudIce particle for which the~~

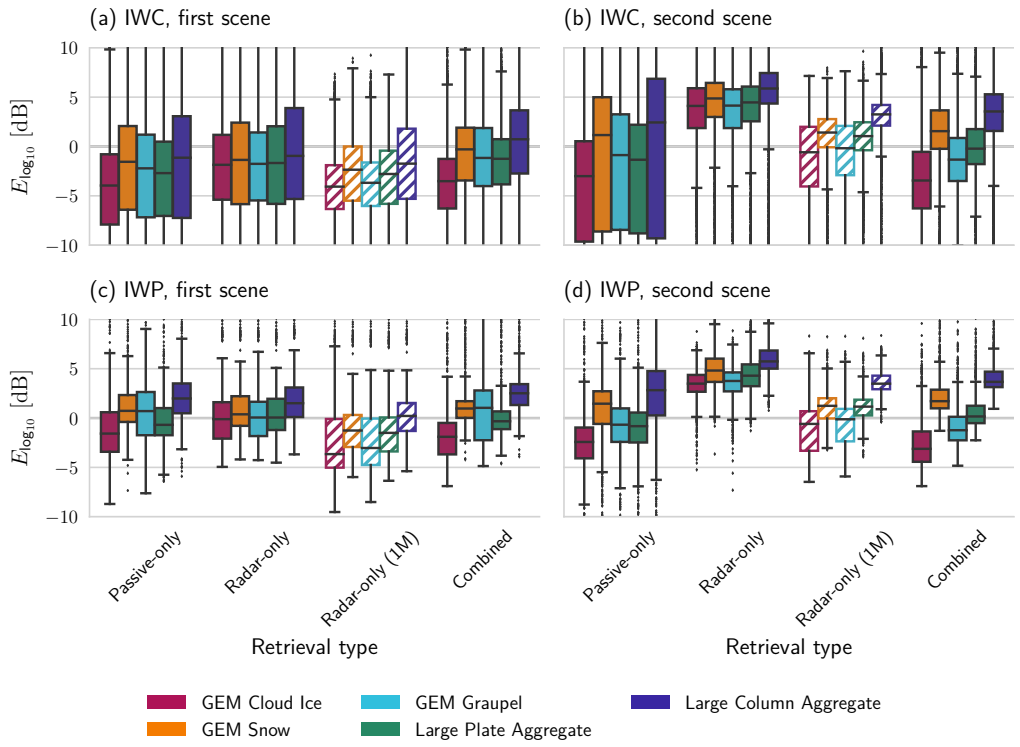

Figure 9. Distributions of the logarithmic retrieval error in IWC and IWP for all tested retrieval methods and particle shapes displayed as box plots. Colored boxes display the interquartile range (IQR) while whiskers show the full range of all points not considered outliers. Points whose distance to the IQR is larger than 1.5 times the width of the IQR are considered outliers and drawn as markers. Two results are shown for the radar-only retrieval, one for the standard version retrieving both PSD moments (solid boxes) and one for the single-moment (1M) version (diagonal hatches).

3.2.2 Particle number ~~densities~~concentrations

Particle number ~~densities~~ concentrations of frozen hydrometeors have been derived from the retrieved N_0^* and D_m parameters by computing the zeroth moment of the corresponding PSD. The resulting particle number ~~density~~ concentration fields are displayed together with the reference field in Fig. 10. To simplify the comparison~~number densities~~, number concentrations are displayed only where the corresponding reference or retrieved IWC is larger than 10^{-6} kg m^{-3}.

Comparing the passive-only and the radar-only retrieval to the reference ~~field~~ fields shows that both methods have little to no skill in predicting number ~~density~~ concentrations. Although the passive-only retrieval partly captures the gradient between very high concentrations at the top of the cloud and the low concentrations at the bottom, it is not at all resolved in the radar-only retrieval. ~~The combined retrieval , however,~~

In contrast to this, the combined retrieval manages to reproduce this gradient in ~~some~~ most parts of the scene. ~~Although its exact structure is not fully reproduced, this clearly shows sensitivity of the retrievals to particle number concentrations.~~

~~The combined retrieval shows the strongest deviations~~ The strongest deviations of the combined results from the reference field ~~between 2 and 3°~~ are observed between 2 ° N and 3° N latitude. Here, the results strongly underestimate the true number concentrations. Comparison with the cloud composition displayed in Panel (a) of Fig. 1 shows that this region contains large amounts of both cloud ice and snow. ~~Since the~~ The retrieval uses only a single hydrometeor species to represent ice in the atmosphere ~~it is~~ and is therefore not able to represent such heterogeneous conditions. Since snow will have ~~the~~ a stronger impact on the observations, the retrieval in these regions ~~tends to predict~~ will likely tend to represent snow rather than ice, which leads to the low retrieved number ~~densities~~concentrations.

~~To further investigate this,~~

Fig. 11 displays scatter plots of the reference and retrieved ~~number density~~ particle number concentrations for all three methods and two particle models from the first test scene. Markers in the plot are color coded according to their homogeneity in the reference scene, here defined as the ratio of the maximum ~~mass density~~ water content of any of the frozen hydrometeor species and ~~total IWC.~~

~~Reference and retrieved particle number concentrations of frozen hydrometeors for the first test scene obtained with the LargePlateAggregate particle model. Panel (a) displays the reference mass concentrations from the model scene. Panel (b), (c) and (d) display the retrieval results for the passive-only, radar-only and combined retrieval. Only values for which the corresponding reference or retrieved IWC was larger than 10^{-6} kg m^{-3} are shown here.~~

the total water content. These results confirm that the passive-only retrieval possesses ~~certain~~ some sensitivity to the particle number ~~density~~ concentrations since the cluster at low ~~reference number densities~~ concentrations corresponding to snow is placed correctly on the diagonal, which is not the case for the radar-only retrieval. The radar-only retrieval does not exhibit any retrieval skill, hardly reproducing any of the variation of the ~~references~~ reference values. Contrary to this, the combined retrieval moves both clusters, the one corresponding to snow and the one at high number concentrations corresponding to cloud ice, towards the diagonal~~, indicating~~ . This indicates that it is capable of distinguishing the microphysical properties of cloud ice and snow. Furthermore, the color coding shows that the strongest deviations between retrieved and reference number ~~densities~~ concentrations occur for grid points where the cloud composition is heterogeneous. ~~Even for the combined retrieval, however, the accuracy of a single retrieval value remains fairly low.~~

The general effect of particle shape on the retrieval results is ~~somewhat~~ similar to what has been observed for IWC, which is why only results for two particle shapes are shown. For the passive-only and combined retrieval, the ~~GemCloudIce model again yields~~ GEM Cloud Ice and Large Column Aggregate models yield the worst retrieval results, ~~leading to a general underestimation of the true particle number density~~while the Large Plate Aggregate performs best. For the radar-only retrieval no noticeable differences are observed between different particle models. ~~Only the results for the GemCloudIce and LargePlateAggregate particle models are shown here since the results for the other particles are mostly similar to those obtained with the LargePlateAggregate model.~~

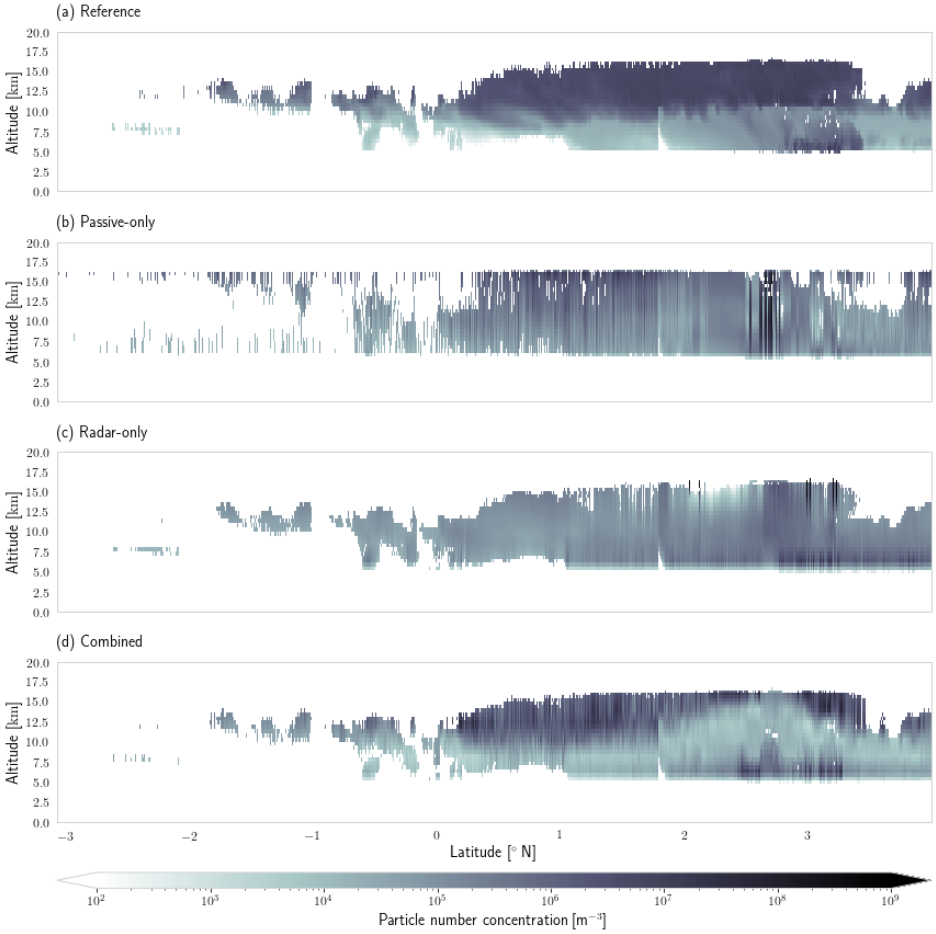

Figure 10. Reference and retrieved particle number concentrations of frozen hydrometeors for the first test scene obtained with the LargePlateAggregate particle model. Panel (a) displays the reference water content from the model scene. Panel (b), (c) and (d) display the retrieval results for the passive-only, radar-only and combined retrieval. Only values for which the corresponding reference or retrieved IWC was larger than 10^{-6} kg m^{-3} are shown here.

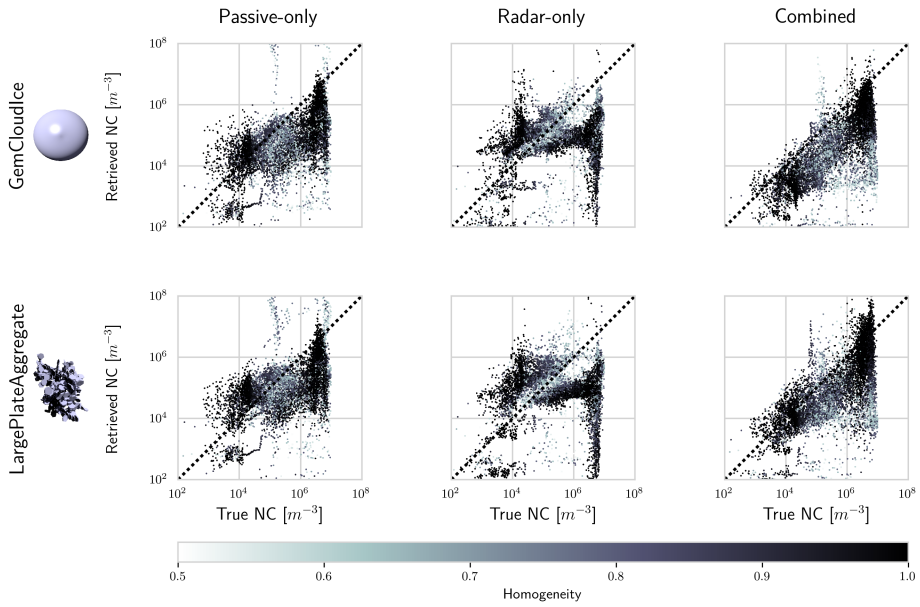

Figure 11. Scatter plots of the retrieved particle number ~~densities~~ concentration (NC) at grid points with reference ~~mass density~~ IWC larger than 10^{-5} kg m^{-3}. Rows show the results for the different particle models used in the retrieval while ~~column~~ columns display ~~the~~ results for ~~the~~ different retrieval methods. The marker color encodes the homogeneity of the corresponding ice mass, which is computed as the ratio of the maximum ~~mass density~~ water content of any of the frozen hydrometeor species and total IWC.

3.2.3 Information content

~~The retrieval results presented above show that the combined observations allow a more accurate retrieval of both mass and particle number density. This confirms the experimental results from Sec. 3.1, that active and passive observations provide complementary information on the microphysics of ice particles. The~~ To quantify the information content of the ~~retrievals can be assessed more quantitatively using the averaging kernel matrix. The trace of the AVK, commonly referred to as the number of~~ single-instrument and the combined observations, the degrees of freedom for signal (DFS) ~~, quantifies the number of independent pieces of information contained in the observations.~~

~~The distributions of the degrees of freedom of each retrieved profile in the test scenes~~ have been computed following Rodgers (2000) by calculating the trace of the averaging kernel matrix

$$\mathbf{A} = (\mathbf{K}^T \mathbf{S}_e^{-1} \mathbf{K} + \mathbf{S}_a^{-1})^{-1} \mathbf{K}^T \mathbf{S}_e^{-1} \mathbf{K}, \tag{9}$$

where $\mathbf{K} = \frac{d\mathbf{F}(\mathbf{x})}{d\mathbf{x}}$ is the Jacobian of the forward model. The information content and its decomposition into contributions from different retrieval quantities are displayed in Fig. ~~14. Not surprisingly, the combined observations exhibit the highest~~ 12.

With respect to ice, the passive-only retrieval yields the lowest information content. ~~Nevertheless, comparison with the DFS values of the active- and passive-only retrieval shows that the observations contain a certain degree of redundancy leading to a lower combined DFS value than the direct sum of~~ For the radar-only retrieval the ~~two.~~

~~The grouping into retrieval quantities furthermore reveals that the largest increase in the information content comes from water vapor, which is not retrieved in~~ information content is significantly higher, on the order of 20 degrees of freedom, but the major part of it is attributed to the D_m parameter. For the combined retrieval, the total information content on ice hydrometeors is increased compared to the radar-only retrieval in regions where the passive-only retrieval provides information on frozen hydrometeors. In addition to that, a clear shift of information content from D_m to N_0^* can be observed over both scenes. ~~Although small, a significant increase in information content is observed for both scenes~~

The information content for rain is much smaller but in relative terms the general behavior is the same as for ice. For RH, no difference is observed for the ~~N_0^* parameter for icehydrometeors. Interestingly, this increase is observed even though the~~ information content ~~in~~ provided by the passive-only ~~observations for N_0^* is close to zero. For the D_m parameter, a small decrease is observed with respect to the radar-only retrieval for both scenes. Since the calculation of the AVK involves the forward model Jacobian, this effect must be related to~~ and combined retrievals. For LCWC, the ~~non-linearity of the forward model~~information content of the combined observations is increased slightly but remains limited to a few degrees of freedom.

3.2.4 Impact of assumed ice particle shape

~~To further investigate the effect~~ The impact of the assumed ice particle shape on the retrieval results ~~, the mass density relations for the tested particle models~~ raises the question whether it also affects the quality of the fit to the observations. To investigate this, the residuals for the radar observations and three ICI channels are displayed in ~~Panel (a) of~~ Fig. ~~15. As can be seen from this plot, the GemCloudIce particle clearly stands out due to its large mass. Except for the fact that the GemSnow particle does not reach down to small particle sizes, the remaining particle models have quite similar in mass-size relations. The extreme density of the GemCloudIce particle model for large particle sizes likely explains the bad performance observedin the results presented above. Similarly, the bad performance of the GemSnow model in terms of retrieved IWC and IWP is likely due to it not covering small particle sizes.~~

~~Also displayed in Fig. 15 (panel (b) and (c)) are the χ^2_y values of the combined retrieval obtained for the tested particle models~~ 13. Each test scene contains a region where the retrieval does not fit the observations well and where substantial deviations between the fitted and true observations are observed. ~~Since the particle shape has considerable effect on sub-millimeter observations (Ekelund et al., 2019), one could hope that the retrieval results can be used to infer the prevailing ice particle type based on the how well the retrieval can fit the observations . Unfortunately, such clear conclusions cannot be drawn from the results. In the first test scene, the best fit is obtained by the GemSnow, GemCloudIce and the LargePlateAggregate particlemodels, although the GemSnow and GemCloudIce models quite clearly yield the worst retrieval performance. For the second scene, similar results are observed . Here, the GemSnow particle consistently gives the lowest χ^2_y value but comparison with Fig. 9 clearly shows that it does not yield the best retrieval performance~~It is also in these regions, where the fits obtained with different particle models differ. These are both regions where the cloud is very thick and both the radar and passive

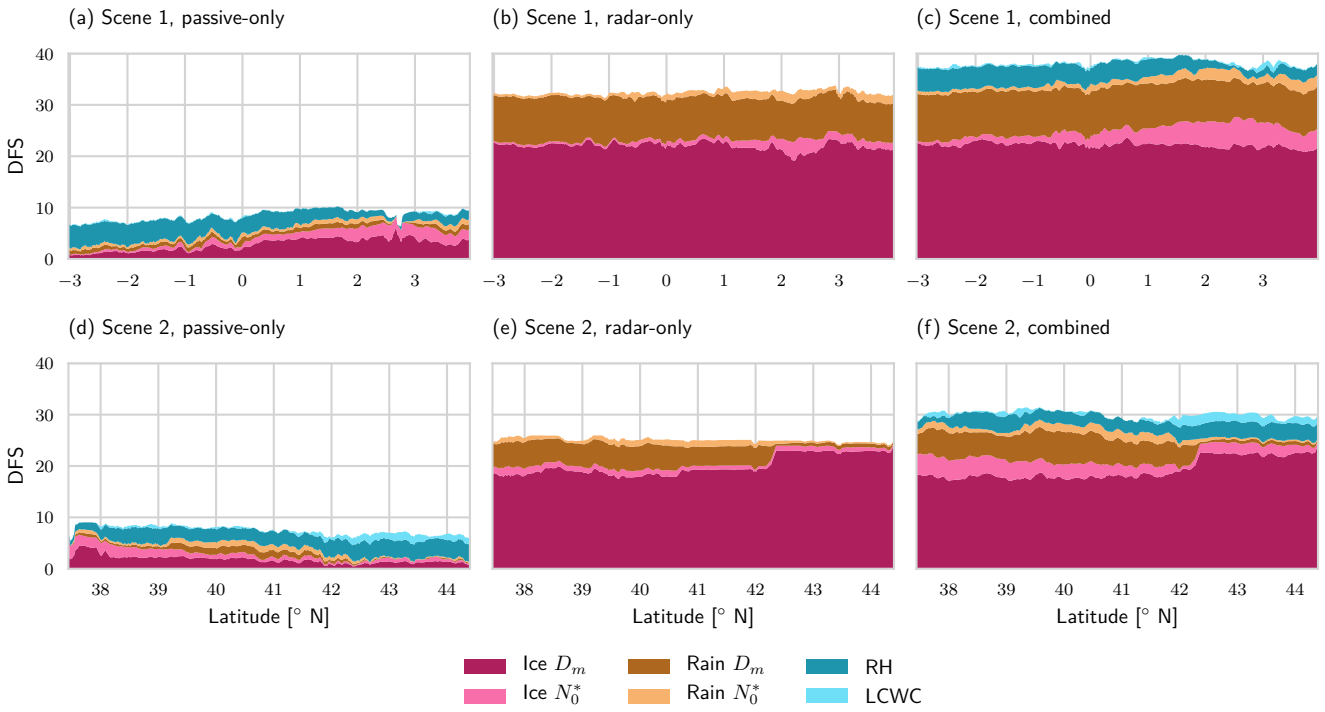

Figure 12. ~~Distributions~~ Degrees of freedom for signal for all retrieval configurations and both test scenes obtained with the Large Plate Aggregate model. The colored areas in each plot represent the contribution to the cumulative degrees of freedom ~~of signal displayed as bar plots grouped by~~ from each retrieval quantity~~and method~~. Results for the first and second test scene are displayed in ~~Panel (a) and for~~ the first and second ~~test scene in Panel (b)~~row, respectively. ~~Markers on~~ The first, second and third panel in each row show the ~~top of bars mark~~ results for the ~~extent of one standard deviation around~~ passive-only, radar-only and the ~~mean of each distribution~~combined retrieval.

observations are likely saturated. Since these are difficult regions for the retrieval it is not clear whether these differences can be related directly to the assumed particle shape. In contrast to this, the retrieval fits the observations well in the remaining parts of the scene. The exception is the GEM Graupel particle, for which quite significant misfits are observed in the first test scene between 0 ° N and 1 ° N latitude.

3.2.5 Humidity and cloud water

The developed passive and combined retrieval algorithms also retrieve profiles of ~~humidity and liquid cloud mass density. For relative humidity~~RH and LCWC. For RH, both retrievals demonstrate sensitivity but no improvement ~~could be~~ was observed in the results of the combined retrieval compared to the passive-only retrieval. ~~Moreover, no suitable retrieval setup was found within the scope of this study which would yield throughout satisfactory performance. Since we do not consider our results representative of what could be achieved with the observational approach, they are not included here.~~

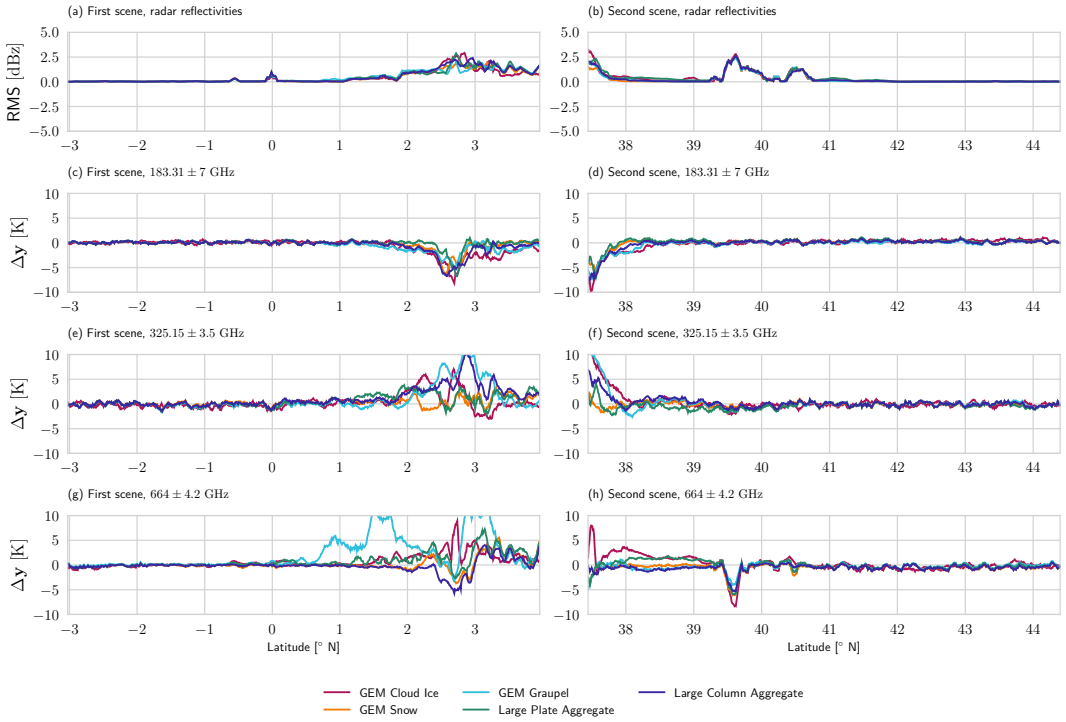

Figure 13. ~~Mass-size relations (Panel~~ Residuals of the fitted observations. First row of panels shows the profile root mean squared error (~~a~~RMS) between fitted ($\hat{\mathbf{y}}$) and ~~χ^2_y values~~ true ($\mathbf{y}$) radar observations for the two test scenes~~(Panel (b) and (c))~~. ~~The final cost curves where smoothed using a running average filter of~~ Rows 2, 3 and 4 show the residual $\Delta\mathbf{y} = \hat{\mathbf{y}} - \mathbf{y}$ for a ~~width~~ selection of ~~20 profiles~~ICI channels.

~~The liquid cloud retrieval, however, revealed an additional synergy of the radar and passive microwave observations. The retrieval results are therefore~~ Results of the LCWC retrieval are shown in Fig. 14~~to serve as a preview for potential additional applications of the combined retrieval approach. Panel (a) of the figure shows the reference and retrieved column-integrated LWC, here referred to as liquid water path (LWP). Although the total LWC is still underestimated~~. For the retrieved LCWC, the combined ~~observations clearly improve the LWP retrievalin all regions except those covered by thick clouds.~~

~~Panel (b) displays the reference LWC drawn as contours on top of the total hydrometeor content. Panel (c) and (d) show the retrieved LWC drawn on top of the retrieved IWC for the passive-only and the combined retrieval. These results show clearly that the combined retrieval is able to detect and retrieve liquid clouds even when they overlap with ice clouds. Although some sensitivity of the passive-only retrieval to LWC can be observed as well, the retrieval puts the cloud too high in the troposphere and underestimates its LWC. This indicates that the radar reflectivity profile contains useful information for the retrieval to better locate cloud water in the atmospheric column~~retrieval yields slightly improved results compared to the passive-only retrieval. The improvements are observed mostly in the retrieved liquid cloud water path (LCWP) in the northern part of the scene. It should be noted that the cloud in this part is a mixed-phase cloud and that both retrievals successfully retrieve IWC

and LCWC. At the center of the scene both retrievals fail to retrieve the LCWC. The reason for this is that in these regions rain is present, whose signal likely swamps any signal from the liquid cloud droplets.

4 Discussion

The principal aim of this study was to investigate the synergies between radar and passive sub-millimeter observations for the retrieval of frozen hydrometeors. To this end, a simplified numerical experiment has been presented, ~~that qualitatively~~ which demonstrates the existence of complementary information in the radar and passive microwave observations. Furthermore, a combined retrieval algorithm has been developed to demonstrate the feasibility of the synergistic ~~retrievals~~ retrieval and further explore their potential as well as current limitations.

The novelty of this work for lies, in part, in the application of ICI's sub-millimeter channels, which sets it apart from the combined retrievals developed for the TRMM and GPM missions. Moreover, the development of a fully consistent variational retrieval in which all retrieval quantities are retrieved simultaneously using the observations from all sensors is also novel. This allows comparison of the combined retrieval to equivalent radar-only and passive-only configurations and therefore a direct analysis of the synergies between the active and passive observations.

4.1 Fundamental synergies

The experiment presented in the first part of this study aimed to ~~establish~~ illustrate the fundamental synergies of ~~the~~ active and passive microwave observations. It compared the cloud signals observed by a radar, a millimeter-wave radiometer and a sub-millimeter-wave radiometer. The results ~~show~~ indicate that the combined observations can ~~simultaneously constrain the horizontal and vertical scaling of~~ constrain the ~~particle size distribution~~size and concentration of particles in the cloud. However, the complementary information content between the active and passive observations depends on both the properties of the observed cloud and the frequency of the observations. For the lower frequencies considered in this study, i.e. the highest frequency channels of the MWI radiometer, the regions where both observations provide complementary information on the particle size distribution of the cloud are limited to very high ~~mass densities~~ water content and particle sizes. It should be noted, however, that since the radar simulations neglect multiple scattering, ~~the results are likely less accurate in this region of the cloud-parameter space~~these results may not fully carry over to space-borne observations. As the passive observing frequency increases, the regions of complementary information content extend down to smaller particle sizes and ~~cloud mass density~~water content. Especially the highest-frequency channels of the ICI radiometer can therefore be expected to provide ~~additional information on the particle size distribution of ice clouds~~complementary information to a W-band radar in a combined observation scenario.

4.2 Combined cloud retrieval

In the second part of the study, we have presented results from a combined, variational cloud retrieval applied to synthetic observations from two test scenes from a ~~high-resolution atmosphere model~~CRM. The results of the combined retrieval were

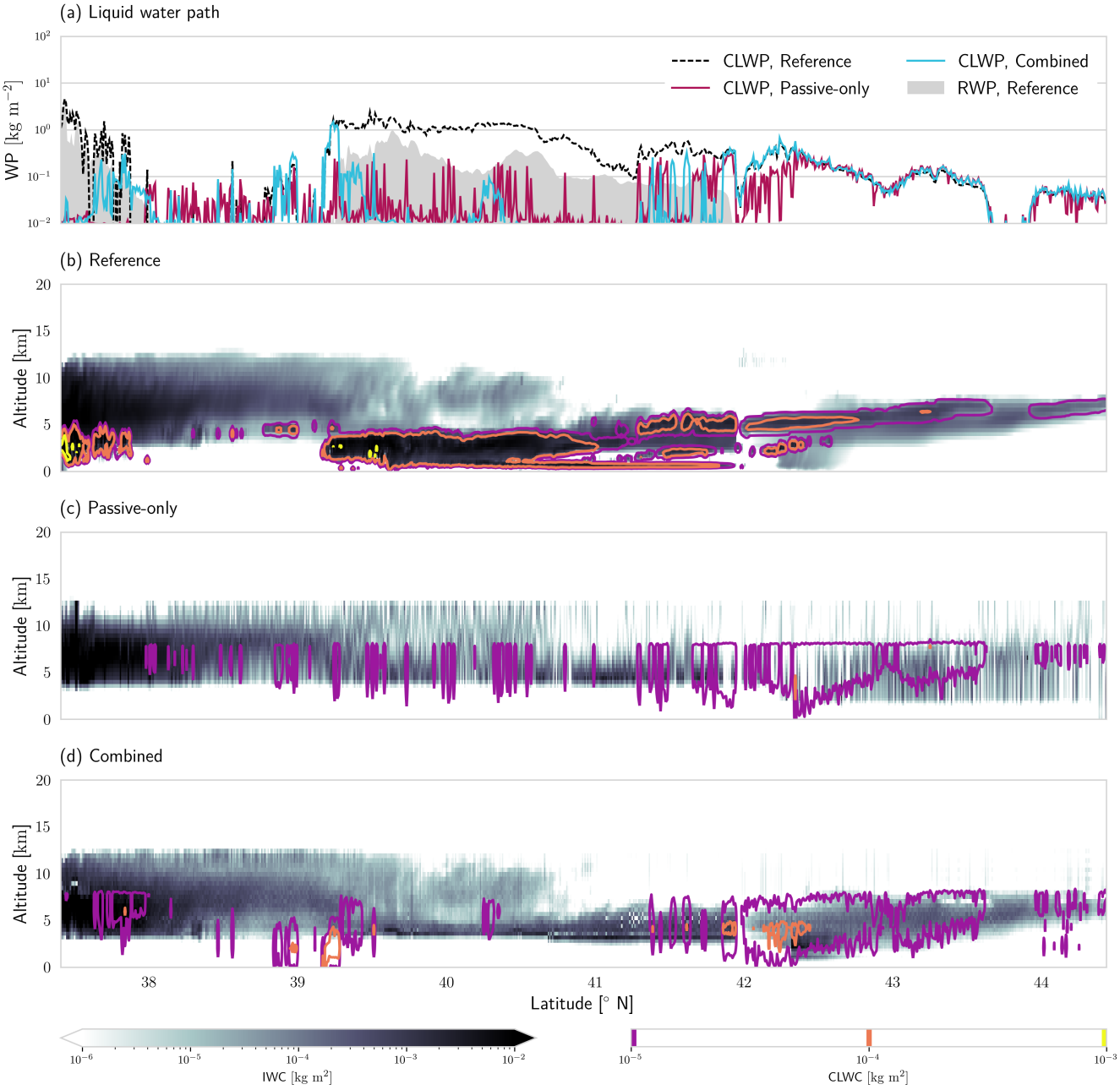

Figure 14. Reference and retrieved ~~LWC~~CLWC and IWC. Panel (a) shows the reference and retrieved LWP for each profile. Panel (b) displays reference LWC contours drawn on top of the total hydrometeor content. Retrieval results for passive-only and combined retrieval are given in Panel (c) and (d).

compared to that of a passive- and a radar-only version of the retrieval algorithm. The simulated observations assumed an airborne viewing geometry and therefore neglected potential errors caused by different or non-overlapping antenna beams as well as inhomogeneity of the atmosphere across the beams. ~~On the other hand, a~~ A source of forward model error was included by applying a more complex microphysics scheme in the simulations than the one used in the retrieval. This ~~allows assessing~~ permits assessment of the retrieval error caused by the simplified modeling of cloud microphysics in the retrieval.

4.2.1 Retrieval performance

Of the three considered retrieval implementations, the passive-only retrieval clearly performs worst in terms of retrieved IWC. It should be noted, however, that the ~~passive only~~ passive-only retrieval presented here has not been fully optimized and should therefore not be taken as representative of the potential performance of the MWI and ICI radiometers for IWC retrievals. To ensure a fair comparison, the retrieval uses almost the same a priori assumptions as the other two retrievals, which in the presented case provide only very limited information on the vertical structure of the cloud. As has been shown also by other studies, the passive observations do provide information on the vertical distribution of ice in the atmospheric column (Wang et al., 2017; Grützun et al., 2018), but the information content is limited to a few degrees of freedom. It is therefore unlikely that the vertical resolution of the passive-only retrieval can be improved drastically without further constraining it a priori, as it is typically done in retrievals that use Monte Carlo integration or neural networks (Pfreundschuh et al., 2018).

With respect to IWP, however, the passive retrieval can perform as well or even better than the radar-only ~~and the combined~~ retrieval. Furthermore, the results in ~~Figure~~Fig. 10 indicate that the passive observations provide some information on the particle number concentrations, which is not the case for the radar observations. This ~~in itself is an interesting result as it shows that even when considered separately, observations from active and passive microwave sensors should be considered complementary to each other in their information content~~shows that passive observations at multiple frequencies can actually constrain the microphysics better than single-frequency radar-only observations alone although at a much lower vertical resolution.

As expected, the radar-only retrieval provides much better IWC retrievals than the passive-only version. However, the results of the two-moment retrieval exhibit systematic deviations from the reference values in certain regions of the cloud. The analysis ~~of the retrieval performance shown in Figure 7, 8 and 10 revealed~~ shown in Fig. 8 and A2 reveals that these are caused by systematic errors in the retrieval of specific hydrometeor species from the GEM model. ~~A likely explanation for this is that the priori assumptions applied~~ Interestingly, the 1M version of the radar-only retrieval did not produce the large errors in the second scene but produces systematic errors for the first test scene. This indicates that the a priori assumptions used in the retrieval do not ~~fit the specific microphysical properties of the species in the model. This hypothesis is confirmed by the radar-retrieved number density fields shown in Fig. 10 and Fig. 11. While the reference distribution has two modes corresponding to ice and snow, the retrieved values are nearly the same throughout the whole scene. Viewed~~ provide a sufficiently good description of how the D_m and N_0^* parameters of the PSD co-vary and that the radar-only observations alone do not constrain both of them well enough. This is plausible also from an information content perspective ~~, this is plausible~~ since the radar provides only one

piece of independent information at each range gate, which is insufficient to determine the two degrees of freedom (N_0^* and D_m) of the PSD. ~~The information on the second degree of freedom must therefore come from the a priori assumptions.~~

~~The a priori assumptions which were used in this study were similar but not identical to what is used in the DARDAR retrievals. Also here it should be noted, that the presented results should not be taken to be representative for the DARDAR product.Rather than this, the DARDAR a priori settings were chosen since they represent well established and validated assumptions for ice cloud retrievals and therefore should provide a reasonable starting point for the development of a combined cloud retrieval.The fact that the a priori assumptions used in the DARDAR retrieval do not agree with the microphysical properties of~~ This hypothesis is confirmed by the radar-retrieved number concentration fields shown in Fig. 10 and Fig. 11. While the distribution of reference values has two modes corresponding to ice and snow~~in the GEM model, does not say much about the general validity of these assumptions~~, the retrieved values are nearly the same throughout the whole scene indicating that the observations themselves provide almost no information on particle concentrations.

Despite ~~the~~ certain visible artifacts in the retrieved IWC field (Fig. 7), the ~~analysis of the results of the combined retrieval presented in Figs. 7 , 8 and in particular 9 shows that it yields , at least for most of the tested particle models, the best~~ combined retrieval yields the best overall performance for IWC and IWP as shown in Fig. 8 and Fig. 9 given that a suitable particle model is used. The benefit of the combined observations is even more pronounced in the retrieved number ~~density fields~~ concentrations (Fig. 10). Here, the passive- and radar-only ~~retrieval showed~~ retrievals show little to no skill in retrieving the ~~particle~~ number concentrations. ~~The combined retrieval , however,~~ In contrast to this, the combined retrieval was able to reproduce the general structure of the number concentration ~~fields~~ field in regions where the cloud composition is homogeneous (Fig. 11). ~~In particular this showed~~ This shows that the combined retrieval is able to distinguish the microphysical properties of ice and snow in the ~~model.~~

4.2.2 ~~Impact of the assumed particle shape~~

~~Although~~ test scenes. Instead of relying on the a priori, the combined retrieval can ~~reduce systematic errors in the retrieved IWC and IWP, its performance can even degrade if an unrealistic particle habit is used, as observed in~~ use information from the observations to constrain the cloud microphysics, which avoids the systematic errors observed in the radar-only retrievals.

The a priori assumptions used in this study were chosen similar to those of the DARDAR-CLOUD product since they represent well established and validated assumptions for ice cloud retrievals. The role of the a priori is to complement the observations with additional information required to make the retrieval problem tractable. For the hydrometeor retrieval this means that the a priori determines how information from the observations, which alone is insufficient to determine both degrees of freedom of the PSD, is distributed between its D_m and N_0^* parameters. For the radar-only retrieval, this works well for cloud systems containing both ice and snow but leads to biased retrievals of both IWC and IWP when this is not the case (Fig. 9~~. In general, the passive-only and the combined retrievals display~~). The DARDAR product uses co-located lidar observations to resolve the ambiguity where observations from both sensors are available. As our results show, this can be achieved also by combining a radar with passive microwave radiometers. However, while the overlap between lidar and radar is restricted to relatively thin clouds, microwave radiometers can provide sensitivity even inside thick clouds.

4.2.2 Impact of the assumed particle shape

Our experiments show a stronger sensitivity to the assumed ~~particle shape~~ ice particle shape for the passive-only and the combined retrievals than the radar-only retrieval. ~~This is plausible since the increased sensitivity~~ The passive observations probe the particle at multiple frequencies and their sensitivity to particle shape, especially of the sub-millimeter ~~radiometer channels~~channels, has been highlighted in several studies ~~(Ekelund et al., 2019; Fox et al., 2019)~~(Ekelund et al., 2020; Fox et al., 2019)
.

~~Given the increased sensitivity of the passive-only and combined retrieval to~~ Only the combined retrieval was able to yield accurate IWC retrievals for both test scenes for suitable choices of the particle model. However, if an unsuitable particle shape is chosen, the ~~assumed particle shape , it would be desirable to know which of the properties of a particle model are most critical for its representativeness. Five different particle models were tested here: The two most dominant from the GEM model and three additional models taken from the ARTS SSDB. The two GEM particles both showed the worst retrieval performance.For the GemCloudIce model~~induced errors may actually outweigh the benefits of the combined retrieval as is the case for the Large Column Aggregate and the GEM Cloud Ice shapes (Fig. 9). Judging from the particle properties displayed in Fig. 4, a likely explanation for ~~its bad performance is its very high density. The GemSnow model has similar density as the 8-ColumnAggregate, but does not reach down to small particle sizes, possibly explaining why it is unsuitable for the retrieval~~ the good performance of the Large Plate Aggregate and the GEM Graupel particle is that their properties are intermediate to those of GEM Cloud Ice and GEM Snow, which are the dominating shapes in the test scenes. For the test scenes considered here, this means that accurate IWC retrievals can be achieved using only a single hydrometeor species with suitable scattering properties which are intermediate to snowflakes and heavily rimed particles. This is in agreement with Ekelund et al. (2020) who found the Large Plate Aggregate to yield good agreement with observations from the GPM Microwave Imager at 183.31 ± 7 GHz. ~~Nonetheless, small performance differences are observed also for the other three models~~

The analysis of the residuals of the retrieval fit (Fig. 13) showed that the residuals for different particle shapes differ most where the cloud is thick. Differences between different particles are observed, but no ~~clear connection to their mass-size relation~~ relationship to the retrieval accuracy in terms of IWC can be established. ~~This indicates that also its specific scattering properties are important factors that determine representativeness of a particlemodel.~~ The GEM Graupel particle, for example, yields accurate IWC retrievals but gives the worst fit for the first test scene. A likely explanation for this is that the retrieved IWC depends mostly on the efficiency with respect to water content of the interaction between the particle and the radiation, whereas the retrieval residual is likely due to the relative efficiencies at different frequencies. Moreover, in the remaining parts of the scenes, there are no differences in the residuals for different particles. This means that the retrieval can fit the observations well regardless of the assumed particle shape and indicates that the observations alone do not strongly constrain the particle shape. This makes it unlikely that particle shape can be retrieved from observations, thus requiring it to be determined a priori.

~~Furthermore, it has been briefly investigated whether the goodness of the fit to the observations can provide information on the suitability of the chosen particle model. In particular, we aimed to address the question whether the combined observations can constrain the dominant particle shape or whether a good fit to the observations can be obtained regardless of the applied~~

It should be noted, that none of the presented retrievals accounts for the error caused by the simplified forward model and the choice of the particle model. ~~Unfortunately, no evidence of a relation between the χ^2_y value and the retrieval performance was observed. It thus remains an open question whether and how information on the ice particle shape can be extracted from microwave observations of ice particles~~This has not been pursued here because of the difficulty of fitting a suitable error model to these errors, which are likely non-Gaussian and scene-dependent. However, it is likely that accounting for them can improve retrieval performance and weaken the impact of the particle choice on the retrieval results.

4.2.3 Humidity and cloud water

As an outlook, ~~we have also included~~ results from the ~~liquid cloud retrieval , that clearly shows its capability to retrieve liquid cloud mass densities even within mixed-phase clouds. Although certain sensitivity to cloud water is observed also for~~ LCWC retrieval have been provided despite it not being a focus of this study. Fig. 14 shows improvements in retrieved LCWP and LCWC in the results of the combined retrieval compared to the passive-only ~~retrieval,~~ retrieval. Although also the ~~addition of the radar signal clearly improved the localization of the cloud in the atmosphere. This explains the observed improvement in the retrieved LWP, since at lower altitude a thicker cloud is required to yield the same passive cloud signal~~passive-only retrieval shows sensitivity to LCWC, the results are less robust than those of the combined retrieval. This shows that combined ~~radar and microwave radiometer observationscan also~~ millimeter and sub-millimeter radiometers, in particular in combination with radar observations, can be used for ~~the profiling of warm and supercooled liquid clouds~~retrieving both frozen and liquid cloud water content in mixed-phase clouds. This conclusion is supported by the information content analysis in Fig. 12, which shows that the passive observations provide some information on LCWC and that this is increased slightly for the combined retrieval.

~~Although no satisfactory results were obtained from the water vapor retrieval, the retrieval results still indicate sensitivity of this setup for retrieving atmospheric humidity.The full exploration of the potential of the combined observations for liquid cloud and water vapor is out of the scope of this study and is left to future investigation.~~

4.2.4 ~~Retrieval method~~

~~The combined retrievalimplementation showed robust performance on fairly distinct and complex cloud scenes. Despite this, both scenes that were considered here contained parts where the OEM minimization did not find a state that results in a good fit to the observations. In contrast to that, the radar-only retrievaldid converge well in most regions where the final cost of~~ For the water vapor retrieval, no significant improvements in the combined retrieval ~~remained high. The inability of the retrieval to fit the observations indicates additional information that is contained in~~ results were observed and also the analysis of the information content does not show any increase in information content. This indicates that the combined observations ~~but which the retrieval method cannot disentangle. Furthermore, the results exhibit visible profile-to-profile variability as well as some artifacts in the form of high-frequency vertical oscillation. We have tried to counteract these by increasing the vertical spatial correlation but to no avail.~~ do not provide any direct synergies for the retrieval of humidity.

~~This raises the question of the suitability of the OEM method applied here . The combined retrieval violates the two fundamental assumptions of the OEM method: The forward model is non-linear and the assumed Gaussian~~

4.2.4 Limitations

An important limitation of this study is its scope: The aim here was not to develop a production-ready combined retrieval product but rather a proof-of-concept to explore this observational approach. The retrieval results presented here should therefore not be interpreted in absolute terms. The primary results are based on the relative performances of the three retrieval methods: Given equivalent a priori assumptions~~do not describe reality very well. In addition to that, the current implementation of the retrieval is computationally very expensive. For further development of the combined retrieval concept it may therefore be advisable to revisit the applied retrieval method in search for a potentially more suitable alternative~~, the combined retrieval demonstrates higher sensitivity to the microphysical properties than the radar-only retrieval and lower errors in terms of IWC than the passive-only retrieval.

4.2.5 ~~Limitations~~

~~Finally, it is important to consider the limitations of this study . The results presented here are~~ Moreover, this study is purely based on simulations and restricted to two selected model test scenes. The validity of the presented results thus ~~to some extent~~ depends on how well cloud microphysics are represented in the GEM model. While this may affect ~~the specific performance results for the tested retrieval methods~~interpretation of the results in absolute terms, the main findings of this work, ~~namely that the combined retrieval shows greater sensitivity to the microphysical properties of ice hydrometeors than the radar- or passive-only retrievals~~which are based on a relative comparison of the retrieval results, should be ~~independent of~~ less dependent on the realism of the test scenes.

~~Furthermore, the forward simulations used to generate the synthetic observations do not consider beam filling issues, assume a slightly unrealistic viewing geometry and neglect multiple scattering in the radar simulations. For~~ As has been stated above, simulated observations used in this study assumed a viewing geometry that is realistic only for airborne observations. They therefore do not provide a realistic assessment of the potential ~~retrieval performance this should certainly be taken into account . Again, it is important to understand the results presented here as a study of the fundamental synergies of active and passive microwave observationsrather than an accurate performance assessment of the combined retrieval~~ of a space-borne satellite mission involving ICI, MWI and a W-band radar. For this it would be necessary to take into account a more realistic viewing geometry, beam-filling errors as well as multiple scattering in the radar observations. Quantifying the effect of these error sources on the retrieval synergies is left for future investigation.

5 Conclusions

The main ~~conclusions from the results presented above are: The complementary information in active and passive microwave observations canconstrain two degrees of freedom of the PSD~~ conclusion from this work is that the combination of radar and sub-millimeter radiometer observations can, to some extent, constrain both the size and number concentration of frozen hydrometeors ~~. This reduces systematic retrieval errors for specific hydrometeor species whose properties are not well described~~

by the a priori assumptions. Especially the sub-millimeter channels of the ICI radiometer contribute to the synergistic information content for ice particles.

In addition to this(Fig. 5). The increased sensitivity of the combined observations to the microphysical properties of hydrometeors helps to improve the accuracy of IWC retrievals and avoid systematic errors observed in an equivalent radar-only retrieval (Fig. 8, 9). Moreover, the combined retrieval also shows improved profiling capabilities for warm and supercooled liquid cloudsshowed clear sensitivity to particle number concentrations and was able reproduce their vertical structure in regions where the cloud composition is homogeneous (Fig. 10, 11).

The results presented in this study particularly highlight the complementarity of the active and passive observations : Although the radar provides observations at high vertical resolution, they contain insufficient information on the microphysical properties of hydrometeors . The passive-only observations, on the contrary, have low vertical resolution, but are more sensitive to cloud microphysics allowing a potentially more accurate IWP retrieval than what can be obtained from the radar alone. A synergistic retrieval using both types of observations allows combining the high vertical resolution of the radar with the sensitivity to cloud microphysics importance of sub-millimeter observations for combined retrievals of frozen hydrometeors. While observations at currently available microwave frequencies provide information complementary to that from a radar only for thick clouds with very large particles ($D_m > 800$ µm, IWC $> 10^{-4}$ kg m^{-3}), frequencies above 200 GHz provide additional information on cloud microphysics (Fig. 5) at smaller particles sizes and water content ($D_m > 200$ µm, IWC $> 10^{-5}$ kg m^{-3}).

Regarding the representation of hydrometeors in the retrieval, our results indicate that complex mixes of hydrometeors can be accurately represented using a single, suitable habit mix. In particular, our results indicate that a suitable habit should have scattering properties that are intermediate between strongly rimed and more snow-flake like particles (Fig. 4, 9).

A direct application of the synergistic retrieval algorithm developed in this study are flight campaigns involving the International Sub-millimetre Airborne Radiometer (ISMAR, Fox et al. (2017)) combined for example with a radar on another aircraft or the Microwave Radar/radiometer for Arctic Clouds (MiRAC, Mech et al. (2019)). The ability of the combined retrieval to constrain two moments of the PSD of frozen hydrometeors should make it a valuable tool for validating the representation of clouds in cloud-resolving or large-eddy simulations which typically employ two-moment schemes. Moreover, since our results indicate retrieval skill also for LCWC in mixed-phase clouds, such observations can be used to study the properties of these clouds which play an important role for the climate of the arctic. The sensitivity to LCWC of the passive observations , which yields more accurate retrievalsof IWC, IWP and particle number densities.

Synergistic retrievals from active and passive microwave observations ideally complement currently available observation systems that combine radar with observations in the visible or infrared. The advantage of combined microwave observations is that they provide sensitivity throughout the whole cloud, where visible and infrared observations would be saturated. Where only information from the radar is available, a retrieval based on optical or infrared observations has to rely on a priori assumptions, which may cause similar systematic errors as what has been observed in this study. In addition to this, our results underline the benefits of ICI's sub-millimeter channels, which significantly improve the sensitivity of the passive observations to smaller particle sizes and mass densities and thus narrow the sensitivity gap between the observing frequencies of traditional

microwave imagers and observations in the infrared and visible domainis also a promising indication for combined ICI/MWI retrievals.

The upcoming launch of the ICI and MWI radiometers thus provides a great opportunity for a potential synergistic cloud-radar missions.Such a mission would have aunique scientific value for the study of frozen hydrometeors because of its ability to better determine the microphysical properties of hydrometeors even inside of thick clouds. Since such information is currently simply not available at a global scale, such a mission would be valuable not only in itself but also for other earth observation systems by establishing more reliable a priori assumptions on cloud microphysics.

The results presented in this study not only show the potential of the combined retrieval approach but also demonstrate its feasibility. Although further work will be required to fully understand the effect of particle shape and PSD, the concept is mature enough to be applied to real observations.Since airborne demonstrators of sub-millimeter radiometers are available already today, the combined retrievals could be applied in future field campaigns to study ice cloud microphysics.

Overall, Ultimately, spaceborne combined radar and sub-millimeter observations can be a way forward towards reducing the large uncertainties in the observational record of ice hydrometeors. The Metop program provides an opportunity for a synergistic radar mission involving the MWI and ICI radiometers. Alternatively, the combination could be realized also by a dedicated small mission, such as the Earth's NexT-generation ICE mission (ENTICE) described in Jiang et al. (2019). The results presented here clearly show the potential this approach and can provide a first step towards the development of a retrieval algorithm for a space-borne configuration. This, however, will require extending the algorithm to the combined active and passive microwave retrievals are a promising concept that deserves further exploration. Regardless whether airborne or spaceborne, combined active and passive microwave observations have great potential to improve the understanding of the microphysical properties of ice hydrometeorsmore complex viewing geometry. Moreover, to quantify the potential benefits of such a mission additional studies will be required to analyze the additional error sources which affect spaceborne observations.

Code availability. All code used to produce the results in this study is available from a public repository (Simon Pfreundschuh, 2019).

Data availability. Data to reproduce the simulations leading to the presented results will be made available on request.

Appendix A: Results from second test scene

The retrieved IWC obtained using the Large Plate Aggregate for the second scene is shown in Fig. A1. Just as the first scene, this test scene contains a region in the south where the final OEM cost, shown in Panel (a), is increased for the passive-only and combined retrievals. This is again a region of very dense cloud consisting of graupel and snow. Qualitatively, the results of the IWC retrieval are very similar to those from the first scene. While the passive-only retrieval provides only very low vertical resolution, both the radar-only and combined retrieval reproduce the vertical structure of the cloud well. The radar-only retrieval consistently overestimates the IWC in the scene, which is not the case for the combined retrieval.

Scatter plots for the retrieval results from the second scene are shown in Fig. A2. Except for the lack of cloud ice in the scene, the results are similar to what has been observed in the first scene: The radar-only retrieval exhibits the same systematic error for the retrieval of snow as in the first scene. Again, this is corrected by the combined retrieval for most of the tested particle shapes. The exception are the GEM Cloud Ice and the Large Column Aggregate particles for which the retrieval does not perform as well.

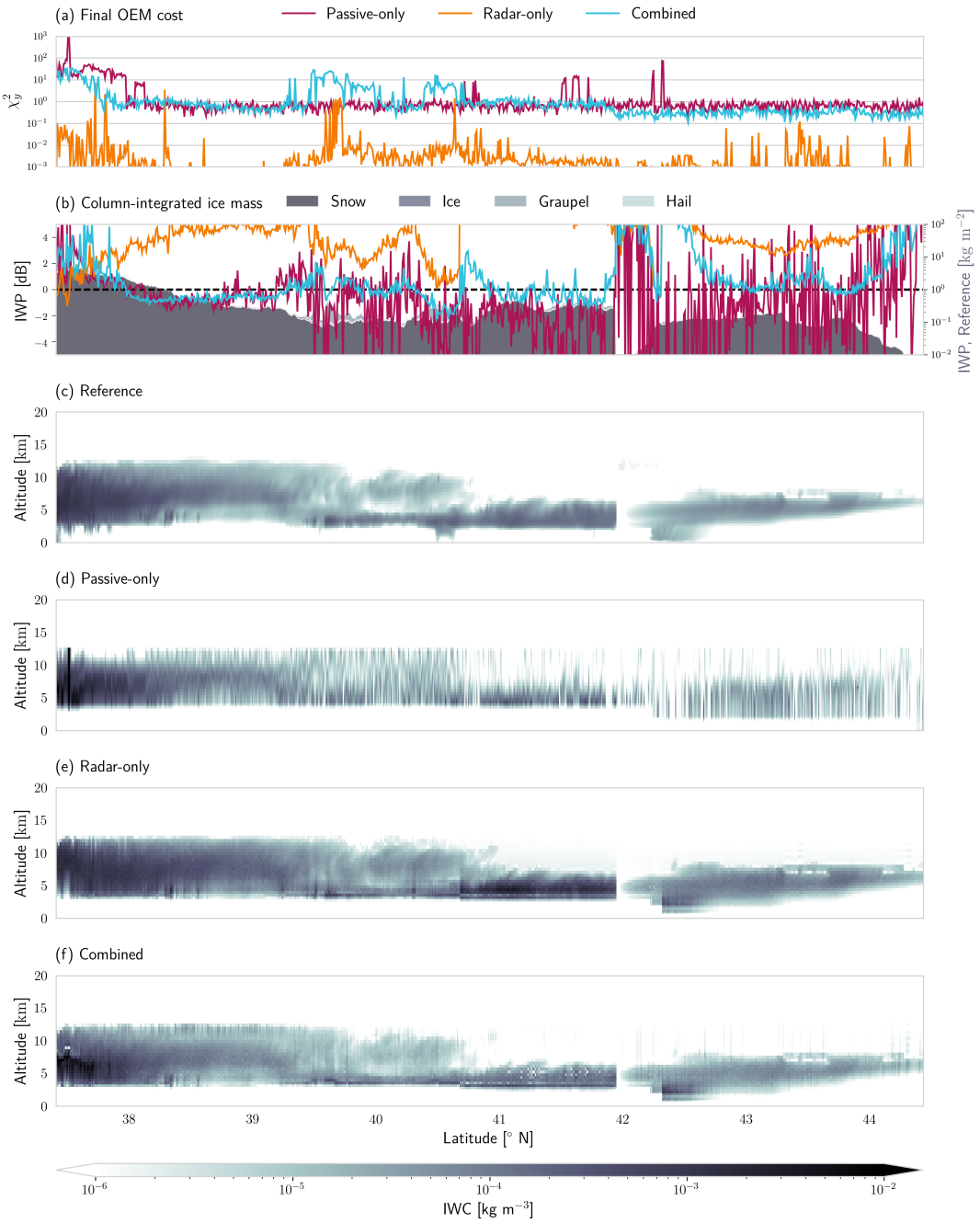

Figure A1. Results of the ice hydrometeor retrieval for the second test scene. Panel (a) displays the value of the χ^2_y diagnostic normalized by the dimension of the measurement space of the corresponding retrieval. Panel (b) shows retrieved IWP in dB relative to the reference IWP. Reference IWP and the contributions from different hydrometeor classes are displayed by the filled areas in the background. Panel (c) displays the reference mass concentrations from the model scene. Panel (d), (e) and (f) display the retrieval results for the passive-only, radar-only and combined retrieval, respectively.

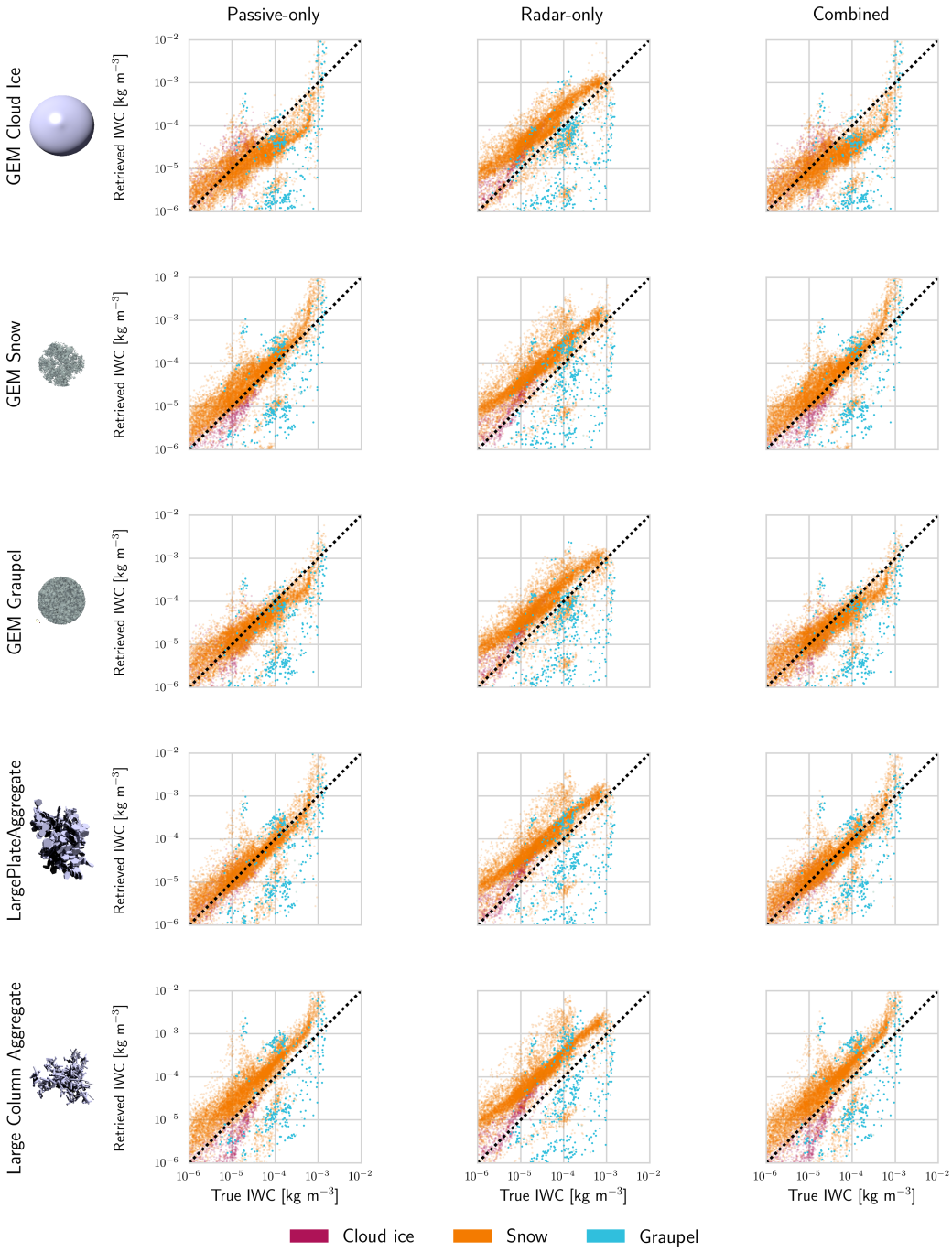

Figure A2. Scatter plots of the reference and retrieved IWC for the second test scene. The rows show the retrieval results for a given assumed ice particle model. The first column of each row displays a rendering of the particle model. The following rows display the results for the passive-only, the radar-only and the combined retrieval.

Author contributions. Simon Pfreundschuh has implemented the retrieval, performed the data analysis and written the manuscript. Patrick Eriksson and Richard Larsson have added code to the ARTS radiative transfer model that was required to perform the presented calculations. Stefan A. Buehler, Patrick Eriksson, Manfred Brath and Simon Pfreundschuh have collaborated on the study that lead to the results presented here. David Duncan and Robin Ekelund have contributed to the conceptualization of the study through comments and advice.

Competing interests. No competing interests are present.

Acknowledgements. The combined and radar-only were developed as part of the ESA-funded study "Scientific Concept Study for Wide-Swath High-Resolution Cloud Profiling" (Contract number: 4000119850/17/NL/LvH). The authors would like to thank study manager Tobias Wehr for his valuable input and guidance.

Furthermore, the authors would like to acknowledge the work of Zhipeng Qu, Howard Barker, and Jason Cole from Environment and Climate Change Canada who produced the model scenes that were used to test the retrieval.

The work of SP, PE and RE on this study was financially supported by the Swedish National Space Agency (SNSA) under grants 150/14 and 166/18.

SB ~~was supported by the Deutsche Forschungsgemeinschaft (DFG, German Research Foundation) under Germany's Excellence Strategy — EXC 2037 'Climate, Climatic Change, and Society' — Project Number: 390683824,~~ is contributing to the Center for Earth System Research and Sustainability (CEN) of Universität Hamburg.

The computations for this study were performed using several freely available programming languages and software packages, most prominently the Python language (The Python Language Foundation, 2018), the IPython computing environment (Perez and Granger, 2007), the numpy package for numerical computing (van der Walt et al., 2011) and matplotlib for generating figures (Hunter, 2007).

The computations were performed on resources at Chalmers Centre for Computational Science and Engineering (C3SE) provided by the Swedish National Infrastructure for Computing (SNIC).

References

Aires, F., Prigent, C., Buehler, S. A., Eriksson, P., Milz, M., and Crewell, S.: Towards more realistic hypotheses for the information content analysis of cloudy/precipitating situations – Application to a hyperspectral instrument in the microwave, Q. J. R. Meteorol. Soc., 145, 1–14, https://doi.org/10.1002/qj.3315, 2019.

Birman, C., Mahfouf, J.-F., Milz, M., Mendrok, J., Buehler, S. A., and Brath, M.: Information content on hydrometeors from millimeter and sub-millimeter wavelengths, Tellus, 69, 1271 562, https://doi.org/10.1080/16000870.2016.1271562, 2017.

Bony, S., Stevens, B., Frierson, D. M., Jakob, C., Kageyama, M., Pincus, R., Shepherd, T. G., Sherwood, S. C., Siebesma, A. P., Sobel, A. H., et al.: Clouds, circulation and climate sensitivity, Nat. Geosci., 8, 261, https://doi.org/10.1038/ngeo2398, 2015.

Boucher, O., Randall, D., Artaxo, P., Bretherton, C., Feingold, G., Forster, P., Kerminen, V.-M., Kondo, Y., Liao, H., Lohmann, U., Rasch, P., Satheesh, S., Sherwood, S., Stevens, B., and Zhang, X.: Clouds and Aerosols, book section 7, p. 571–658, Cambridge University Press, Cambridge, United Kingdom and New York, NY, USA, https://doi.org/10.1017/CBO9781107415324.016, 2013.

Brath, M., Fox, S., Eriksson, P., Harlow, R. C., Burgdorf, M., and Buehler, S. A.: Retrieval of an ice water path over the ocean from ISMAR and MARSS millimeter and submillimeter brightness temperatures, Atmos. Meas. Tech., 11, 611–632, https://doi.org/10.5194/amt-11-611-2018, 2018.

Buehler, S. A., Mendrok, J., Eriksson, P., Perrin, A., Larsson, R., and Lemke, O.: ARTS, the Atmospheric Radiative Transfer Simulator – version 2.2, the planetary toolbox edition, Geosci. Model Dev., 11, 1537–1556, https://doi.org/10.5194/gmd-11-1537-2018, 2018.

Cazenave, Q., Ceccaldi, M., Delanoë, J., Pelon, J., Groß, S., and Heymsfield, A.: Evolution of DARDAR-CLOUD ice cloud retrievals: new parameters and impacts on the retrieved microphysical properties, Atmos. Meas. Tech. Discuss., 12, https://doi.org/10.5194/amt-12-2819-2019, 2018.

Cazenave, Q., Ceccaldi, M., Delanoë, J., Pelon, J., Groß, S., and Heymsfield, A.: Evolution of DARDAR-CLOUD ice cloud retrievals: new parameters and impacts on the retrieved microphysical properties, Atmos. Meas. Tech., 12, 2819–2835, https://doi.org/10.5194/amt-12-2819-2019, 2019.

Côté, J., Gravel, S., Méthot, A., Patoine, A., Roch, M., and Staniforth, A.: The operational CMC–MRB global environmental multi-scale (GEM) model. Part I: Design considerations and formulation, Mon. Weather Rev., 126, 1373–1395, https://doi.org/10.1175/1520-0493(1998)126<1373:TOCMGE>2.0.CO;2, 1998.

Delanoë, J., Protat, A., Testud, J., Bouniol, D., Heymsfield, A. J., Bansemer, A., Brown, P., and Forbes, R.: Statistical properties of the normalized ice particle size distribution, J. Geophys. Res.-Atmos., 110, https://doi.org/10.1029/2004JD005405, 2005.

Delanoë, J., Heymsfield, A. Protat, A., Bansemer, A., and Hogan, R.: Normalized particle size distribution for remote sensing application, J. Geophys. Res.-Atmos., 119, 4204–4227, https://doi.org/10.1002/2013JD020700, 2014.

Duncan, D. I. and Eriksson, P.: An update on global atmospheric ice estimates from satellite observations and reanalyses, Atmos. Chem. Phys., 18, 11 205, https://doi.org/10.5194/acp-18-11205-2018, 2018.

Ekelund, R., Eriksson, P., and Pfreundschuh, S.: Using passive and active observations at microwave and sub-millimetre wavelengths to constrain ice particle models, Atmos. Meas. Tech. Discuss., 13, https://doi.org/10.5194/amt-13-501-2020, 2019.

Ekelund, R., Eriksson, P., and Pfreundschuh, S.: Using passive and active observations at microwave and sub-millimetre wavelengths to constrain ice particle models, Atmos. Meas. Tech., 13, 501–520, https://doi.org/10.5194/amt-13-501-2020, 2020.

Eliasson, S., Buehler, S. A., Milz, M., Eriksson, P., and John, V. O.: Assessing observed and modelled spatial distributions of ice water path using satellite data, Atmos. Chem. Phys., 11, 375–391, https://doi.org/10.5194/acp-11-375-2011, 2011.

Eriksson, P., Ekelund, R., Mendrok, J., Brath, M., Lemke, O., and Buehler, S. A.: A general database of hydrometeor single scattering properties at microwave and sub-millimetre wavelengths, Earth Syst. Sci. Data, 10, 1301–1326, https://doi.org/10.5194/essd-10-1301-2018, 2018.

Eriksson, P., Rydberg, B., Mattioli, V., Thoss, A., Accadia, C., Klein, U., and Buehler, S. A.: Towards an operational Ice Cloud Imager (ICI) retrieval product, Atmos. Meas. Tech. Discuss., https://doi.org/10.5194/amt-13-53-2020, 2019.

Eriksson, P., Rydberg, B., Mattioli, V., Thoss, A., Accadia, C., Klein, U., and Buehler, S. A.: Towards an operational Ice Cloud Imager (ICI) retrieval product, Atmos. Meas. Tech., 13, 53–71, https://doi.org/10.5194/amt-13-53-2020, 2020.

Evans, K. F., Wang, J. R., Racette, P. E., Heymsfield, G., and Li, L.: Ice Cloud Retrievals and Analysis with the Compact Scanning Submillimeter Imaging Radiometer and the Cloud Radar System during CRYSTAL FACE, J. Appl. Meteorol., 44, 839–859, https://doi.org/10.1175/JAM2250.1, 2005.

Fox, S., Lee, C., Moyna, B., Philipp, M., Rule, I., Rogers, S., King, R., Oldfield, M., Rea, S., Henry, M., Wang, H., and Harlow, R. C.: ISMAR: an airborne submillimetre radiometer, Atmos. Meas. Tech., 10, 477–490, https://doi.org/10.5194/amt-10-477-2017, 2017.

Fox, S., Mendrok, J., Eriksson, P., Ekelund, R., O'Shea, S. J., Bower, K. N., Baran, A. J., Harlow, R. C., and Pickering, J. C.: Airborne validation of radiative transfer modelling of ice clouds at millimetre and sub-millimetre wavelengths, Atmos. Meas. Tech., 12, 1599–1617, https://doi.org/10.5194/amt-12-1599-2019, 2019.

Geer, A. J., Baordo, F., Bormann, N., Chambon, P., English, S. J., Kazumori, M., Lawrence, H., Lean, P., Lonitz, K., and Lupu, C.: The growing impact of satellite observations sensitive to humidity, cloud and precipitation, Q. J. R. Meteorol. Soc., 143, 3189–3206, https://doi.org/10.1002/qj.3172, 2017.

Grecu, M., Olson, W. S., and Anagnostou, E. N.: Retrieval of Precipitation Profiles from Multiresolution, Multifrequency Active and Passive Microwave Observations, Journal of Applied Meteorology, 43, 562–575, https://doi.org/10.1175/1520-0450(2004)043<0562:ROPPFM>2.0.CO;2, 2004.

Grecu, M., Olson, W. S., Munchak, S. J., Ringerud, S., Liao, L., Haddad, Z., Kelley, B. L., and McLaughlin, S. F.: The GPM Combined Algorithm, J. Atmos. Oceanic Technol., 33, 2225–2245, https://doi.org/10.1175/JTECH-D-16-0019.1, 2016.

Grützun, V., Buehler, S. A., Kluft, L., Mendrok, J., Brath, M., and Eriksson, P.: All-sky information content analysis for novel passive microwave instruments in the range from 23.8 to 874.4 GHz, Atmos. Meas. Tech., 11, 4217–4237, https://doi.org/10.5194/amt-11-4217-2018, 2018.

Hou, A. Y., Kakar, R. K., Neeck, S., Azarbarzin, A. A., Kummerow, C. D., Kojima, M., Oki, R., Nakamura, K., and Iguchi, T.: The Global Precipitation Measurement Mission, Bull. Amer. Met. Soc., 95, 701–722, https://doi.org/10.1175/BAMS-D-13-00164.1, 2014.

Hunter, J. D.: Matplotlib: A 2D graphics environment, Comput. Sce. Eng., 9, 90–95, https://doi.org/10.1109/MCSE.2007.55, 2007.

Jiang, J. H., Yue, Q., Su, H., Kangaslahti, P., Lebsock, M., Reising, S., Schoeberl, M., Wu, L., and Herman, R. L.: Simulation of Remote Sensing of Clouds and Humidity From Space Using a Combined Platform of Radar and Multifrequency Microwave Radiometers, Earth Space. Sci., 6, 1234–1243, https://doi.org/10.1029/2019EA000580, 2019.

Jiménez, C., Buehler, S., Rydberg, B., Eriksson, P., and Evans, K.: Performance simulations for a submillimetre-wave satellite instrument to measure cloud ice, Q. J. R. Meteorol. Soc., 133, 129–149, https://doi.org/10.1002/qj.134, 2007.

Kummerow, C., Barnes, W., Kozu, T., Shiue, J., and Simpson, J.: The tropical rainfall measuring mission (TRMM) sensor package, Journal of atmospheric and oceanic technology, 15, 809–817, 1998.

Kummerow, C. D., Randel, D. L., Kulie, M., Wang, N.-Y., Ferraro, R., Munchak, J. S., and Petkovic, V.: The Evolution of the Goddard Profiling Algorithm to a Fully Parametric Scheme, J. Atmos. Oceanic Technol., 32, 2265–2280, https://doi.org/10.1175/JTECH-D-15-0039.1, 2015.

Liebe, H. J., Hufford, G. A., and Cotton, M. G.: Propagation modeling of moist air and suspended water/ice particles at frequencies below 1000 GHz, in: AGARD conference proceedings 542: Atmospheric propagation effects through natural and man-made obscurants for visible to mm-wave radiation, pp. 3.1–3.10, Palma de Mallorca, Spain, 17–20 May 1993, 1993.

Mech, M., Kliesch, L.-L., Anhäuser, A., Rose, T., Kollias, P., and Crewell, S.: Microwave Radar/radiometer for Arctic Clouds (MiRAC): first insights from the ACLOUD campaign, Atmospheric Measurement Techniques, 12, 5019–5037, https://doi.org/10.5194/amt-12-5019-2019, 2019.

Milbrandt, J. A. and Yau, M. K.: A multimoment bulk microphysics parameterization. Part II: A proposed three-moment closure and scheme description, J. Atmos. Sci., 62, 3065–3081, https://doi.org/10.1175/JAS3534.1, 2005.

Munchak, S. J. and Kummerow, C. D.: A Modular Optimal Estimation Method for Combined Radar–Radiometer Precipitation Profiling, J. Atmos. Oceanic Technol., 50, 433–448, https://doi.org/10.1175/2010JAMC2535.1, 2011.

Perez, F. and Granger, B. E.: IPython: A System for Interactive Scientific Computing, Computing in Science Engineering, 9, 21–29, https://doi.org/10.1109/MCSE.2007.53, 2007.

Pfreundschuh, S., Eriksson, P., Duncan, D., Rydberg, B., Håkansson, N., and Thoss, A.: A neural network approach to estimating a posteriori distributions of Bayesian retrieval problems, Atmos. Meas. Tech., 11, 4627–4643, https://doi.org/10.5194/amt-11-4627-2018, 2018.

Prigent, C., Aires, F., Wang, D., Fox, S., and Harlow, C.: Sea-surface emissivity parametrization from microwaves to millimetre waves, Q. J. R. Meteorol. Soc., 143, 596–605, https://doi.org/10.1002/qj.2953, 2017.

Rodgers, C. D.: Inverse methods for atmospheric sounding: theory and practice, vol. 2, World scientific, https://doi.org/10.1142/3171, 2000.

Rosenkranz, P. W.: Absorption of microwaves by atmospheric gases, in: Atmospheric remote sensing by microwave radiometry, edited by Janssen, M. A., pp. 37–90, John Wiley and Sons, Inc., New York, USA, 1993.

Rosenkranz, P. W.: Water vapor microwave continuum absorption: A comparison of measurements and models, Radio Sci., 33, 919–928, https://doi.org/10.1029/98RS01182, 1998.

Simon Pfreundschuh: mcrf – A microwave cloud retrieval framework, https://doi.org/10.5281/zenodo.3467316, 2019.

Stamnes, K., Tsay, S.-C., Wiscombe, W., and Laszlo, I.: DISORT, a general-purpose Fortran program for discrete-ordinate-method radiative transfer in scattering and emitting layered media: documentation of methodology, Tech. rep., Tech. rep., Dept. of Physics and Engineering Physics, Stevens Institute of . . . , 2000.

Stephens, G. L., Vane, D. G., Boain, R. J., Mace, G. G., Sassen, K., Wang, Z., Illingworth, A. J., O'connor, E. J., Rossow, W. B., Durden, S. L., Miller, S. D., Austin, R. T., Benedetti, A., and Mitrescu, C. a.: THE CLOUDSAT MISSION AND THE A-TRAIN, Bull. Amer. Met. Soc., 83, 1771–1790, https://doi.org/10.1175/BAMS-83-12-1771, 2002.

Tanelli, S., Durden, S. L., Im, E., Pak, K. S., Reinke, D. G., Partain, P., Haynes, J. M., and Marchand, R. T.: CloudSat's Cloud Profiling Radar After Two Years in Orbit: Performance, Calibration, and Processing, IEEE T. Geosci. Remote, 46, 3560–3573, https://doi.org/10.1109/TGRS.2008.2002030, 2008.

The Python Language Foundation: The Python Language Reference, https://docs.python.org/3/reference/index.html, 2018.

van der Walt, S., Colbert, S. C., and Varoquaux, G.: The NumPy Array: A Structure for Efficient Numerical Computation, Computing in Science Engineering, 13, 22–30, https://doi.org/10.1109/MCSE.2011.37, 2011.

Waliser, D. E., Li, J.-L. F., Woods, C. P., Austin, R. T., Bacmeister, J., Chern, J., Del Genio, A., Jiang, J. H., Kuang, Z., Meng, H., Minnis, P., Platnick, S., Rossow, W. B., Stephens, G. L., Sun-Mack, S., Tao, W.-K., Tompkins, A. M., Vane, D. G., Walker, C., and Wu, D.: Cloud ice: A climate model challenge with signs and expectations of progress, J. Geophys. Res.-Atmos., 114, https://doi.org/10.1029/2008JD010015, 2009.

Wang, D., Prigent, C., Aires, F., and Jimenez, C.: A Statistical Retrieval of Cloud Parameters for the Millimeter Wave Ice Cloud Imager on Board MetOp-SG, IEEE Access, 5, 4057–4076, https://doi.org/10.1109/ACCESS.2016.2625742, 2017.

Xie, X., Crewell, S., Löhnert, U., Simmer, C., and Miao, J.: Polarization signatures and brightness temperatures caused by horizontally oriented snow particles at microwave bands: Effects of atmospheric absorption, J. Geophys. Res.-Atmos., 120, 6145–6160, 2015.

Bibliography

Brath, M., Ekelund, R., Eriksson, P., Lemke, O., and Buehler, S. A.: Microwave and submillimeter wave scattering of oriented ice particles, Atmospheric Measurement Techniques Discussions, 2019, 1–38, https://doi.org/10.5194/amt-2019-382, 2019.

Cazenave, Q., Ceccaldi, M., Delanoë, J., Pelon, J., Groß, S., and Heymsfield, A.: Evolution of DARDAR-CLOUD ice cloud retrievals: new parameters and impacts on the retrieved microphysical properties, Atmos. Meas. Tech., 12, 2819–2835, https://doi.org/10.5194/amt-12-2819-2019, 2019.

Delanoë, J. and Hogan, R.: DARDAR-CLOUD, URL `www.icare.univ-lille1.fr//projects_data/dardar/docs/varcloud-algorithm_description-v1.0.pdf`, 2010.

Delanoë, J., Protat, A., Testud, J., Bouniol, D., Heymsfield, A. J., Bansemer, A., Brown, P., and Forbes, R.: Statistical properties of the normalized ice particle size distribution, J. Geophys. Res.-Atmos., 110, https://doi.org/10.1029/2004JD005405, 2005.

Delanoë, J., Heymsfield, A. Protat, A., Bansemer, A., and Hogan, R.: Normalized particle size distribution for remote sensing application, J. Geophys. Res.-Atmos., 119, 4204–4227, https://doi.org/10.1002/2013JD020700, 2014.

Ekelund, R., Eriksson, P., and Pfreundschuh, S.: Using passive and active observations at microwave and sub-millimetre wavelengths to constrain ice particle models, Atmos. Meas. Tech., 13, 501–520, https://doi.org/10.5194/amt-13-501-2020, 2020.

Eriksson, P., Jamali, M., Mendrok, J., and Buehler, S. A.: On the microwave optical properties of randomly oriented ice hydrometeors, Atmos. Meas. Tech., 8, 1913–1933, https://doi.org/10.5194/amt-8-1913-2015, 2015.

Eriksson, P., Ekelund, R., Mendrok, J., Brath, M., Lemke, O., and Buehler, S. A.: A general database of hydrometeor single scattering properties at microwave and sub-millimetre wavelengths, Earth Syst. Sci. Data, 10, 1301–1326, https://doi.org/10.5194/essd-10-1301-2018, 2018.

Eriksson, P., Rydberg, B., Mattioli, V., Thoss, A., Accadia, C., Klein, U., and Buehler, S. A.: Towards an operational Ice Cloud Imager (ICI) retrieval product, Atmos. Meas. Tech. Discuss., https://doi.org/10.5194/amt-13-53-2020, 2019.

Grecu, M., Olson, W. S., and Anagnostou, E. N.: Retrieval of Precipitation Profiles from Multiresolution, Multifrequency Active and Passive Microwave Observations, Journal of Applied Meteorology, 43, 562–575, https://doi.org/10.1175/1520-0450(2004)043<0562:ROPPFM>2.0.CO;2, 2004.

Grecu, M., Olson, W. S., Munchak, S. J., Ringerud, S., Liao, L., Haddad, Z., Kelley, B. L., and McLaughlin, S. F.: The GPM Combined Algorithm, J. Atmos. Oceanic Technol., 33, 2225–2245, https://doi.org/10.1175/JTECH-D-16-0019.1, 2016.

Hou, A. Y., Kakar, R. K., Neeck, S., Azarbarzin, A. A., Kummerow, C. D., Kojima, M., Oki, R., Nakamura, K., and Iguchi, T.: The Global Precipitation Measurement Mission, Bull. Amer. Met. Soc., 95, 701–722, https://doi.org/10.1175/BAMS-D-13-00164.1, 2014.

Jiang, J. H., Yue, Q., Su, H., Kangaslahti, P., Lebsock, M., Reising, S., Schoeberl, M., Wu, L., and Herman, R. L.: Simulation of Remote Sensing of Clouds and Humidity From Space Using a Combined Platform of Radar and Multifrequency Microwave Radiometers, Earth Space. Sci., 6, 1234–1243, https://doi.org/10.1029/2019EA000580, 2019.

Kummerow, C., Barnes, W., Kozu, T., Shiue, J., and Simpson, J.: The tropical rainfall measuring mission (TRMM) sensor package, Journal of atmospheric and oceanic technology, 15, 809–817, 1998.

Kummerow, C. D., Randel, D. L., Kulie, M., Wang, N.-Y., Ferraro, R., Munchak, J. S., and Petkovic, V.: The Evolution of the Goddard Profiling Algorithm to a Fully Parametric Scheme, J. Atmos. Oceanic Technol., 32, 2265–2280, https://doi.org/10.1175/JTECH-D-15-0039.1, 2015.

Milbrandt, J. A. and Yau, M. K.: A multimoment bulk microphysics parameterization. Part II: A proposed three-moment closure and scheme description, J. Atmos. Sci., 62, 3065–3081, https://doi.org/10.1175/JAS3534.1, 2005.

Munchak, S. J. and Kummerow, C. D.: A Modular Optimal Estimation Method for Combined RadarRadiometer Precipitation Profiling, J. Atmos. Oceanic Technol., 50, 433–448, https://doi.org/10.1175/2010JAMC2535.1, 2011.

Rodgers, C. D.: Inverse methods for atmospheric sounding: theory and practice, vol. 2, World scientific, https://doi.org/10.1142/3171, 2000.

Xie, X., Crewell, S., Löhnert, U., Simmer, C., and Miao, J.: Polarization signatures and brightness temperatures caused by horizontally oriented snow particles at microwave bands: Effects of atmospheric absorption, Journal of Geophysical Research: Atmospheres, 120, 6145–6160, 2015.